

**Broadband microwave permittivity
measurements
of blood for hydration monitoring**

Submitted in partial fulfilment of the requirements of the
Degree of Doctor of Philosophy
(Queen Mary University of London)

Presented by
WESLEIGH DAWSMITH

Statement of originality

I, Wesleigh Dawsmith, confirm that the research included within this thesis is my own work or that where it has been carried out in collaboration with, or supported by others, that this is duly acknowledged below and my contribution indicated. Previously published material is also acknowledged below.

I attest that I have exercised reasonable care to ensure that the work is original, and does not to the best of my knowledge break any UK law, infringe any third party's copyright or other Intellectual Property Right, or contain any confidential material.

I accept that the College has the right to use plagiarism detection software to check the electronic version of the thesis.

I confirm that this thesis has not been previously submitted for the award of a degree by this or any other university.

The copyright of this thesis rests with the author and no quotation from it or information derived from it may be published without the prior written consent of the author.

Signature:

Date: 31/07/2020

Abstract

In the UK, dehydration and malnutrition affects vulnerable patients, costing the NHS an estimated £13 billion. Whilst a patient's hydration levels is usually determined by fluid balance or plasma osmolality methods, these have a slow turnaround time and are invasive. New approaches that are non-invasive, real-time and easy to use need to be developed to improve dehydration prevention. The present study modified an NPL broadband microwave permittivity system by inverting the dielectric probe to allow for the broadband permittivity measurement of microliter fluid samples. The system was extensively characterised using solutions of NaCl and pure water. While some calibration artifacts were introduced, overall the measured permittivity response was only 3% below the expected absolute permittivity. To determine if blood permittivity changed during dehydration, blood permittivity measurements were taken from healthy athletes (who cycled at a high intensity in a 35°C, 40% humidity environment for 80 min) and compared to changes in blood osmolality and body mass. We demonstrated a correlation existed between blood osmolality and permittivity at a range of frequencies, suggesting the technique has the potential to monitor hydration in sportspeople. Finally, to determine exactly which components were affecting the permittivity profile during dehydration, a range of NaCl, bovine HCT and BSA concentrations in physiological osmotic solutions were measured at frequencies between 0.5 GHz to 20 GHz using our inverted probe method. We demonstrated a strong linear correlation between the real and imaginary permittivity when varying concentrations of HCT, BSA and osmolality. However, while little difference was found between the frequency-permittivity profile of HCT and BSA for both the real and imaginary permittivity, significant difference existed compared to NaCl, with a window existing at 20 GHz where measurements could be made independent of NaCl. Overall microwave dielectric measurements were found to be suitable for measuring changes in blood hydration.

Acknowledgments

Firstly, thank you to my primary supervisor Dr Tina Chowdhury, who changed my way of thinking and made me a new person. A huge thank you to my lead industrial supervisor at NPL, Dr Richard Dudley, it is thanks to you I understand the importance of patients and conducting preliminary studies. I will carry this with me for life (or till I get amnesia). A huge thank you to my secondary supervisor, Dr Robert Donnan, you were always there when I need you, and your support and insight were invaluable. Final thank my supervisor, Dr Nobuoki Ohtani, I could not have progressed without your input. I am sorry the project did not quite go in the direction you hoped.

A big thank you for all the support I received from the staff at QMUL. A special shout out to the technicians: Chris Mole, Shafir Iqbal, Alice Williams, Dennis Ife and Eric Di Federico. A huge thank you to Vicky Kwaku for the implants (for outreach), Ben Milson and Mark Ariyanayagam for their support with H&S queries, Dr David Barrett and Dr James Taylor (fellow PhD students in our group) for showing me the ropes and Sarah Coleman, whom without I would likely not be submitting.

At NPL I wish to give a huge thank you to Dr Andrew Gregory for helping me understand dielectrics and lending me equipment. A warm thank you to Dr Mira Naftaly for her help and support over the years, I would have 1 paper less without her. A jokey thank you to Dr Imran Mohamed, no jokes here, keep moving on, nothing to see here. Seriously though, I could not have wished for a better office mate. Finally, a big thank you also, to Colin Towey, for his help and support with the human trials at St Mary's University.

I wish to thank my family, especially my mum, Chantelle Dawsmith. Thank you for the cheap rent, free food and your proofreading services which were great greatly appreciated and often undervalued. Thank you to my brother, Aston Dawsmith, who I spent many an hour gaming with to relax. Good luck being a physics teacher. Finally thank you to my dad, Nigel Dawsmith, for not dying on me during write up, that would have been a real downer.

Finally thank you to the EPSRC and NPL for funding this PhD (CASE EP/N50953X/1).

Table of Content

Statement of originality.....	I
Abstract.....	II
Acknowledgments.....	III
List of figures.....	VIII
List of tables	XIII
List of abbreviations	XIV
1. The current clinical problem with measuring dehydration and current measurement techniques	1
1.1 Introduction to detecting and measuring hydration	2
1.2 The social economic impact of poor hydration.....	3
1.3 Hydration Control.....	5
1.3.1 Defining hydration status.....	5
1.3.2 Blood Composition	7
1.3.3 Controlling Hydration.....	8
1.3.4 Effect of dehydration on blood composition.....	10
1.4 Current and future hydration monitoring techniques	11
1.4.1 Commonly used clinical methods to measure hydration	11
1.4.2 Rarely used clinical methods to measure hydration	14
1.4.3 State of the art hydration measurement technologies and products.	16
2. Technology selection and microwave permittivity theory .	20
2.1 Blood dielectric technology for measuring changes in hydration levels	21
2.1.1 Why blood dielectrics measurements were pursued for hydration detection	21
2.1.2 Challenges with measuring blood dielectrics.....	23
2.2 Dielectric measurements theory	24
2.2.1 Microwave dielectric theory	24
2.2.2 The effect of blood components on dielectric measurement of water	29
2.3 Thesis overview, Aims and Objectives	38

3. Characterisation of the inverted dielectric probe setup	41
3.1 Introduction	42
3.2 Normal dielectric probe setup and measurements.....	43
3.2.1 Experimental setup.....	43
3.2.2 Calibration and measurement method	44
3.3 Microliter inverted dielectric probe design, setup, measurement and characterisation	46
3.3.1 Experimental setup.....	46
3.3.2 Probe justification	47
3.3.3 Calibration and measurement method	48
3.4 Characteristics of the inverted dielectric probe	49
3.4.1 Effect of calibration and sample volume on the inverted microliter dielectric setup and the characterisation of the 'bump' in the data.....	49
3.4.2 Modelling the inverted dielectric probe in CST	55
3.4.3 Effect of time on the inverted microliter dielectric setup	57
3.4.4 Performance characteristics of the microliter dielectric setup.....	62
3.5 Summary of the microliter dielectric setup	68
4. Exercise induced dehydration causes changes in the permittivity of whole blood	69
4.1 Introduction	70
4.1.1 The effect of exercise induced dehydration on blood composition	70
4.1.2 The effect of exercise induced dehydration on body metrics.....	73
4.2 Methods	74
4.2.1 Human trials ethics approvals, MTA's and volunteer criteria	74
4.2.2 Experimental overview – Human trials 1	75
4.2.3 Experimental overview – Human trials 2	76
4.2.4 General Methodologies	77
4.3 Results: The effect of dehydration on bloods properties	83
4.3.1 Participant biometrics	83
4.3.2 Real permittivity.....	84
4.3.3 Imaginary permittivity	87
4.3.4 Blood osmolality, glucose and oxygen	90
4.3.5 Infrared spectrum	92
4.4 Discussion: The effect of dehydration on blood properties	94
4.4.1 Real permittivity.....	94
4.4.2 Imaginary permittivity	95
4.4.3 Infrared spectrum	95
4.4.4 The effect of sample size on whole blood osmolality.....	97
4.5 Summary of findings	98

5. Microwave frequency dependent dielectric properties of blood as a potential technique to measure hydration	99
5.1 Introduction	100
5.1.1 The effect of %HCT, albumin and osmolality on the dielectric properties of blood	100
5.1.2 The effect of other blood components and variables on the dielectric properties of blood	101
5.2 Methods	103
5.2.1 Experimental overview	103
5.2.2 Materials and equipment	104
5.2.3 Making fluids with known osmolality	104
5.2.4 Making fluids with known albumin concentrations	105
5.2.5 Making fluids with known %HCT	107
5.2.6 Making fluids with known glucose concentration	107
5.3 Results: The effect of blood components on the permittivity of water	108
5.3.1 %HCT	108
5.3.2 Albumin	109
5.3.3 NaCl	110
5.3.4 Glucose	111
5.3.5 The effect of blood components on osmotic waters permittivity ..	112
5.4 Discussion: The effect of blood components on the permittivity of water	113
5.4.1 %HCT	113
5.4.2 Albumin	113
5.4.3 NaCl	114
5.4.4 Glucose	115
5.4.5 Effect of %HCT, albumin and osmolality on the real permittivity .	115
5.4.6 Effect of %HCT, albumin and osmolality on the imaginary permittivity	116
5.4.7 Limitation of the work	117
5.5 Summary of findings	119
6. Final discussion and future work.....	120
6.1 Final discussion on the key findings	121
6.1.1 Inverted dielectric probe work	121
6.1.2 Human blood measurement work.....	122
6.1.3 Assessing the potential to measure hydration in bovine blood	122
6.2 Analysis of the methodologies used and thoughts on the direction of future work.....	124
6.2.1 Inverted dielectric probe work	124

6.2.2	Human blood measurement work.....	125
6.2.3	Assessing the potential to measure hydration in bovine blood	127
6.2.4	Other areas of research	128
List of publications		131
Conference and symposium contributions		131
References		133
Appendix.....		138

List of figures

Figure 1.1: The relationship for fluid and electrolyte movement between the plasma, interstitial and intracellular components ¹⁴	6
Figure 1.2: The average weight of water (%) stored in different regions of a health adult body. The red boxes highlight the three key areas.....	6
Figure 1.3: (Top) Composition of blood in a blood vessel ¹⁶ . (Bottom) Left: blood when freshly collected into a vacutainer. Right: average blood volumetric makeup after being centrifuged.	8
Figure 1.4: A summary of the process the body undergoes when dehydration ¹⁷	9
Figure 2.1: The polarisation mechanism dielectric materials can undergo ⁷⁴	25
Figure 2.2: The relation between the complex permittivity, real permittivity, imaginary permittivity and the loss tangent.	26
Figure 2.3: The relation between frequency and the time constant of relaxation on the strength of the displacement field ⁷³	28
Figure 2.4: A) The electron covalent bonds of a water molecule. B) The H-bonds in water when not under the effects of an electric field. Note the orientation is random, and results in no net charge. C) The water molecules aligning with the orientation of an applied electric field.....	29
Figure 2.5: The dipole nature of water molecules, with a positive dipole ($\delta+$) surrounding the hydrogen atoms, and a negative dipole ($\delta-$) surrounding the oxygen atom ¹⁴	31
Figure 2.6: The effect of temperature on the dielectric properties of water.	32
Figure 2.7: The effect of physiological osmolality on the dielectric properties of water.	34
Figure 2.8: The effect of increased protein (albumin) concentration on the dielectric properties of osmotic water.....	35
Figure 2.9: The effect of increased RBCs on the dielectric properties of osmotic water.	36

Figure 3.1: Normal Dielectric setup used for large fluid volumes.	44
Figure 3.2: A) The inverted dielectric setup used. The dielectric probe has been shown with its holding case removed. B) The frame used to hold the probe in place. Note the metal rods (red ovals) used to hold the probe in place, 6 from left to right and 6 from front to back. C) An example of water being pipetted onto the tip of the probe.	47
Figure 3.3: Permittivity measurement of ~200 μ l of horse blood made using the inverted dielectric probe setup. Notice that there is an uncharacteristic bump in the data at around 5.5 GHz.	49
Figure 3.4: The effect of water sample volume on the permittivity when calibrated using 200 μ l of water. Notice no bump is present for the 200 μ l sample.	50
Figure 3.5: The permittivity of 200 μ l salt water (290 mOsmol/kg) measured when 200 μ l of water was used during calibration. Notice the slight bump around 5.5 GHz.	51
Figure 3.6: The shape of 200 μ l droplets on a 9.5mm wooden rod covered in tin foil (as COVID-19 prevented lab access to get real photos). A) Saltwater (NaCl) droplet (high osmolality > 300 mOsmol/kg. B) Tap water droplet (low osmolality < 10 mOsmol/kg). C) Overlay of the tap water droplet onto the saltwater droplet. The arrows highlight the overlay line. D) A zoom in of the difference between the two droplets.	52
Figure 3.7: The effect of varying the sample volume of water on the real permittivity measured at different calibration volumes of water, A) 200 μ l, B) 160 μ l, C) 140 μ l, D) 100 μ l.	53
Figure 3.8: The effect of varying the sample volume of water on the imaginary permittivity measured at different calibration volumes of water, A) 200 μ l, B) 160 μ l, C) 140 μ l, D) 100 μ l.	54
Figure 3.9: A) CST model of the tip of the dielectric probe (cross-section) with a droplet of water on top. The results show the electric field lines and strength at 0.5 GHz, with the electric field remaining within the sample at all frequencies measured (0.5-20 GHz). B) Overlay of the simulation on top of the probe with a 200 μ l droplet of water.	56
Figure 3.10: The broadband effect of time on the A) real permittivity and B) imaginary permittivity, of water samples left on the tip of a dielectric probe. The effect of time on the C) real permittivity and D) imaginary permittivity, of water	

samples left on the tip of a dielectric probe at 2GHz. Notice that the permittivity plateaus by 8 minutes.	58
Figure 3.11: (L) Setup used to heat the probe tip to control its temperature. (R) Zoom in of the heat cuff made from heat shrink wire casing, resistive nichrome wire and 10mm O-rings.....	59
Figure 3.12: The effect of time and gravity on the A) real and B) imaginary permittivity of 40% HCT 288mOsmol/kg solution. The effect of time on a specific frequency (9 GHz) can be seen to impact the C) real and D) imaginary permittivity in a linear fashion, except between 0-10 minutes, where an additional temperature effect can be seen influencing the measurement.	61
Figure 3.13: The repeatability of the A) real permittivity and B) Imaginary permittivity measured using the inverted dielectric setup when measuring using 0.1M NaCl (n=6). (Red) 3.S.D. error bars placed around the mean. (Black) %3.S.D.....	63
Figure 3.14: The calibration error (n=5) of the mean (n=6) A) real permittivity and B) Imaginary permittivity measured using the inverted dielectric setup when measuring using 0.1M NaCl (n=5). (Red) 3.S.D. error bars placed around the mean. (Black) %3.S.D.....	65
Figure 3.15: Example of the mean (n=6) % difference between a 0.1M NaCl solution measured using a dielectric probe in the normal setup vs the probe in the inverted setup. The mean absolute % difference across the frequency spectrum was 1.5% for the real permittivity and 2.3% for the imaginary permittivity.....	67
Figure 4.1: The effect of change in mass on the real permittivity of whole blood for participants 1-8. The insert shows frequencies between 0.5-3.5 GHz. Note that for participants 3-7, there is a clear trend where dehydration inferred through mass loss leads to a drop in the real permittivity.....	85
Figure 4.2: The effect of dehydration (tracked through loss in body mass) on the real permittivity of whole human blood at 2 GHz for A) participant 1-8, B) participant 3-7 and C) participant 5-7. D) The effect of dehydration (tracked through osmolality increases) on the real permittivity of whole human blood for participant 5-7.	86

Figure 4.3: The effect of change in mass on the imaginary permittivity of whole blood for participants 1-8. The insert shows frequencies between 17.0-20.0 GHz. Note that for participants 3-7, there is a clear trend where dehydration inferred through mass loss leads to a drop in the imaginary permittivity.....88

Figure 4.4: The effect of dehydration (tracked through loss in body mass) on the imaginary permittivity of whole human blood at 18 GHz for A) participant 1-8, B) participant 3-7 and C) participant 5-7. D) The effect of dehydration (tracked through osmolality increases) on the imaginary permittivity of whole human blood for participant 5-7.....89

Figure 4.5: The relation between exercise induced dehydration via body mass loss and A) blood oxygen saturation, B) mean blood glucose (n=1-3) and C) % change in blood osmolality, for the second set of human trials. D) The temperature of the blood at the time of measurement relative to the temperature of the room. E) The relation between exercise induced dehydration via body mass loss and % change in whole blood osmolality, for the first set of human trials..91

Figure 4.6: The effect of dehydration (shown by mass loss) on the VIS-NIR absorption spectra of whole blood diluted 1:9 in saline for participants 5-8 respectively measured with a 1mm path-length. The insert shows wavelengths between 510-590. Note that there is a general trend of dehydration resulting in an increase in the absorption at the peak around 535 and 570 nm.93

Figure 4.7: The VIS-NIR absorption spectra for a range of blood components dissolved in water measured with a 1mm path-length.93

Figure 5.1: The change in osmolality caused by increasing albumin concentrations..... 106

Figure 5.2: The mean (n=6) A) real and C) imaginary permittivity of physiological concentrations of %HCT (35 % - 50 %) diluted in osmotic water (288mOsmol/kg) measured between 0.5 -20 GHz at 0.1 GHz intervals. The mean (n=6) B) real and D) imaginary permittivity plotted against %HCT at a range of frequencies demonstrated the highly linear relation between the two, with $R^2 > 0.999$ across all frequencies measured, not just the sample shown. 108

Figure 5.3: The A) real and C) imaginary permittivity (n=1) of physiological concentrations of albumin (3.5 – 5.5 g/dl) diluted in osmotic water (288mOsmol/kg) measured between 0.5 -20 GHz at 0.1 GHz intervals. The B)

real and D) imaginary permittivity (n=1) plotted against albumin at a range of frequencies demonstrated the highly linear relation between the two, with $R^2 > 0.98$ across all frequencies measured, not just the sample shown. 109

Figure 5.4: The mean (n=6) A) real and C) imaginary permittivity of physiological osmolality's (250 - 350 mOsmol/kg, 0.134 - 0.188 M) diluted in osmotic water (288mOsmol/kg) measured between 0.5 -20 GHz at 0.1 GHz intervals. The mean (n=6) B) real and D) imaginary permittivity plotted against osmolality at a range of frequencies demonstrated the highly linear relation between the two, with $R^2 > 0.80$ across all frequencies measured, not just the sample shown. 110

Figure 5.5: The mean (n=5) A) real and B) imaginary permittivity of a (red) high physiological concentration of glucose (200 mg/dl) diluted in deionised water, compared against the permittivity of (blue) deionised water. The (black) % difference between the two can also be seen, with the absolute % difference for the real permittivity being 0.056%, with the absolute % difference for the imaginary permittivity being 0.119%. 111

Figure 5.6: The change in A) real and C) imaginary permittivity (calculated from the gradients of permittivity values with respect to changes in blood component concentration seen in Figure 5.2-4) for an increase in (Red) %HCT by 5 %, (green) albumin by 1 g/dl and (blue) osmolality by 10 mOsmol/kg, plotted between 0.5 -20 GHz at 0.1 GHz intervals. The similarities between the B) real and D) imaginary permittivity profile of (blue) albumin and (Red) %HCT are highlighted. 112

Figure 6.1: Proposed inverted dielectric probe setup with a low permittivity cup to measure larger sample volumes. 124

Figure 6.2: Scanning electron microscopy (SEM) image of sickle RBCs in a A) oxygenated and B) Deoxygenated state. Image adapted from (A.Abay,2019)¹³⁷. C) Shape of haemoglobin in normal and sickle cell anaemia (adapted from¹³⁸) 129

List of tables

Table 1.1: Medical conditions caused by the increase or decrease of total body electrolyte and water levels within an individual, moving them from an euhydrated state.	5
Table 1.2: Commonly used clinical methods to measure hydration. Accuracy and complexity increase further down the table.	13
Table 1.3: Rarely used clinical methods to measure hydration. Accuracy and complexity increase further down the table.	15
Table 1.4: State of the art portable hydration measurement technologies and products attempting to come to market.	18
Table 3.1: The min and max mean absolute % difference across the frequency spectrum of a 0.1M NaCl solution measured using a dielectric probe in the normal setup vs the probe in the inverted setup.	67
Table 4.1: Biometrics of participants from study 1.	83
Table 4.2: Biometrics of participants from study 2.	83

List of abbreviations

ADH – Antidiuretic hormone

HCT – Haematocrit

%HCT – % Haematocrit

IR – Infrared

LED – Light emitting diode

MRI – Magnetic resonance imaging

MTA – Material transfer agreement

NIR – Near infrared

NMR – Nuclear magnetic resonance

RBC – Red Blood Cells (erythrocyte)

RH – Relative Humidity

3.S.D. – 3 standard deviations

%3.S.D. – % 3 standard deviations

SOP – Standard operating procedures

TBP – Total blood protein

WBC – White blood cells (leucocytes)

Chapter 1

The current clinical problem with measuring dehydration and current measurement techniques

1.1 Introduction to detecting and measuring hydration

Individuals can sense dehydration through the thirst response and react by consuming fluids. The thirst response is driven by mechanoreceptors in the brain that can quantify the changes in the volume and ion concentrations of the blood. Using biochemical pathways these mechanoreceptors control the individual's hydration by regulating the amount of fluid and ions retained or expelled by the body. Due to its direct link to our bodies own hydration control pathways, blood plasma osmolality is the clinical gold standard typically used by clinicians for measuring hydration in the NHS.

While the body's thirst response is typically reliable, it has limits. The ageing process causes the receptors in the brain to become less sensitive, resulting in the elderly having a high tendency to dehydrate due to not consuming enough fluids, which can cause or worsen health conditions. When exercising, athletes sweat not just water but also salt. Due to the thirst response only informing us to drink, it can result in the body experiencing dehydration caused by a lack of ions in the body. Finally, vulnerable individuals such as premature babies or patients suffering from stroke or diabetes are unable to rely on their thirst response. Whilst plasma osmolality measurements will inform on the individual's hydration, it requires regular blood samples to track the hydration response accurately, which is costly, time-consuming and invasive. As such, there is a need to find novel methods to accurately measure hydration both in real-time and non-invasively.

1.2 The social economic impact of poor hydration

Dehydration leads to three social-economic impacts: economic cost, effect on individual short-term health and effect on individual long-term health. While these impacts are easy to assess at an individual scale, the true extent on a national level is hard to determine in part due to dehydration both causing and worsening a range of different medical conditions.

To date, there has been no comprehensive review into the economic costs of dehydration. In 2004 it was estimated that proper hydration could save the NHS £0.95 billion¹ from reducing the number of patients staying in hospitals. In 2015, the cost of malnutrition and hydration was estimated to cost the NHS over £13 billion². While both of the presented studies looked at the financial cost of dehydration on NHS, there is also the economic cost to the workplace which needs to be considered. Just a 2% drop in body fluid mass (which is easily achievable) causes a measurable drop in both intellectual^{3,4,5} and physical^{6,7} performance and increases susceptibility to illness. As such it can be assumed that dehydration has a significant unreported economic cost to the workplace, caused by both a loss of productivity and time off due to illness.

Dehydration also has an immediate effect on an individual's health. Mild dehydration typically causes symptoms like a dry mouth, headache, more concentrated urine, and drops in intellectual and physical performance. As dehydration progresses the individual will begin to overheat, have orifices around the body become dry and unlubricated, before eventually falling into a coma ultimately culminating in death if not treated.

The long-term health effects of dehydration can be just as devastating due to its effect on existing health conditions. Individuals on medication risk overdosing while dehydrated, as the body lacks the volume of blood plasma required to dilute the medication sufficiently⁸. Diabetics with high blood glucose (which can be caused by dehydration) urinate more frequently to dispel glucose, which can perpetuate their dehydration⁹. For patients with acute renal failure on dialysis, there is the need to manage their water and salt consumption between sessions, to prevent fluid build-up in the body which can lead to further conditions like heart failure and death¹⁰. Ultimately, the failure to control and maintain the correct

hydration can have a serious impact on individuals with long term existing health conditions.

The lack of understanding around the impact of dehydration and the number of people affected is best highlighted when looking at death rates. In the UK only 934 death certificates mentioning malnutrition and dehydration on them in England and Wales in 2014¹¹, this is substantially less than the 12,000 additional deaths estimated to be caused by dehydration related acute kidney failure alone each year¹². It is likely that the true death rate from dehydration is hard to determine due to its ability to worsen existing health conditions making numbers more complicated to calculate. However, the large disparity between figures helps highlight just how little is known about the true extent and cost of dehydration.

1.3 Hydration Control

1.3.1 Defining hydration status

Hydration status refers to the overall hydration of a human at a given time and is determined by the total water (H₂O) and electrolyte (ions: Na⁺, Cl⁻, K⁺, Mg²⁺) levels in the body. The different types of hydration are best summarised in Table 1.1.

Table 1.1: Medical conditions caused by the increase or decrease of total body electrolyte and water levels within an individual, moving them from an euhydrated state.

		Water Level		
		High	Normal	Low
Electrolyte Level	High	Euhydrated	Hypernatremia	Hypernatremia
	Normal	Hyperhydrated	Euhydrated	Dehydrated
	Low	Hyponatremia	Hyponatremia	Euhydrated

Within the body, 3 different regions exist where water and ions are stored: intercellular space, extracellular space and blood plasma. As an individual's hydration changes, the balance of water and electrolytes between the regions shifts. The intercellular fluid refers to the fluid inside the cells and typically accounts for 40% of the total body weight. The intercellular fluid is separated from the interstitial fluid by the cell membrane, which contains ion regulation gates and channels, allowing the two fluid compartments to exist at different osmolalities. The interstitial fluid is made up of the fluid around the outside of cells and corresponds to around 16% of the total body weight. This fluid acts as an intermediary fluid between the intercellular fluid and the plasma, as demonstrated in Figure 1.1. Plasma is the third store of fluid in the body and is separated from the intercellular fluid by the blood vessel wall, through which water and small molecules can be exchanged. The plasma typically accounts for around 4% of the total body weight and is the bodies mass transport system. As plasma is moved and mixed quickly throughout the body, it acts as the equalising fluid of the body, helping resolve local hydration deficits. The interstitial fluid and plasma

can be referred to together as extracellular fluid and is summed up well by Figure 1.2¹³.

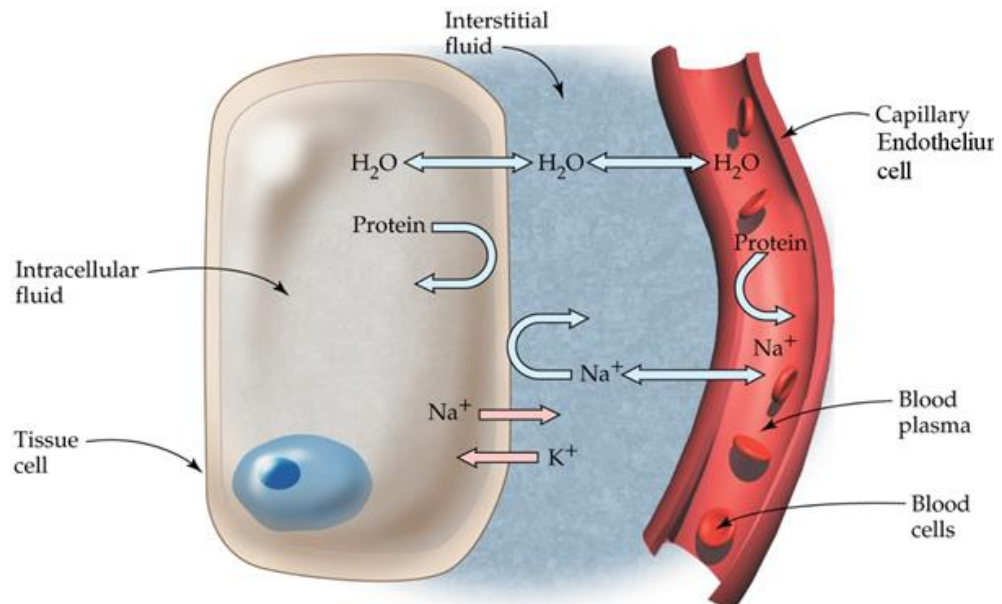


Figure 1.1: The relationship for fluid and electrolyte movement between the plasma, interstitial and intracellular components¹⁴.

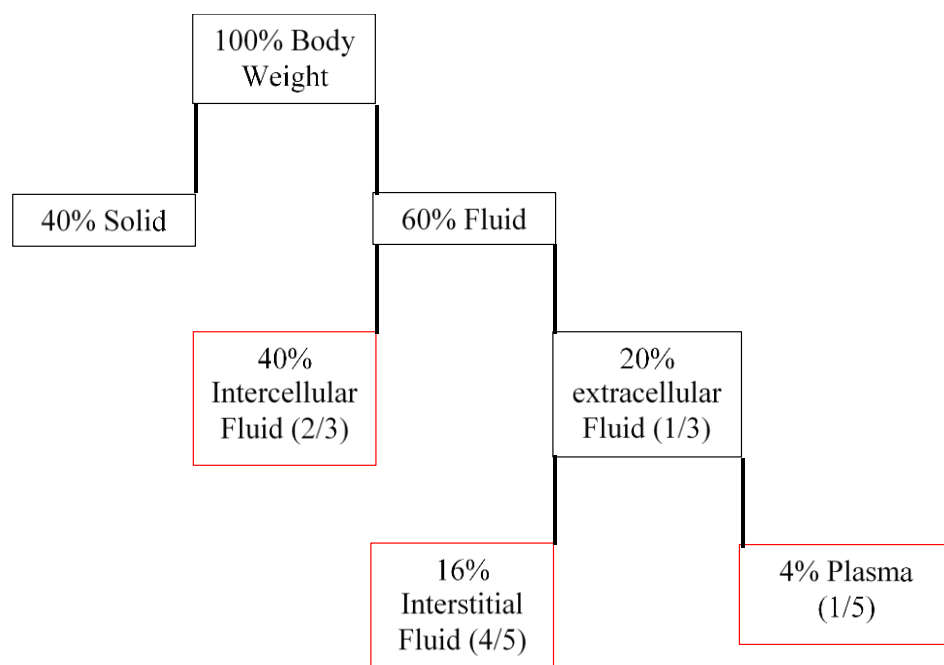


Figure 1.2: The average weight of water (%) stored in different regions of a health adult body. The red boxes highlight the three key areas.

1.3.2 Blood Composition

Blood (Figure 1.3) is a multifunctional tissue with three distinct components, each with their own features and functions. They are: RBC's (erythrocyte), plasma and other blood components which include WBC (leucocytes) and clotting factors¹⁵. RBC's makeup ~45% of the blood by volume¹⁵ and are specialist oxygen-carrying cells with no nucleus and a biconcave disk shape. RBC's are packed with the protein haemoglobin which bonds to oxygen and gives blood its distinctive red colour.

Plasma makes up ~55% of blood¹⁵ and is a water-based fluid filled with ions, proteins, and other components needing transporting. The key ions in the plasma are sodium (Na⁺), potassium (K⁺) and chloride (Cl⁻), which help maintain normal cell function. The main blood proteins can be split into 3 main groups: albumins, which are responsible for regulating the osmotic pressure of blood, globulins, which assists in immune function and hormone transporting, and fibrinogen which helps with clotting. Over 1000 globulin proteins can be further sub-divided into α 1-globulin, α 2-globulin, β -globulin and γ -globulin. Finally, there are the substances being transported in the plasma, which includes: hormones, glucose and waste products like CO₂, lactate and urea.

Making up only ~1% of the total blood volume¹⁵, immune cells and clotting factors play two important roles. The immune component is comprised of 5 different types of WBC, most noticeably neutrophils and monocytes. The WBC's are responsible for fighting off disease and infection throughout the body, using the blood as a transport system. The clotting factor component of blood is made up of platelets and an assortment of other substances, which upon the detection of damage to blood vessels, goes through a cascade of reactions to form a clot.

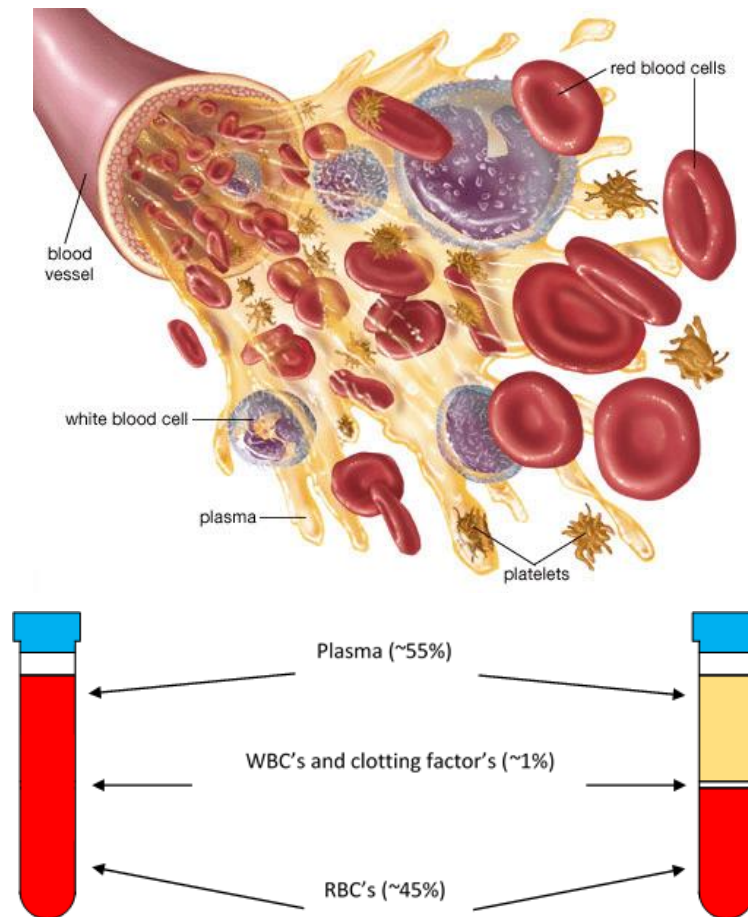


Figure 1.3: (Top) Composition of blood in a blood vessel¹⁶. (Bottom) Left: blood when freshly collected into a vacutainer. Right: average blood volumetric makeup after being centrifuged.

1.3.3 Controlling Hydration

Controlling the body's hydration response is the hypothalamic-renal feedback system which has been well summarised by S. N. Thornton, 2010¹⁷ and can be seen summarised in Figure 1.4. When dehydration begins, the interstitial component is the first area from which water is lost when the body undergoes dehydration, resulting in an increase in interstitial ion concentration. This increase results in an increase in osmotic pressure outside the cells and results in water leaving the cells to enter the interstitial region. The loss of water in the cells results in cells shrinking. This shrinkage is detected by the receptor in the hypothalamus, which causes 2 main responses. Firstly, the brain releases a hormone which induces the thirst response. Secondly, receptors located in the hypothalamus sends a neural signal to the hippocampus, which increases secretion of the antidiuretic hormone (ADH) from the posterior pituitary. The ADH then travels to

the kidney via the bloodstream and causes more ion free water to be reabsorbed. To help rebalance the intracellular and interstitial components, water from the blood plasma begins to move into the interstitial region. This results in a fall in plasma volume. This is detected by volume receptors in the kidney, which results in the increased release of the enzyme renin. The renin causes a cascade of reactions to occur, resulting in the increase of angiotensin II in the blood. This increase is detected by the adrenal gland, which increases its secretion of the steroid hormone, aldosterone. This in turn increases the amount of sodium being reabsorbed by the kidneys, which in turn increases serum sodium concentration.

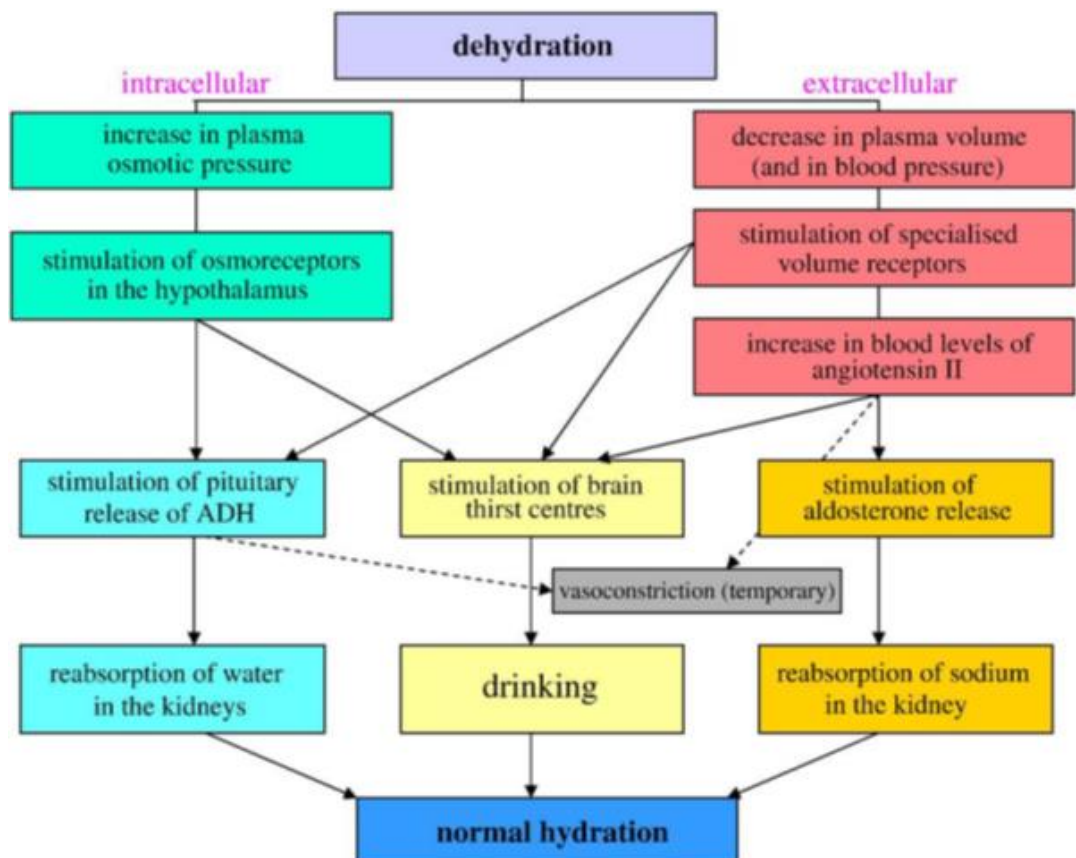


Figure 1.4: A summary of the process the body undergoes when dehydration¹⁷.

1.3.4 Effect of dehydration on blood composition

When the body undergoes dehydration, blood is one of the most impacted tissues in the body, due to its role acting as an equilibrium medium between different tissues and organs in the body. It is for this reason that the current routinely used clinical gold standard is plasma osmolality, a derivative of whole blood composition. When an individual dehydrates, a decrease in the plasma volume occurs, which is complemented by an increase in plasma Na^+ , K^+ , Cl^- , Mg^{2+} , osmolality, %HCT and total protein^{18,19}.

1.4 Current and future hydration monitoring techniques

Whilst blood plasma osmolality is the current gold standard for hydration monitoring and tracking, a range of other techniques exist which can be used to track hydration. Each of these techniques come with their own advantages and disadvantage which will be explored in this section. When comparing hydration monitoring devices, there are a range of variables which need to be considered including: how it works, how long it takes to make a measurement, size, cost, training requirements, how invasive the test is and how reliable it is to hydration.









1.4.1 Commonly used clinical methods to measure hydration

Table 1.2 outlines some of the most commonly used techniques used to measure hydration with increasing complexity and have been well documented in previous works^{20,21,22,23}. While non-invasive and free, the thirst response is a poor measure of hydration, triggering only after the individual has dehydrated. Further, as there is only one sensation, it can only tell you to consume fluids and does not inform on salt needs.

Urine volume and colour is another free way to determine one's hydration, however like all other urine-based hydration measurements, it comes with an inherent inaccuracy in the sampling time, with measurements being made on a fluid which acts as a mean of an individual's hydration since they last urinated, and does not account for fluids consumed within the last hours. To reduce perception uncertainty, urine colourimetry can be used, however, this comes at a cost. To further increase the accuracy when using urine measurements, specific gravity or osmolality tests can be used. Specific gravity tests offer a quick hand-held way of measuring hydration, while urine osmolality provides a higher accuracy, but requiring a more costly benchtop unit. The next step up in complexity is the fluid balance technique. This technique is commonly used in the care environment, where invasive blood tests not an option or practical. This technique is labour intensive requiring staff to measure fluid consumed and expelled. More advance monitoring can be achieved by calculating salt consumed in meals along with expected sweat rate to allow for salt monitoring as well. The gold standard measurement technique involves taking blood samples, with serum osmolality informing on the salt to water ratio of the body. Such tests

are however costly and slow, requiring a trained phlebotomist and analyst. The usefulness of the result is often impeded by slow turn arounds in hospital labs and the need for multiple readings to track an individual over time. Enhanced blood testing can go further and providing information on %HCT (inferring plasma volume as RBC volume remains constant) and blood protein levels, allowing for a more thorough diagnosis of dehydration to be given.






Table 1.2: Commonly used clinical methods to measure hydration. Accuracy and complexity increase further down the table.

Name	Summary of technology	Advantages	Disadvantages
Thirst ²⁴ 	Sensation generated by a drop in plasma volume and an increase in plasma osmolality.	<ul style="list-style-type: none"> - Free - No training required - Tells you when to drink fluids - Non-invasive 	<ul style="list-style-type: none"> - Only activated once you are dehydrated. - Cannot distinguish between water and salt needs.
Urine volume and colour by eye 	Examining the colour and volume of an individual's urine. Dehydration results in less, more concentrated urine.	<ul style="list-style-type: none"> - Free - Little training required - Non-invasive 	<ul style="list-style-type: none"> - Delay response (only works when you urinate). - Low sensitivity not informing on fluid consumed within the last hour
Urine colour ²⁵ 	Measuring urine colour using a colorimeter or spectroscopy.	<ul style="list-style-type: none"> - Little training required - Non-invasive 	<ul style="list-style-type: none"> - Same as 'urine volume and colour by eye' - Medium cost. - Benchtop device
Urine specific gravity ^{25,26} 	The specific gravity of urine is typically measured using a refractometer. High urea concentration results in a higher refractive index.	<ul style="list-style-type: none"> - Little training required - Non-invasive - Cheap - Hand held device 	<ul style="list-style-type: none"> - Same as 'urine by eye'
Urine osmolality ^{25,27} 	Examining the concentration of salts in a set weight of urine.	<ul style="list-style-type: none"> - Little training required - Non-invasive 	<ul style="list-style-type: none"> - Same as 'urine by eye' - Medium cost. - Benchtop device
Fluid balance technique ²⁸ 	Measuring the weight of fluid consumed, against the weight of fluid expelled.	<ul style="list-style-type: none"> - High sensitivity to water needs, can be expanded to include salt. 	<ul style="list-style-type: none"> - Labour intensive - Medium training required - Equipment intensive - Medium cost - Susceptible to human error
Plasma / Serum osmolality 	Examining the concentration of salts in a set weight of blood plasma or serum.	<ul style="list-style-type: none"> - High sensitivity to changes in hydration 	<ul style="list-style-type: none"> - Labour intensive - Medium training required - Equipment intensive - Medium cost - Benchtop device - Invasive
Enhanced blood test (Plasma osmolality, %HCT and TBP) 	Examining the concentration of salts in a set weight of blood plasma or serum. Informs on RBC and protein concentration.	<ul style="list-style-type: none"> - High sensitivity to changes in hydration - Informs on water and salt needs 	<ul style="list-style-type: none"> - Labour intensive - Medium training required - Equipment intensive - Medium cost - Benchtop devices - Invasive

1.4.2 Rarely used clinical methods to measure hydration

Table 1.3 outlines some of the less commonly used techniques used to measure hydration with and have been well documented in previous works^{20,21,22,23}. Saliva osmolality tests can be quick to perform, are relatively cheap per sample and required little training to carry out. However, this test is a poor gage of hydration in all but the most extreme of circumstances and suffer from inaccuracy related to recently consumed food and water. Tear osmolality has an established weak link with hydration. While not technically invasive, tear osmolality risks causing discomfort to the individual, due to the proximity with which the hand-held device needs to be placed near the eye. While the collection device is handheld, the method is not portable, being tied down by a benchtop analyser. Bio-impedance spectroscopy can be portable or benchtop, depending on the device, with the latter having a higher accuracy. By using different frequencies, the water content of the intercellular and extracellular space can be examined. These devices are non-invasive and can detect small changes in total body water, but struggle with electrolytes. MRI can be used to detect hydrogen molecules (and therefore water) within the body with a very high sensitivity, allowing for changes to be measured. However, the devices require large amounts of space to operate, are costly to run and maintain and require specialist operators and analysts. Further, whole-body measurements can take up to 1 hour, with small movements causing inaccuracies. There are few locations where MRIs are available, with NaMRI machines (which can analysis Na for further hydration tracking) numbering a handful countrywide. Stable isotope dilution offers a high degree of accurate for tracking an individual's hydration, allowing for both water and salts to be tracked. However, the technique is a poor measure of whole-body hydration, as it requires tissue biopsies, which makes it invasive. Further, the technique is expensive, requiring specialist isotopes and staff to be conducted and has to be planned in advance, due to the isotopes requiring time to diffuse into the tissue. When it comes to hydration monitoring neutron activation analysis is the most accurate method for determining hydration, allowing for the determination of total body water and salt levels. While the technique is non-invasive, it requires the subject to be irradiated, which carries a level of risk. Further, the low number of devices available, along with cost and expertise required, makes this an impractical method of determining hydration.

Table 1.3: Rarely used clinical methods to measure hydration. Accuracy and complexity increase further down the table.

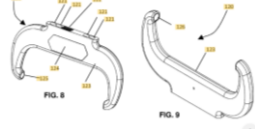



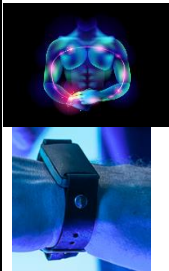
Name	Summary of technology	Advantages	Disadvantages
Saliva osmolality ^{29,30} 	Examining the concentration of salts in a set weight of saliva fluid.	<ul style="list-style-type: none"> - Little training required - Non-invasive 	<ul style="list-style-type: none"> - Weakly linked to hydration, being affected by recently consumed food and water - Medium cost - Benchtop device
Tear osmolality ^{31,32} 	Examining the concentration of salts in a set weight of tear fluid.	<ul style="list-style-type: none"> - Portable handheld device - Quick turnaround time 	<ul style="list-style-type: none"> - Semi-invasive - Weakly linked to hydration - Medium cost - Benchtop analyser
Bio-impedance spectroscopy ^{33,34,35} 	Changes in body composition results in a change in electric impedance of the body which can be measured. Different frequencies measure different components.	<ul style="list-style-type: none"> - Sensitivity to changes in hydration - Non-invasive - Can distinguish between intercellular and extracellular water - Little training required 	<ul style="list-style-type: none"> - Requires a base line measurement - Portability sacrifices accuracy.
MRI / ²³ Na MRI ^{36,37,38,39,40} 	Magnetic resonance imaging allows for the quantification of water and Na in the body. This can allow changes in body water and salt to be measured over multiple readings.	<ul style="list-style-type: none"> - Very accurate - Can inform on salt and water changes - Non-invasive 	<ul style="list-style-type: none"> - Requires a base line measurement - Very costly - Limited number of machines available - Whole body measurements are time consuming - Susceptible to error from movement - Specially trained staff needed
Stable isotope dilution D_2O	The individual consumes a known volume of a non-radioactive isotopes of the substance being measured. By comparing pre and post isotope dilution levels in a known volume, the total substance in a biopsy can be determined.	<ul style="list-style-type: none"> - Very accurate - Can inform on salt and water changes 	<ul style="list-style-type: none"> - Very costly - Time consuming - Delayed response time from start of measurement. - Invasive
Neutron activation analysis 	Radioactively activated individuals are placed into a full body radiation detector, where the gamma ray energy emitted from them is measured. The energy emitted is specific to each element, with the intensity being relative to the quantity of the element.	<ul style="list-style-type: none"> - Very accurate - Can inform on salt and water changes - Non-invasive 	<ul style="list-style-type: none"> - Very costly - Limited number of machines available - Irradiates the subject - Difficult to make measurements over time - Specially trained staff needed - Time consuming



1.4.3 State of the art hydration measurement technologies and products.

From Table 1.2 and Table 1.3, it can be seen that to date, there is no method to accurately measuring hydration in a non-invasive real-time manner for the everyday person. Table 1.4 outlines some of the modern attempts to solve this diagnostics problem. Ultrasound technology is well established as a safe non-invasive method for imaging deep into the body. More recent studies have examined its ability to measure hydration having found that changes in tissue water resulted in a change in ultrasound transmission speed, making it a potential candidate for a new method. The MX3 saliva osmometer aims to streamline saliva hydration monitoring with a handheld non-invasive device. While the technical specifications of the device have yet to be released, the device is likely to suffer from the same poor link to hydration, as current saliva osmolality measurements. Miniaturized NMR relaxometry offers a cheaper, more portable benchtop solution for non-invasively measuring muscle water, compared to that of a typical MRI. While unable to detect salt, this technology has been shown to be able to differentiate between water in the intercellular and extracellular components. Surface impedance has been used to measure skin hydration for decades, however, a new wave of wearables with in-built skin impedance and wrist motion tracking (to detect when you drink) are attempting to determine and individual's hydration. While these devices are non-invasive and wearable, they suffer from comfort complaints, having to be fitted tightly to 'work'. While current gold standard Bio-impedance spectroscopy methods used 4 fixed points of contact, ARUA band aims to perform bio-impedance measurements using only 2 points of contact between the left wrist and the right hand. To date, the technology has been marred with inaccuracy claims and has yet to make it through a clinical study. Infrared technology is well established in the medical setting and is routinely used in pulse oximeters to measure blood oxygen saturation in a non-invasive wearable manner. However, companies (LVL, Sixty) are looking to use NIR to measure hydration. This is due to water having a range of peaks in the NIR region, along with a high absorption value, making small changes noticeable. To date however, no company has succeeded in bringing this technology to market. In recent times dielectric measurements have started to gain traction as a potential method for measuring hydration, thanks to its high sensitivity measuring changes in individual blood components. While broadband dielectric

spectroscopy typically requires a benchtop device, as shown by the success of recent glucose monitor, the technology has the potential to be made non-invasive and wearable by selecting the correct frequencies. Currently however, no dielectric database exists for companies to draw on. Sweat patches (developed by GE, Gatorade and a range of research institutions) look to measure both water and salt expulsion rates in order to determine hydration, despite there being no clear link between sweat rate and hydration status. However, such devices have the benefit of being wearable and non-invasive.

Table 1.4: State of the art portable hydration measurement technologies and products attempting to come to market.

Name	Summary of technology	Advantages	Disadvantages
Ultrasound 	<p>The link between ultrasound velocity and muscle water content has been well explored with increases in muscle water content resulting in a decreased ultrasound velocity⁴¹. This technique proved so successful, the authors of the work were granted multiple patents for the work^{42,43}. To date however, no commercial product has come out of this research.</p>	<ul style="list-style-type: none"> - Non-invasive - Real-time - Sensitive linear response to change in muscle water content - Wearable (leg cuff) 	<ul style="list-style-type: none"> - Only informs on local muscle water content - No product taken to market yet, cost is unknown
Silvia osmolality ^{44,45} 	<p>Measures saliva osmolality using the new "electrochemical test strip" technology.</p>	<ul style="list-style-type: none"> - Non-invasive - Handheld - Measurement within seconds - Cheap 	<ul style="list-style-type: none"> - Not real time - Not wearable - Weak link to hydration, being affected by recently consumed food and water - Not yet commercially available (will be soon)
NMR relaxometry ⁴⁶ 	<p>Measure water content using portable NMR relaxometry.</p>	<ul style="list-style-type: none"> - Non-invasive - Highly sensitive to changes in local muscle water. - Measurement within minutes. 	<ul style="list-style-type: none"> - Small benchtop device - Not real-time - Unknown cost
Surface Impedance 	<p>While handheld surface impedance devices used to measure skin hydration have been around for a while, a new wave of wrist mounted watches claiming to be able to measure hydration using the technology have started to emerge. Requires being very tightly fitted to an individual's skin. Uses skin impedance to determine an individual's hydration.</p>	<ul style="list-style-type: none"> - Non-invasive - Real-time - Wearable - Low cost 	<ul style="list-style-type: none"> - Low accuracy for measuring hydration - Likely to only be measuring skin hydration. - Require an uncomfortably tight fit to work.
Bio-impedance spectroscopy 	<p>Bio-impedance is typically used to measure body composition measured using four points of contact method (one on each wrist and ankle). Recently a company has tried to measure hydration using 2 points of contact (left wrist and right fingers) impedance technique, however it has been plagued with inaccuracy claims.</p>	<ul style="list-style-type: none"> - Non-invasive - Effectively real-time - Wearable - Low cost 	<ul style="list-style-type: none"> - Unproven accuracy for measuring hydration, with developers looking at software patch problems.

Name	Summary of technology	Advantages	Disadvantages
<p>Infrared^{47,48}</p> 	<p>Despite numerous companies (BSK athletic – Ivi, Sixty – Sixty, and Halo Wearables - Halo H1) developing devices to measure hydration using a wrist mounted red or IR LED system, there is little to no evidence in the literature showing that such a thing is possible for hydration measurements. The author believes the main draw (while misguided), comes from water having a range of high absorption peaks around 0.5-3 μm, which could be used to measure changes in water content using powerful enough devices which are not wrist mountable^{49,50}.</p>	<ul style="list-style-type: none"> - Non-invasive - Real-time - Wearable - Low cost 	<ul style="list-style-type: none"> - No proven link to hydration (Likely to only provide information of water content, as salt levels are hard to detect using IR at low concentrations without high energy sources)
<p>Dielectric measurements</p>	<p>Dielectric spectroscopy techniques (Microwave) have been shown to be able to detect changes in hydration in a range of different tissues^{51,52,53,54,55}, with changes in the real and imaginary permittivity being correlated to changes in tissues weight. More recently, this technique has shown promise for correlating to blood hydration, having been shown to be highly sensitive to changes in 3 key blood hydration markers: salt⁵⁶, %HCT^{57,58,59} and protein^{60,61} content.</p>	<ul style="list-style-type: none"> - Has been shown to accurately measure changes in protein, salt and %HCT (water to RBC ratio). - Effectively real time - Can be wearable 	<ul style="list-style-type: none"> - Expensive - Can be invasive and non-wearable
<p>Sweat Patch^{62,63,64}</p> 	<p>While there has been shown to be no link between sweat composition and hydration, a lot of research has been put into sweat patch hydration monitors for use in sports and the military (by the likes of GE, Gatorade, and multiply research institutions). These contain chemical and electric sensors which can measure the composition of a localised region of sweat via chemical reactions, but typically needs an external device to read the data from the patch.</p>	<ul style="list-style-type: none"> - Non-invasive - Real-time - Wearable - Low cost per patch - Informs on water and salt 	<ul style="list-style-type: none"> - No proven link to hydration, with salt expulsion depending on diet - only informs on localised hydration

Chapter 2

Technology selection and microwave
permittivity theory

2.1 Blood dielectric technology for measuring changes in hydration levels

This section covers the selection process for the most suitable biological measurands and technology for measuring hydration.

2.1.1 Why blood dielectrics measurements were pursued for hydration detection

Biological measurement and selection

When it comes to measuring hydration, there are a range of biological measurands which have been correlated to hydration and measured noninvasively including: weight, urine, tears, saliva, muscle, skin, and blood. However, not all of them are reliable markers for hydration, and only one could be taken forward.

Weight was ruled out as a marker due to this highly variable nature, being affected by more than just body hydration, including the consumption of food and bowel movements. Further, it could not be measured accurately using a portable device. Urine was ruled out as a marker, as the measurement frequency is dependent on urination, and has a poor relation to hydration, due to the infrequency with which human urinate. Tears were ruled out as a marker, due to their poor link to hydration, with the body dehydrating significantly before seeing drops in tear osmolality. Further, not everyone is comfortable with putting objects in / near their eye. Saliva was ruled out as a marker, as its content is not solely dependent on hydration, with food and drink affecting its composition. While muscle looked like a good candidate, being really accessible and changing composition relative to hydration⁴¹, it was not selected due to the potential of localised hydration variations risking misinforming on the hydration of the whole individual. Skin was deselected for a similar reason, while also suffering from being heavily affected by the humidity of the local environment⁶⁵.

This left blood to be examined. While it is not as accessible as muscle or skin, existing medical devices like pulseoximeters⁶⁶ (measuring blood oxygen saturation) and glucose monitors^{67,68} (blood glucose) have shown it is possible to measure blood properties non-invasively using small wearable devices. Another reason to focus on blood relates to our comprehensive understanding of its

behaviour during changes in hydration status, which is severely lacking for other tissues. Further, this tissue is already the biological measurand of choice for the clinical gold standard hydration test, osmolality. This, along with its unquestionable direct link to hydration (having the body's own thirst response being dependent on blood osmolality and volume) makes it the ideal biological measurands to use.

Technology selection

Having identified blood as the optimal biological measurand to measure hydration, the technology to be used needed to be selected. From the literature review in Table 1.2 and Table 1.3 above, the following technologies were identified as an option: MRI, NMR, NIR, bio-impedance, ultrasound, dielectrics. MRI measurements techniques were not taken forward for a range of reasons, while they offer a highly accurate way to measure both the water and sodium levels within a human, the devices were not portable, being room-sized. Further, the limited number of NaMRI available would hamper research efforts. In recent years the size of NMR technology has been shrunk to the size of small benchtop devices⁴⁶. While small, such devices are still not wearable, and likely never could be. This coupled with their limited resolution, inability to inform on salt needs and cost, make NMR an unsuitable technology to take forward. NIR was not selected to be taken forward due to the uncertainties over its ability to measure hydration. While lots of start-ups are claiming to be developing NIR technology in their wearables to measure hydration due to high absorption of water in this region^{69,70}, no device has yet to display capabilities in measuring blood water levels. Further, as this technology has no sensitivity to salt levels, it would only provide limited information on hydration. In the last 20 years, bio-impedance technologies have come a long way, allowing for the differentiation between water and salt⁷¹ stored in the intracellular and extracellular spaces using different frequencies. However, while this technology can be small and accurate, attempts to make it wearable have been met with inaccuracies⁷², making it unsuitable to take further. Ultrasound has been shown to be sensitive to changes in muscle water content, giving it the potential to measure the hydration⁴¹. However, as a non-invasive wearable ultrasound hydration monitor has been patented⁴³, it would not be

commercially viable to work on the technology. Further, there is no evidence to suggest it can detect changes in salt levels or be adjusted to work with blood.

The final technology to be examined is dielectrics. Studies have already shown that dielectrics are not just sensitive to water and salt concentrations, but also blood %HCT and blood proteins⁶⁰. As such, this technology has the potential to give more blood parameters than the current gold standard. However, for dielectric spectroscopy results to be traceable, they typically required chunky benchtop VNAs to make measurements. This data can however inform the creation of single or multi-frequency wearable patch/resonator devices which could lead to an informative wearable hydration monitor. As there is already a solid foundation for this technology, and an understanding of how blood components affect measurements, the author believes dielectric technologies offer the best opportunity for measuring the hydration of blood, and by extension, humans.

2.1.2 Challenges with measuring blood dielectrics

Within the literature (and explained below in section 2.2) a basic understanding exists describing how blood components affect the dielectric properties of blood. There are however some issues which need to be addressed over the course of this thesis in order to move towards the development of a wearable hydration monitor.

While stated as a strength above, being able to measure more than just water and salt also poses a problem. This is because the effect of any one variable could be drowned out by another. Determining how each of the variables overlap and interact is a vital step in assessing the viability of this technology. Such data would then be needed to inform decisions surrounding which frequency or frequencies, are needed to best measure hydration. Finally, a non-invasive wearable device would need to be made (potentially taking the form of a patch antenna or resonator), which could measure the dielectric of the blood through the skin.

2.2 Dielectric measurements theory

Having determined that measuring blood dielectric offers the best chances to improving hydration monitoring, this section will now give the reader a brief introduction of the science underpinning the technology, with an emphasis on water and blood constituents. Dielectric theory with a specific focus on blood has previously been covered in detail in other's theses^{73,61}.

2.2.1 Microwave dielectric theory

Polarisation mechanisms of materials in electric fields

A material is considered to be a dielectric if it is an insulator which can be readily polarised opposing the applied electric field it is placed under, typically because the material in question contains some form of charge or dipole. The degree to which the material is polarised is dictated by the composition and structure of the material and ultimately determines the materials permittivity, ϵ . While it is common to express permittivity relative to free space, ϵ_0 , to get the relative permittivity, ϵ_r , this is not always necessary.

$$\epsilon_r = \frac{\epsilon}{\epsilon_0} \quad \text{Equation 1}$$

When an electric field, E , is applied to a material, it leads to the material becoming polarised, causing the separation of charge within the material, resulting in the formation of an electric dipole moment, p . The total sum of all the electric dipole moments within a set unit volume of material determines the materials polarisation, P . The polarisation of a material causes a decrease in the electric field strength occurring within the material, resulting in the generation of a displacement field, D , which is proportional to both the strength of the applied electric field and the materials permittivity.

$$D = \epsilon_0 E + P = \epsilon E \quad \text{Equation 2}$$

When placed in an electric field, there are typically four types of polarisation mechanisms a dielectric material can undergo (see Figure 2.1), these are: Electronic, Ionic, Orientational and Interfacial.

Electronic polarisation occurs when a dipole moment is generated by the electron cloud of a neutral atom moves toward the source of the applied electric field, while the positive nucleus moves in the direction of the field. Ionic polarisation is caused when positive and negative ions of an ionic lattice are displaced, with the positive ions moving in the direction of the field, while the negative ions move opposing the field. This movement results in electronic dipole movement within the ionic structure. Orientational polarisation occurs when free-moving polar molecules within liquids and gases (which typically cancel each other out over a large enough area), align parallel to the field, leading to the overall polarisation of the material. Interfacial polarisation is where the free charges in the material are able to move within the confinement of the boundaries of the material, with positive charges moving in the direction of the field, while negative charges move opposing the field.

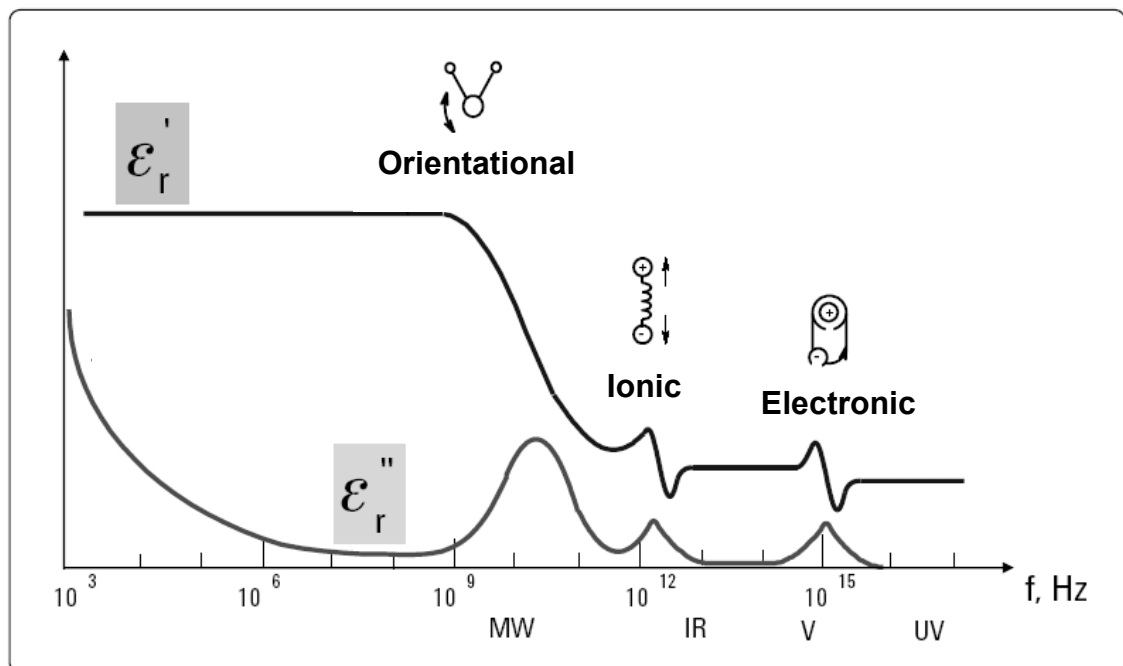


Figure 2.1: The polarisation mechanism dielectric materials can undergo⁷⁴.

Complex Permittivity

When the material is removed from the electric field, the energy used to create the polarisation is re-emitted, with the material returning to its equilibrium state as the polarisation dissipates. As a result, dipolar materials can be thought of as an energy store. However, as the application of the electric field induces the moment of charged particles, some of this stored energy is lost in the form of heat. The energy is lost as heat for a range of reasons including collisions between particles, the breaking of intermolecular bonds or the overcoming of electrostatic interactions. To accurately represent both the energy stored, and the energy lost during polarisation, the permittivity is represented as a complex term:

$$\epsilon = \epsilon' - i\epsilon'' \quad \text{Equation 3}$$

Where, ϵ' , is the real permittivity (a.k.a. dielectric constant) of the material and is a lossless measure of the energy stored in the material. ϵ'' , is the out-of-phase imaginary permittivity (a.k.a. loss factor) of the material and represents the energy lost and i , is the imaginary number $\sqrt{-1}$. The losses of the system can be reported in the form of a loss tangent (see Figure 2.2), $\tan\delta$, which is the ratio of the real and imaginary permittivity:

$$\tan\delta = \frac{\epsilon''}{\epsilon'} \quad \text{Equation 4}$$

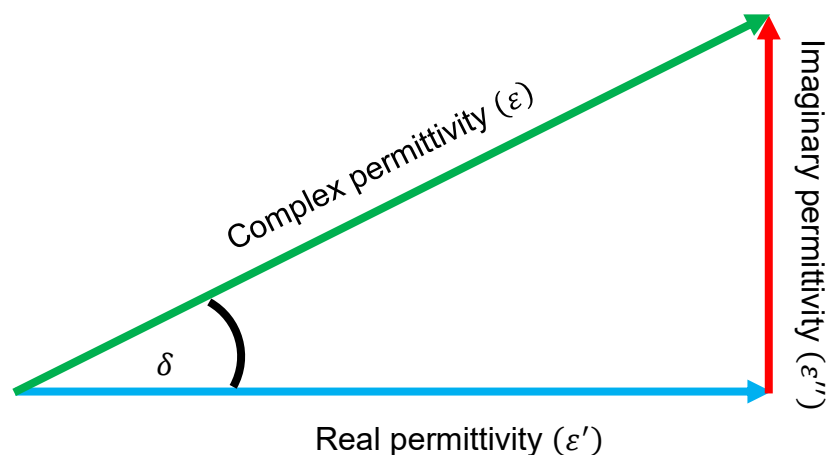


Figure 2.2: The relation between the complex permittivity, real permittivity, imaginary permittivity and the loss tangent.

Frequency dependence

Up until now, the complex permittivity of a material has only been examined with respect to a static electric field. However, when a material is subjected to a time-varying microwave signal, the same polarisation mechanisms occur, but the dielectric behaviour of the material is instead dependent on the (angular) frequency (ω) of the applied oscillating electric field. Equations 1, 2 and 4 can therefore be better generalised as:

$$\epsilon_r(\omega) = \frac{\epsilon(\omega)}{\epsilon_0} \quad \text{Equation 5}$$

$$\epsilon(\omega) = \epsilon'(\omega) - i\epsilon''(\omega) \quad \text{Equation 6}$$

$$\tan\delta = \frac{\epsilon''(\omega)}{\epsilon'(\omega)} \quad \text{Equation 7}$$

This frequency-dependent property comes about due to a property known as time constant of relaxation, τ . When a material is exposed to an electric field, the material does not align instantaneously with the field, having to overcome its viscosity (due to being a non-ideal fluid) as well as any bonds present between molecules. The time constant of relaxation therefore refers to the time taken for the material to align with the field and is dependent on the polarisation mechanism as well as the materials properties.

As a result of this delay in alignment, the power from the oscillating applied electric field and the resulting displacement field generated in the material become out of phase by an amount equal to the time constant of relaxation, with the displacement field being dragged back down by the oscillating applied electric field, before it has had time to reach an equivalent maximum as seen in Figure 2.3. It is this relationship between the frequency and the time constant which ultimately affects the strength of the displacement field generated, and therefore the materials measured permittivity.

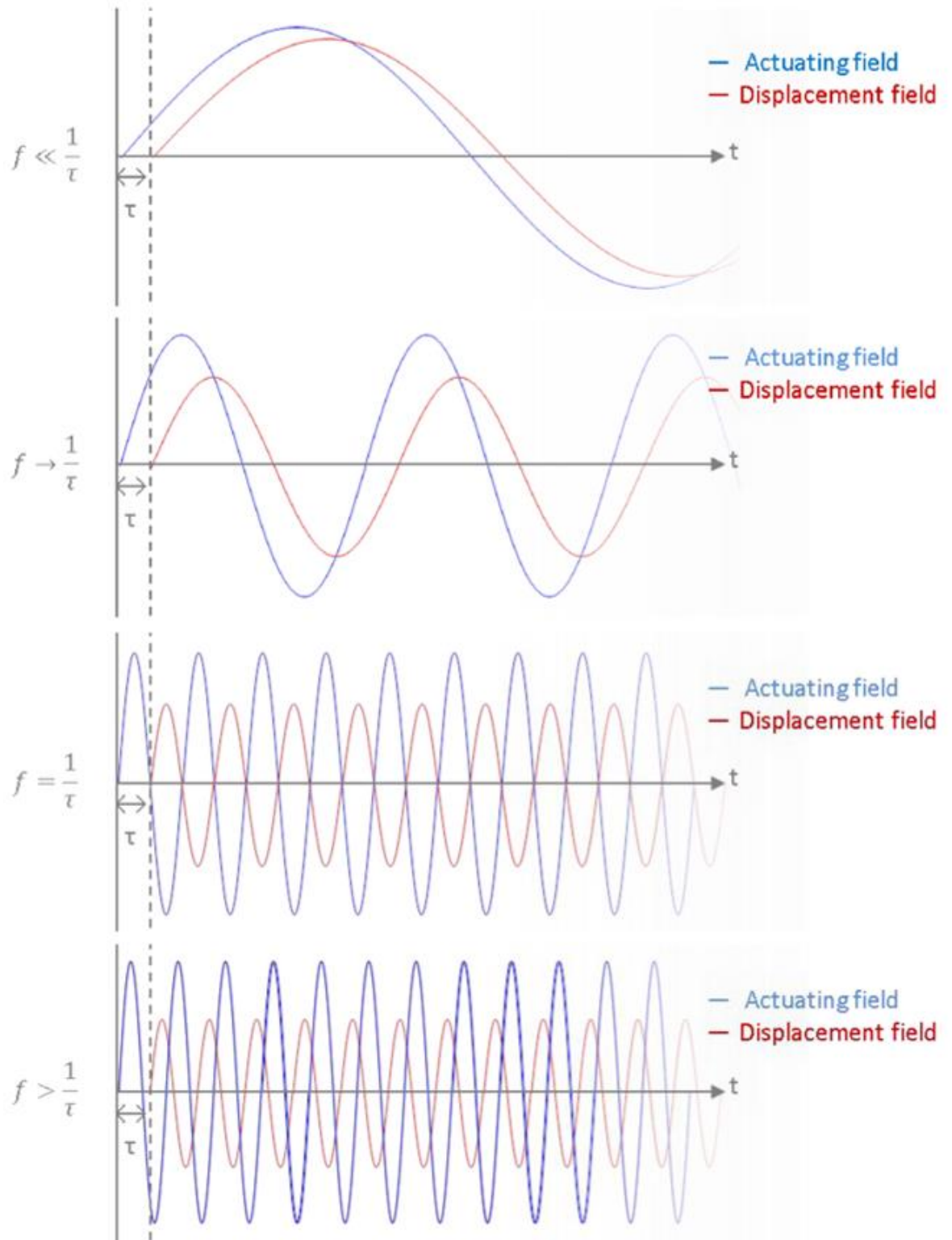


Figure 2.3: The relation between frequency and the time constant of relaxation on the strength of the displacement field⁷³.

2.2.2 The effect of blood components on dielectric measurement of water

On Earth, water is the key component to life, acting as the main biological solvent within nearly all organisms. Because of this, it is important to understand what made water such an important fluid, the sources of its dielectric properties and its dielectric response to changes in its environment.

Waters composition and interactions

Water molecules are simple in their composition, being made up of two hydrogen atoms covalently bonded to a single oxygen atom as seen in Figure 2.4.A. Due to water being a small molecule, the remaining unbound negatively charged electron pairs from the oxygen atom try to repel each other, resulting in a 104.5° angle being formed between the hydrogen atoms, rather than the expected 180° . This bend in the water molecule leads to water becoming a dipolar molecule, with a positive dipole (δ^+) being present around the hydrogen atoms, while a negative dipole (δ^-) exists at the other end around the oxygen atom as seen in Figure 2.5.

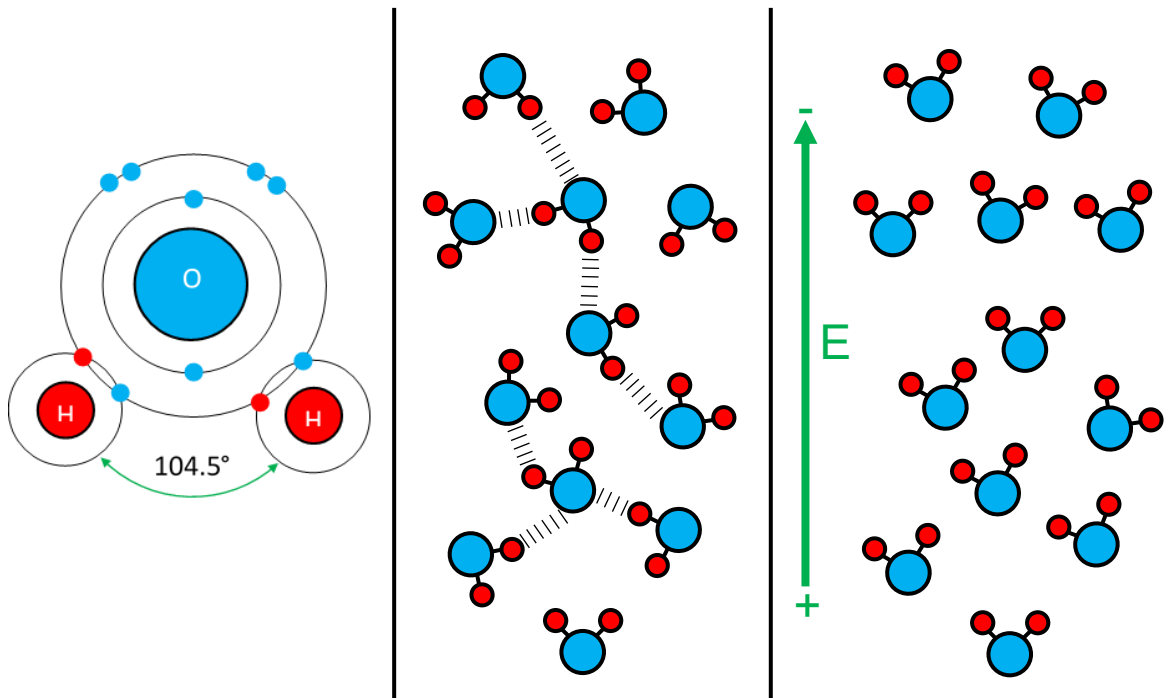


Figure 2.4: A) The electron covalent bonds of a water molecule. B) The H-bonds in water when not under the effects of an electric field. Note the orientation is random, and results in no net charge. C) The water molecules aligning with the orientation of an applied electric field.

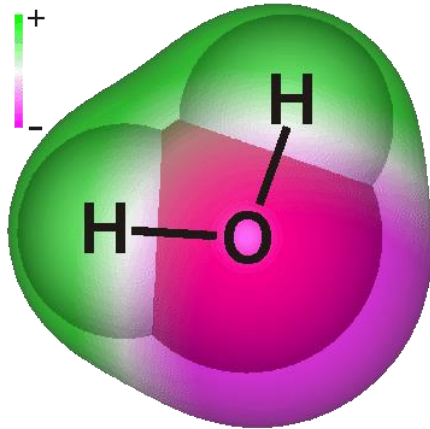
This in turn leads to water possessing a range of unique properties when interacting with other water molecules in a solution. Due to the dipolar nature of water molecules, electrostatic forces (namely H-bonds) between the negative dipole on an oxygen atom, and the positive dipole on a neighbouring hydrogen atoms are formed (Figure 2.4.B). These H-bonds act as a store of energy within the solution, requiring energy to be made, and releasing energy when broken. It is the ease with which water molecules can form electrostatic forces with other molecules, along with its small size (being able to reach and interact with areas on a solute larger solvent molecules would be unable to reach), which gives water its exceptional solvent properties when dissolving other chemicals.

Waters' dielectric properties

At microwave frequencies, it is this orientational polarisation which dominates the dielectric response of water. When water molecules are not under the effects of an electric field, they align themselves randomly (Figure 2.4.B), and over a large enough sample, with a net neutral charge, despite each molecule having a dipole in its own right. However, when water molecules are placed in an applied electric field, the water molecules on average, align themselves with the electric field (Figure 2.4.C), with a time constant of relaxation of ~ 8 ps at room temperature⁷⁵.

Bound and unbound water

With water being a small, highly polar molecule (Figure 2.5), it interacts strongly with charged molecules like electrolytes, which can affect how it interacts with



applied electric fields. When water is not surrounded by charged particles, it is said to be unbound water and behaves accordingly. However, when a charged particle is present, a thin film of immovable water molecules surrounds the charged particle⁷⁶. As such, when placed in an applied electric field, bound water is unable to move and partake in the polarisation response.

Figure 2.5: The dipole nature of water molecules, with a positive dipole ($\delta+$) surrounding the hydrogen atoms, and a negative dipole ($\delta-$) surrounding the oxygen atom¹⁴.

Effect of temperature, time constant and viscosity on waters' permittivity

Changes in kinetic energy at an atomic level result in and are measured as, changes in temperature. It is the changes occurring at the atomic level, which ultimately control the changes seen in the materials properties as the temperature increases.

At higher temperatures, water molecules have a higher kinetic energy. As a result, the water molecules are able to deviate more from the alignment of the applied electric field. Because of this, less polarisation of the molecules occurs, meaning less energy is stored to be re-emitted when the field is removed and the sample relaxes, resulting in the dielectric constant decreasing with the increase in temperature. Further, as higher temperatures allow water molecules to resist alignment with the applied electric fields, fewer electrostatic H-bonds between water molecules are broken. As less unrecoverable energy is lost breaking bonds, it results in a reduction in the loss factor as seen in Figure 2.6.

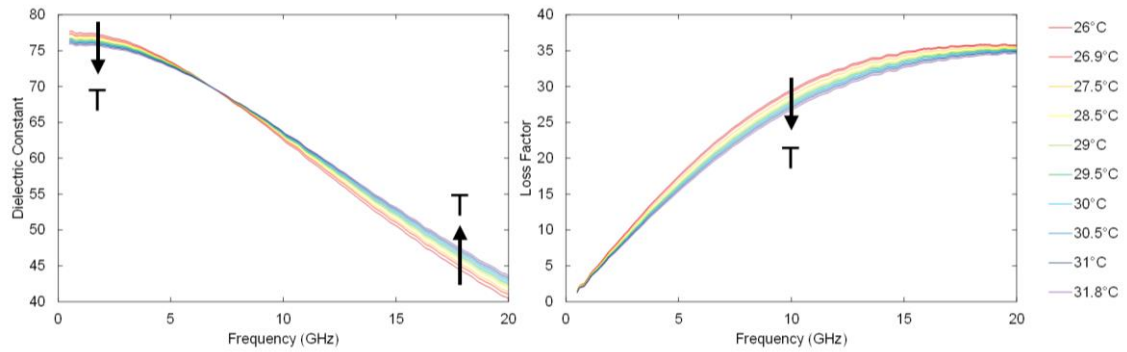


Figure 2.6: The effect of temperature on the dielectric properties of water.

The response of the dielectric constant of water with respect to temperature is, however, further complicated due to the dielectric constant being dependent on the time constant, which is in turn dependent on both temperature directly as well as the temperature-dependent viscosity.

At higher temperatures, water molecules possess more kinetic energy. As a result, within a sample of water, there are fewer hydrogen bonds present at a given time as they are easier to overcome. Because of this, the water molecules are able to align quicker with an external applied electric field, resulting in a reduced time constant. This bond-based temperature dependence of the time constant can be seen explained using the temperature-dependent Gibbs energy of activation of reorientation equation:

$$\tau = \frac{h}{k_b T} e^{\frac{\Delta G}{RT}} \quad \text{Equation 8}$$

Where h is Planck's constant ($6.63 \times 10^{-34} \frac{\text{m}^2 \text{kg}}{\text{s}}$), k_b is the Boltzmann's constant ($1.38 \times 10^{-23} \frac{\text{J}}{\text{K}}$), R is the gas constant ($8.31 \frac{\text{J}}{\text{K mol}}$), ΔG is Gibbs free energy and T is the temperature⁷⁷. As well as explaining the decrease in the relaxation time of the sample, it also helps explain why the relaxation of water shifts to higher frequencies with increased temperatures.

The time constant of relaxation for water is also dependent on temperature due to viscosity. At higher temperatures the viscosity of water decreases, which results in a decrease in the resistive forces acting on the rotating molecule, reducing the time taken for the molecule to align with the external applied electric

field, and therefore the time constant. The effect of viscosity on the electric field can be described using:

$$\tau = \frac{\pi\eta(T)r^3}{k_bT} \quad \text{Equation 9}$$

Where r is the effective radius of the molecule and η is the viscosity of the fluid. Where the temperature-dependent viscosity can be examined using:

$$\eta(\tau) = \eta_0 e^{\left(\frac{E_\eta}{K_bT}\right)} \quad \text{Equation 10}$$

Where, E_η , is the system activation energy. This high dependence on temperature sees the relaxation of water vary significantly from ~17 ps at 0.2°C to ~7 ps at 35°C.

Effect of ions / electrolytes on waters' permittivity

With electrolytes being ions, when placed in an applied electric field, they are given kinetic energy and react by moving themselves towards the source of their opposing charge. As the ions move through the fluid they are suspended in, they collide with other molecules, dissipating some of their kinetic energy as heat. As there is no restorative force present, these ions do not re-emit this energy, contributing significantly toward the loss of the system. As a result, increased concentrations of ions in water result in an increase in the imaginary permittivity. The contribution of ions to the loss is, however, very frequency-dependent, dropping at the rate of 1/frequency in the microwave region. At lower frequencies, ions are induced to travel further, resulting in more collisions and therefore a larger loss. However, at high frequencies, the ions do not have enough time to move before the applied electric field flips, resulting in less movement and a lower loss. The contributions of ions to the imaginary permittivity is described by the conductivity term seen in $Conductivity = \frac{i\sigma}{\omega\epsilon_0}$ Equation

11, where σ is the ionic conductivity of the ion present. At biological concentrations, ions no longer have a significant effect on the loss over 10 GHz, becoming negligible around 20 GHz⁶⁰ as seen in Figure 2.7.

$$\text{Conductivity} = \frac{i\sigma}{\omega\epsilon_0} \quad \text{Equation 11}$$

For the real permittivity, increases in ion concentration cause a small decrease in the permittivity. This small decrease is due to the ions (which possess a lower permittivity than water) occupying more of the volume which had been occupied by high permittivity water, resulting in the overall reduction in the permittivity. The ions further contribute to the decrease in the permittivity, as they surround themselves with bound water, which does not react readily with an applied electric field.

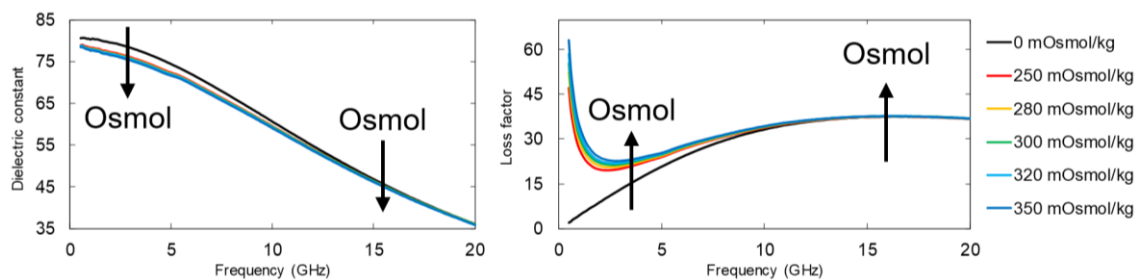


Figure 2.7: The effect of physiological osmolality on the dielectric properties of water.

The effect of ions on water is also temperature-sensitive in several ways and is dependent on the hydrated ion radius, which is unique to each ion. At higher temperatures, the increased motion present in water molecules results in the disruption of the ion solvation shells, resulting in a reduction in the ions hydration radius. With less bound water around the molecule, the ions can move more readily through the solvent, resulting in an increase in the loss. The higher temperatures also reduce the viscosity of the water, making it easier for the ions to move within the solution, increasing conductivity. This increase causes higher losses to occur at lower frequencies.

Effect of proteins on waters' permittivity

Blood is a protein-rich fluid where the concentration of proteins present changes significantly with changes in hydration¹⁹. Proteins carry out a wide variety of important roles within the body, including DNA replication, transportation of smaller molecules, hormone control and digestion. Blood contains upwards of 8g/dl of protein, so the effects of it changing concentration need to be understood.

In terms of structure, proteins are large, complex, organic molecules, made up of lots of amino acid chains bound together in up to 4 levels of hierarchical structure. The primary structure is made of a single amino acid chain and becomes one of two secondary structures, either α -helix or a β -sheet due to the formation of hydrogen bonds between atoms on the peptide backbone. The tertiary structure is formed when multiple α -helix's and β -sheet's come together due to hydrophobic interactions, before being held together by hydrogen bonds, salt bridges and disulfide bonds. The quaternary structure is made up of 2 or more tertiary structure elements, held together using the same interactions present at the tertiary structure. As a result of their large, flexible, less-polar structure, proteins have a low permittivity (typically less than 10) at high frequencies⁷⁸.

In terms of proteins effect on the permittivity of water, increasing the concentration of protein results in a drop in both the real and imaginary permittivity as seen in Figure 2.8. This decrease is proportional to the volume fraction of water being displaced and is due to proteins having a significantly lower permittivity due to the reasons described above. Further, due to the outer edge of proteins being hydrophilic, containing some polar groups, a layer of bound water forms a hydration shell around the molecule, further reducing the permittivity. Finally, increasing the concentrations of protein in the water causes an increase in its viscosity. This causes the spectra to shift and relax at lower frequencies.

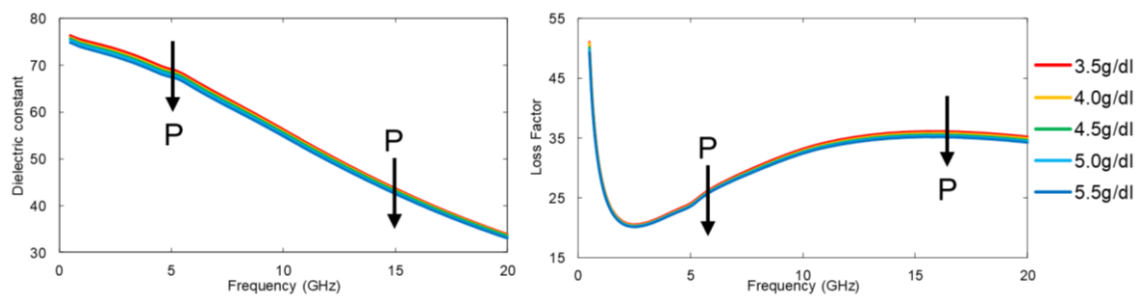


Figure 2.8: The effect of increased protein (albumin) concentration on the dielectric properties of osmotic water.

Effect of RBCs on waters' permittivity

Within the blood, RBCs make up a major portion of its composition, on average making up 45% of its overall volume. As RBCs are unable to leave the cardiovascular system (unless a trauma occurs), unlike plasma, as an individual dehydrates, its volume fraction within the blood increases, as the amount of plasma decreases.

RBCs are specialist oxygen-carrying cells with a biconcave disc shape. Like all animal cells, the cell membrane is made from a phospholipid bilayer, containing ions channels to allow ions to move in and out of the cell, as well as containing a range of surface antigens. The phospholipid membrane is free-flowing and is held together by hydrophobic interactions stemming from the hydrophilic tails present on the lipid molecules. Unlike most other cells, the RBCs interior has no nucleus, with the majority of the space being packed with the iron-rich oxygen-binding protein, haemoglobin. The interior of the cell also contains water like all other cells, albeit, at a low rate of 65%⁷⁹.

When the concentration of RBCs is increased in a solution of saline water, both the real and imaginary permittivity measured fall as seen in Figure 2.9. This is due to the low permittivity of haemoglobin (around $10^{78,80}$) relative to water, along with its high prevalence within the RBC. However, unlike other cells, RBCs do not exhibit α -depression⁸¹. While the reason for this is unknown, it is speculated that this is due to: the reduced number of ion channels, the fact that the cell has no strong charges present on its membrane, its biconcave shape or, that the effect is just drowned out.

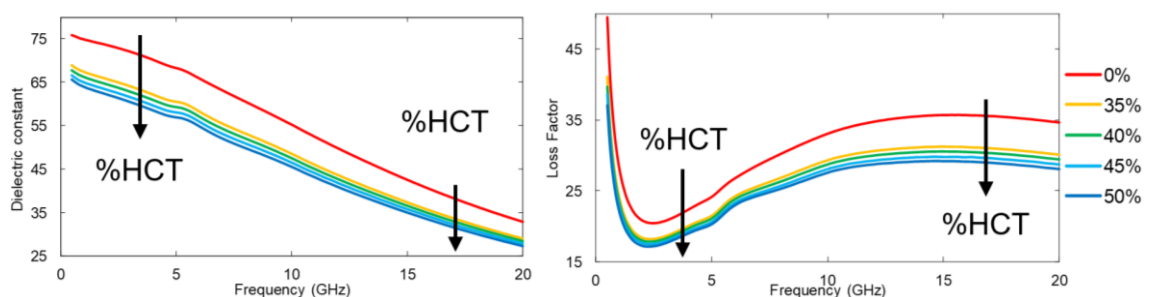


Figure 2.9: The effect of increased RBCs on the dielectric properties of osmotic water.

Effect of other blood components on waters' permittivity

So far, the effects of varying salts, proteins and RBC'S on the permittivity of water has been examined. In total, these constituents make up ~99% of blood's volume, with the remainder being comprised of WBCs and the blood clotting components. While these remaining blood components would have a small impact on the permittivity measured, their effect has been shown to be negligible⁶⁰. Further, while these blood constituent's volume fraction increases during dehydration, the increase is negligible due to their initial low composition rate in blood and would be dwarfed when compared to changes in %HCT, osmolality and protein. As a result, these components can be thought of as adding a small fix constant to the permittivity of blood, and as such, they will not be discussed or examined further, due to them not changing significantly during changes in hydration.

2.3 Thesis overview, Aims and Objectives

Overall, while the true financial cost of hydration can only be guessed at, the effect of dehydration on an individual's health is well understood, ranging from small drops in physical and mental performance, to death. As such monitoring hydration effectively is vital. Unfortunately, current gold standard tests are slow and invasive, resulting in their use being limited.

The body's hydration state is in constant fluctuation, with localised hydration changes being averaged out against the blood, which is constantly being rebalanced by the hypothalamic-renal feedback systems. As such, it was determined any new hydration monitor should measure blood hydration to accurately measure hydration status.

There are currently a range of different technologies being developed for use as an easy to use non-invasive hydration monitor. However, only dielectrics was found to be sensitive to changes in osmolality, %HCT and blood protein levels, making it the optimal technology to take forward for further analysis. As such, following further investigation, it was determined that the microwave region offered the best opportunity for hydration measurements, with the loss factor being highly sensitive to osmolality, while the dielectric constant could measure %HCT and albumin levels.

Aims and objectives

Aim 1: To test the ability of a commercially available 9.5 mm dielectric probe to measure the broadband microwave complex permittivity of microliter fluid droplets and analyse its performance.

Hypothesis: The inverted dielectric setup could be used to measure the permittivity of microliter fluid droplets while only introducing minor errors.

Objectives: We examined the systems repeatability and calibration error using a 0.1M NaCl solution. The accuracy was determined by comparing results from the inverted setup with a normal dielectric setup. Time and volume dependence were examined using a solution of pure water.

Project outcome: The system was found to be suitable for measuring the complex permittivity of microliter solutions with the introduction of small errors. These errors were deemed to be insignificant for the tasks being performed using the inverted setup.

Aim 2: Determine whether the complex permittivity of whole human blood changed when athletes dehydrate during strenuous exercise.

Hypothesis: Exercise-induced dehydration will result in a change in the complex permittivity of whole human blood.

Objectives: The complex permittivity of whole blood were collected from athletes at time = 0,40 and 80 min and the complex permittivity was measured using the inverted dielectric setup. All athletes were dehydrated by cycling at 15/20 on the Borg's SPI in a 35°C 40% humidity environment with no fluid consumption allowed.

Project outcome: Exercise-induced dehydration was found to cause measurable changes in the complex permittivity of whole blood.

Aim 3: We developed a dielectric measurement technique that could potentially determine hydration levels in blood.

Hypothesis: The microwave dielectric properties of blood were dependent on HCT and albumin concentrations and the osmolality of the solution.

Objectives: The present study examined the effects of physiological osmotic solutions with NaCl (280 mOsmol/kg to 300 mOsmol/kg), HCT (35% to 50%) and albumin (3.5 g/dl to 5.5 g/dl) isolated from bovine blood on the dielectric properties measured at frequencies spanning from 0.5 GHz to 20 GHz using an open-ended coaxial probe.

Project outcome: The dielectric measurement technique has the potential to determine hydration levels in blood solutions with varying composition.

Chapter 3

Characterisation of the inverted dielectric probe setup

3.1 Introduction

When measuring the broadband dielectric properties of a fluid, large volumes of sample are typically used, as the fields generated by the probe theoretically spread out to infinity in all directions, with the field strength decaying at a rate of $\frac{1}{r^2}$ ⁸². Typically, this means that a 9.5mm probe should be surrounded by at least a 6 cm³ block of fluid to prevent the generation of serious inaccuracies. However, obtaining such a quantity of sample is not always possible. To make 6 repeat measurements of blood at 3 hydration levels would require an individual to donate 648ml (~1.1 pint) of blood while undergoing a gruelling exercise regime. As such a new approach was needed to allow for the broadband measurements of small samples. Resonators have exceptional sensitivities for measuring the dielectric properties of small samples, however, they are very frequency specific⁸³, making them uneconomical for broadband applications. Instead, the author proposed using a commercially available 9.5mm broadband dielectric probe in an inverted setup, such that microliter samples could be measured. This chapter will firstly go over how the probe is operated in its normal specified setup, before moving on to characterising the inverted setup and methods used, before finally characterising the behaviour and errors of the system.

3.2 Normal dielectric probe setup and measurements

This section will outline the setup and measurement methods used for a typical dielectric measurement setup where the sample size exceeds the electric field range of the probe.

3.2.1 Experimental setup

Dielectric measurements were made using a VNA (Rohde and Schwarz ZVB-20 vector network analyser) which was attached to a 9.5mm diameter open-ended coax dielectric probe (Keysight 855070E series⁸⁴) via a coaxial cable (HP 85132E). The VNA was connected to a controlling laptop via a National Instrument HS+ GPIB to USB cable. The system was calibrated using the proprietary Tkcal (NPL) software which uses a least-squares calibration method, while data was recorded using the proprietary Tkdsen (NPL) software which used full-wave modal analysis⁸⁵. Both software's operated on the assumption that the sample was large enough such that fringe effects were avoided (which may not always have been the case). The dielectric probe was held in a downwards position using a clamp stand, with a Pyrex glass beaker containing the sample resting on a scissor stand. The setup can be seen in explained in Figure 3.1.

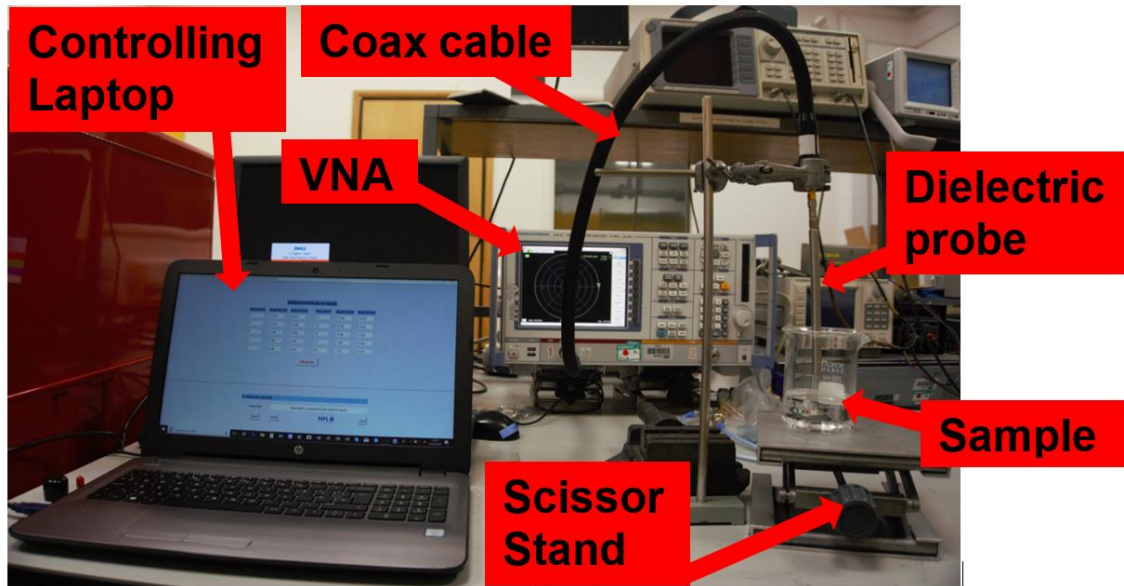


Figure 3.1: Normal Dielectric setup used for large fluid volumes.

3.2.2 Calibration and measurement method

Calibration

The system was calibrated using 3 standards: air, short and pure water. Once the system was set up, the VNA was set to measure between 0.5-20 GHz at Interval 0.1 GHz. Once the VNA had warmed up and all materials had reached room temperature (typically achieved by leaving samples exposed to the air for 30 minutes), an air temperature measurement was taken using a digital thermometer, which was inputted into the Tkcal calibration software. To begin the calibration, three short measurements were performed by placing a polished piece of copper onto the tip of the probe, such that the outer and inner conductors were bridged. Next, one air measurement was taken by leaving the probe clean and exposed to air. Finally, one pure water measurement was taken by filling a Pyrex beaker with the solution and raising it to the probe using a scissor stand, such that 2 cm of the tip of the probe was submerged. When using a transparent fluid, a check was made prior to the measurement to ensure no air bubbles were

trapped on the tip of the probe, which could have skewed the measurement due to the relatively low dielectric value of air. If bubbles were present, the Pyrex beaker was lowered, and the probe cleaned carefully using blue tissue (such that no residue was present, and the probe was not moved), before the steps above were repeated. The Tkcal software then completed the calibration. Next, the Tkdsen (NPL) software was opened, and a sample of DMSO was measured and compared against the currently accepted values to ensure the calibration was within an acceptable range (± 0.1 of the UKAS accepted value for the temperature measured between 1-19 GHz at 2 GHz intervals). If this was not the case, the calibration process was repeated.

Measurement

Once the dielectric system had been calibrated, the Tkdsen (NPL) software was opened. A clean Pyrex beaker was obtained, and the solution being tested poured into it. The Pyrex beaker was then brought up to the probe tip using a scissor stand such that 2 cm of the probe was submerged. A permittivity measurement of the sample was then taken between 0.5-20.0 GHz at 0.1 GHz intervals. The sample was then lowered, and the probe cleaned ready for the next measurement.

3.3 Microliter inverted dielectric probe design, setup, measurement and characterisation

When measuring the dielectric properties of blood, there are 2 key challenges from a measurement perspective. The first of these is that it is not always possible to get enough blood to surround most of the electric field generated by the probe. Secondly, as blood is opaque, it is not possible to tell if air bubbles have been introduced during the setup phase, and are therefore present during the measurement, which could degrade the scientific significance of the data. To get around some of these problems, the author proposed using the dielectric probe in an inverted position. This section aims to give the reader an understanding of how the system worked, as well as describe its characteristic behaviours.

3.3.1 Experimental setup

The inverted dielectric setup uses a similar setup as described in section 3.3.1 above, this included the same proprietary software. The key differences are that instead of being held pointing downward with a clamp stand, the dielectric probe was instead held in a fixed upwards position using a specially built frame. Secondly, rather than using a scissor stand to move a Pyrex beaker up to the probe, the sample was moved from the Pyrex beaker on and off the tip of the probe using a 200 μ l pipette (pipette4u – AHN Biotechnologie). The setup can be seen in Figure 3.2. To prevent damage to the probe from falling fluid, electrical joints were waterproofed with a layer of clingfilm followed by Sellotape. 10 mm O-rings were also situated along the probe to catch any falling fluid (using hydrostatic forces due to the close fit with the 9.5 mm probe).

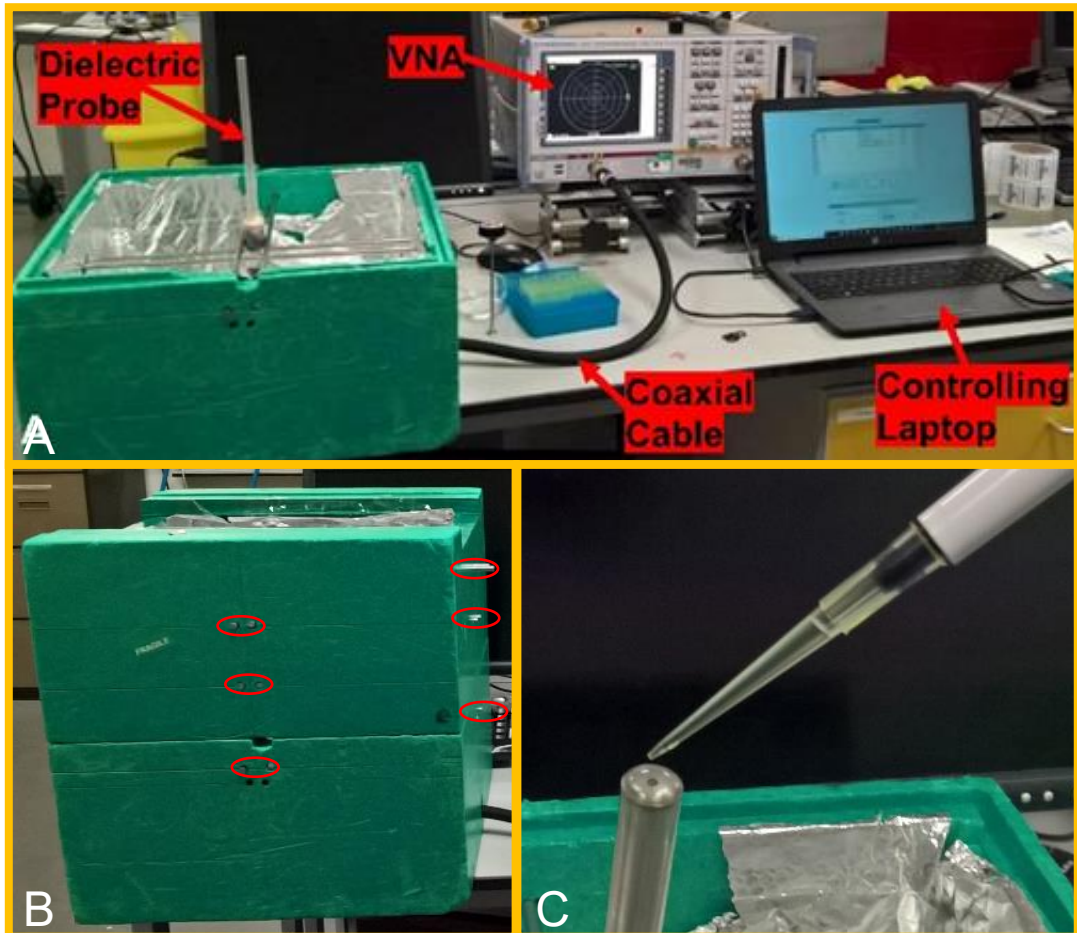


Figure 3.2: A) The inverted dielectric setup used. The dielectric probe has been shown with its holding case removed. B) The frame used to hold the probe in place. Note the metal rods (red ovals) used to hold the probe in place, 6 from left to right and 6 from front to back. C) An example of water being pipetted onto the tip of the probe.

3.3.2 Probe justification

For our experiment, a commercially available 9.5mm diameter dielectric probe (Keysight 855070E) was used. There were 2 key reasons behind the probe's selection. Firstly, the frequency range with which an open-ended coax dielectric probe works is inversely proportional to its size, with small diameter probes typically offered a higher sensitivity at higher frequencies (9.5mm diameter probe optimised to work between 0.5-20 GHz). Secondly, the probe was just big enough to hold a microliter droplet of sample for measurement.

3.3.3 Calibration and measurement method

Calibration

The system was calibrated using a similar method as described in section 3.2.2 above. One of the key differences being that the water calibration measurement was carried out by pipetting 200 μl of the pure water from the Pyrex beaker onto the tip of the probe, with the measurement being made within 5 seconds (the significance of making the measurement within 5 seconds will be explained in section 3.4.3). If bubbles were seen on the top of the sample (not at the tip of the probe as was the case for the normal setup and occurring much less frequently), the sample was pipetted off into the waste bin and the probe cleaned. The second key difference related to the validation of the calibration. As all other commonly used well-characterised materials were unable to hold a 200 μl droplet on the tip of the probe, a sub-standard check was performed using a 200 μl water sample to check the calibration was within an acceptable range. The system error shall be discussed in section 3.4.4 covering this.

Measurement

Measurements of samples were made using a similar method as described in section 3.2.2 above. One of the key differences being that a 200 μl sample was pipetted onto the tip of the probe from a Pyrex beaker using a pipette, with the measurement being made within 5 seconds. The sample was then pipetted off, and the probe cleaned. The probe was then left for 3 minutes before the next measurement took place (the significance of leaving the probe for 3 minutes will be explained in section 3.4.3).

3.4 Characteristics of the inverted dielectric probe

3.4.1 Effect of calibration and sample volume on the inverted microliter dielectric setup and the characterisation of the ‘bump’ in the data

During preliminary studies, it was noticed that that unexpected ‘bumps’ would appear in the dielectric measurement data as highlighted in Figure 3.3 when ~200 μl of blood was pipetted onto the tip of the probe and 200 μl of water was used during the calibration.

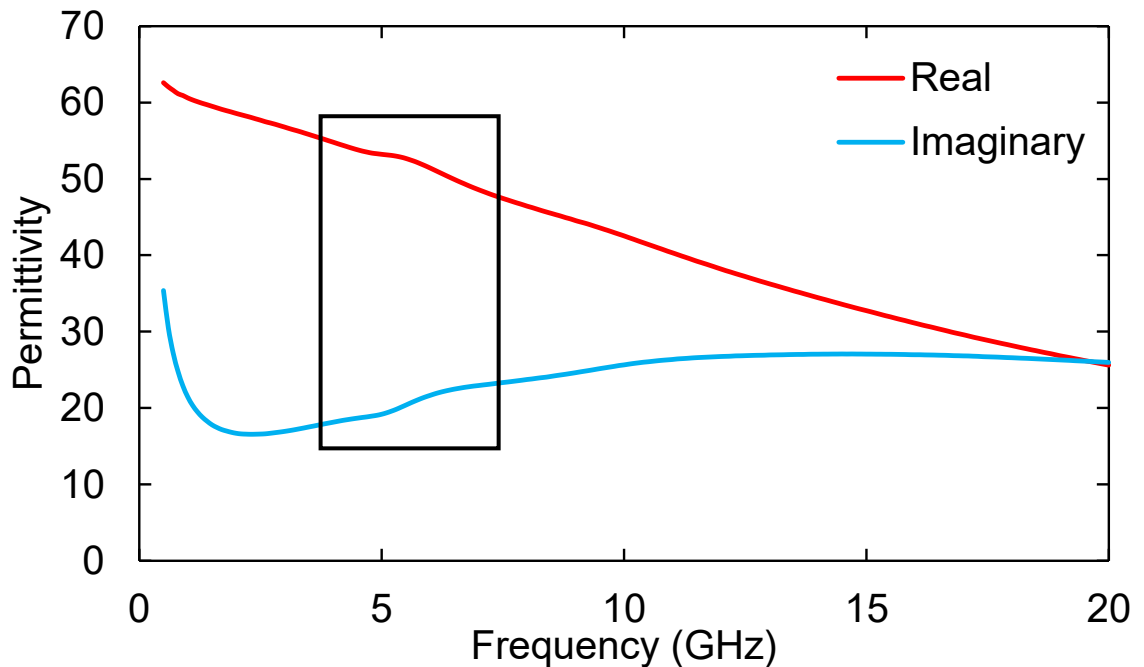


Figure 3.3: Permittivity measurement of ~200 μl of horse blood made using the inverted dielectric probe setup. Notice that there is an uncharacteristic bump in the data at around 5.5 GHz.

Unfortunately, due to blood having a tendency to stick to the inside of the pipette, it is described as only ~200 μl . As a result, it was initially theorised that this bump in the data was an artefact caused by differences between the calibration volume size and the sample volume size. A further test on varying water sample size showed that increasing or decreasing the volume of the water sample away from

the 200 μl calibration volume resulted in increased deviation from the expected smooth water curve as seen in Figure 3.4.

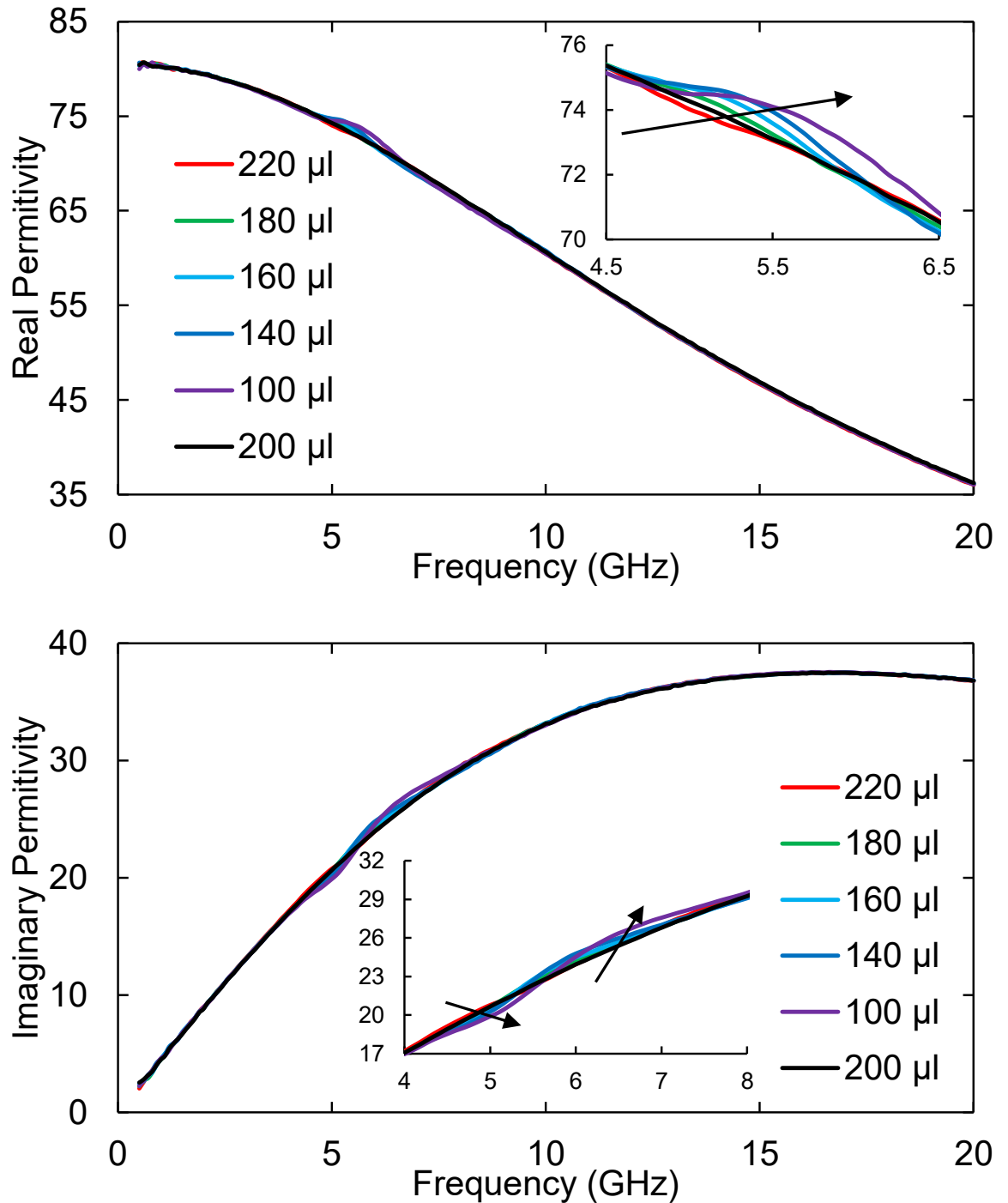


Figure 3.4: The effect of water sample volume on the permittivity when calibrated using 200 μl of water. Notice no bump is present for the 200 μl sample.

However, when making measurements using 200 μl of saltwater (290 mOsmol/kg), a solution which pipettes easily, the same characteristic bumps reappeared (Figure 3.5), albeit, more subtly. This led the author to believe that the bumps in the data were not caused by variation from the calibration volume alone, but also the shape of the calibration droplet. This conclusion was reached by the physical examination of the shape of the two droplets as seen in Figure 3.6. Here the saltwater droplet has a shorter and wider profile compared to the lower osmolality water droplet. This change in volume and shape was due to the NaCl increasing the surface tension of the water⁸⁶. As such, the saltwater droplet no longer had the same shape or volume as the calibration water volume, resulting in the subtle “bump” seen in the data.

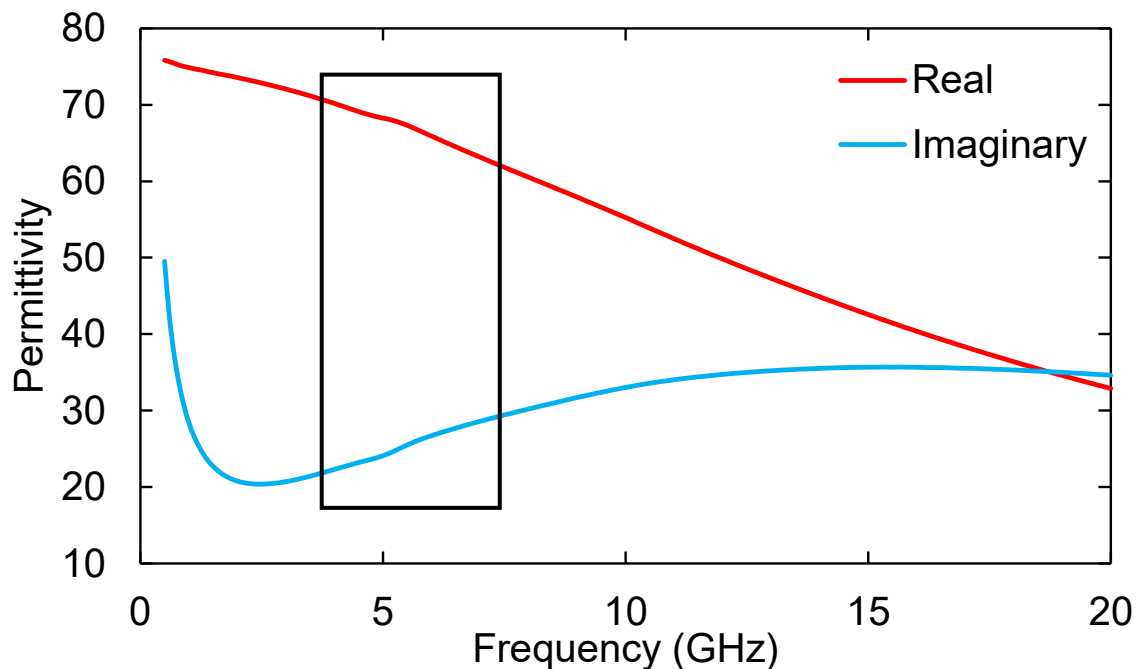


Figure 3.5: The permittivity of 200 μl salt water (290 mOsmol/kg) measured when 200 μl of water was used during calibration. Notice the slight bump around 5.5 GHz.

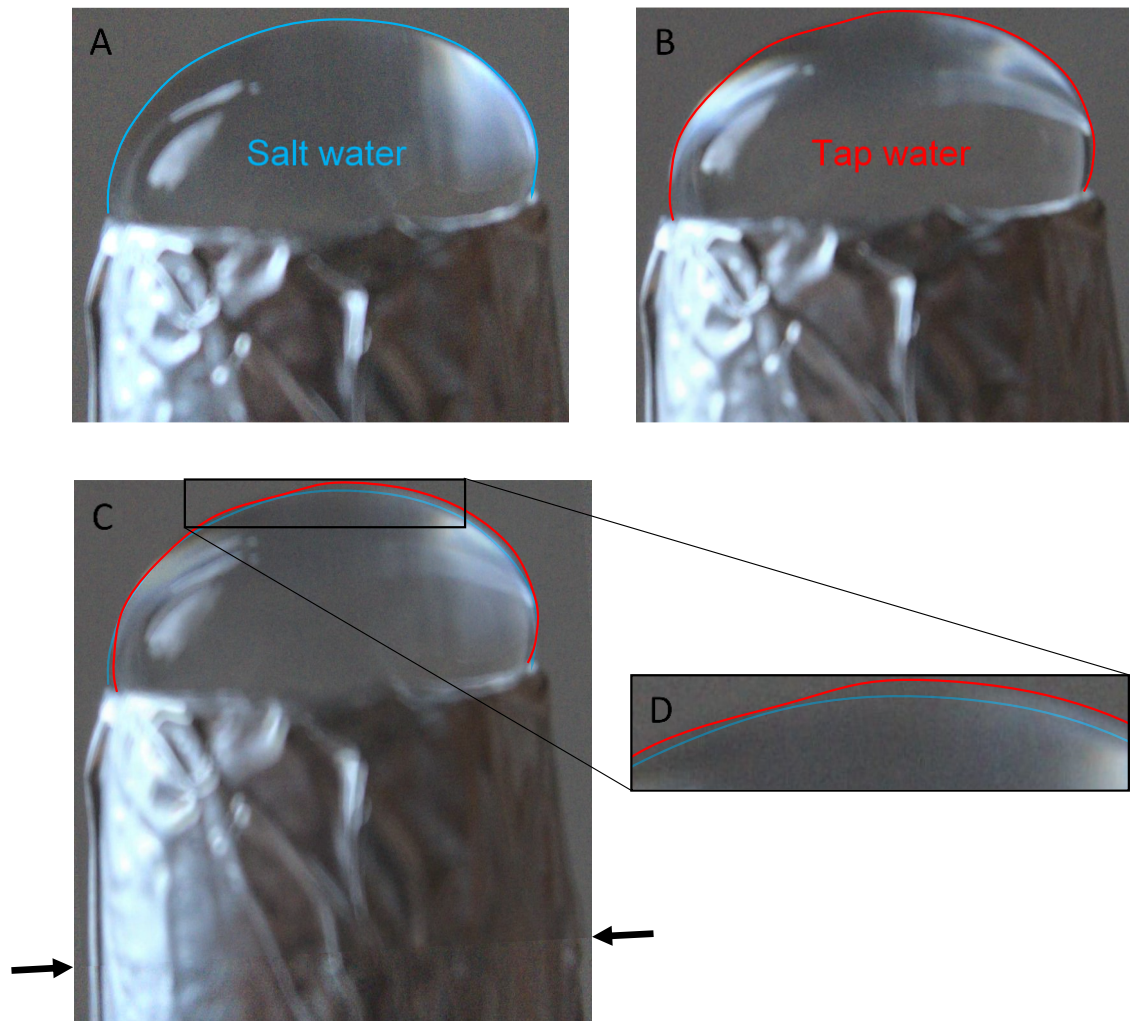


Figure 3.6: The shape of 200 μ l droplets on a 9.5mm wooden rod covered in tin foil (as COVID-19 prevented lab access to get real photos). A) Saltwater (NaCl) droplet (high osmolality > 300 mOsmol/kg). B) Tap water droplet (low osmolality < 10 mOsmo/kg). C) Overlay of the tap water droplet onto the saltwater droplet. The arrows highlight the overlay line. D) A zoom in of the difference between the two droplets.

To finish characterising the ‘bump’ in the data one final set of experiments were conducted looking at the effect changing the calibration fluid size had on the data. This was done by measuring varying volumes of water at different calibration volumes (200 μl , 160 μl , 140 μl , 100 μl), with the results for the real permittivity being seen in Figure 3.7 with the imaginary permittivity being seen in Figure 3.8.

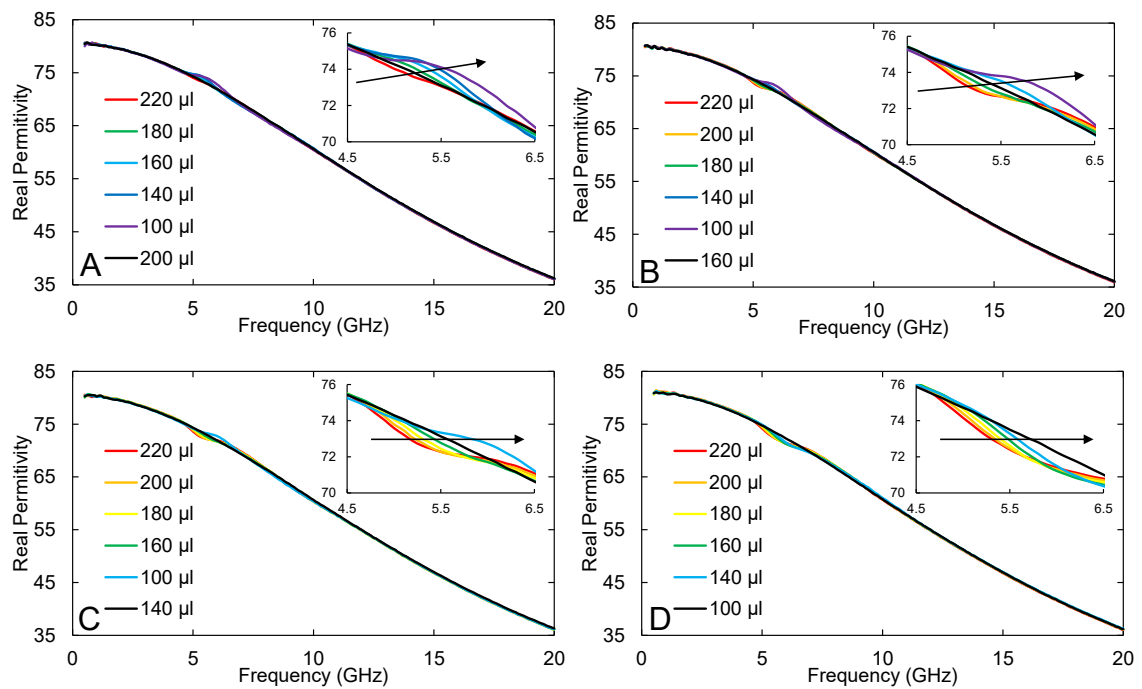


Figure 3.7: The effect of varying the sample volume of water on the real permittivity measured at different calibration volumes of water, A) 200 μl , B) 160 μl , C) 140 μl , D) 100 μl .

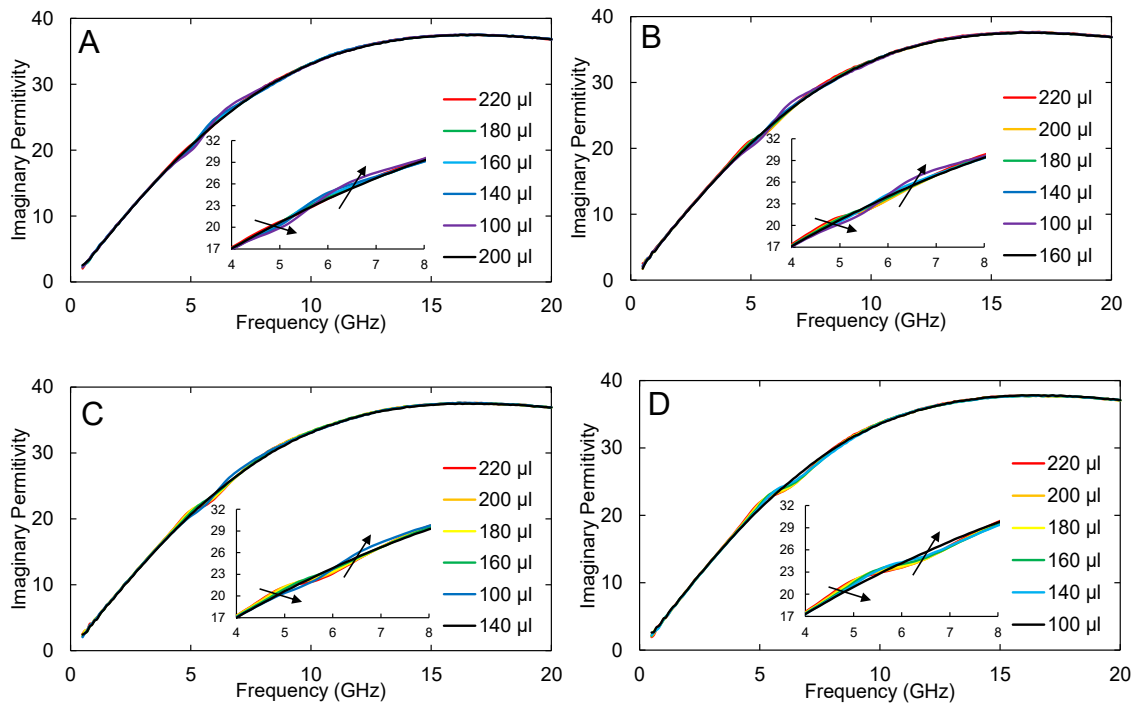


Figure 3.8: The effect of varying the sample volume of water on the imaginary permittivity measured at different calibration volumes of water, A) 200 μl , B) 160 μl , C) 140 μl , D) 100 μl .

It can be seen in these figures, that when the sample volume measured was equal to the calibration volume, the measurement of water was smooth as expected. This tells us that this bump ultimately is a calibration artefact which can be accounted for. However, as the smoothest results occurred even at low calibration volumes, there is likely an error being introduced, meaning the results measured are not a 'true' traceable permittivity measurement. This error will be examined later in section 3.4.4.

3.4.2 Modelling the inverted dielectric probe in CST

To help determine the effect of small sample sizes on the electric field generated by the dielectric probe, a frequency domain computational model examining this effect was made. This was performed using CST STUDIO SUITE 2018 running a Finite Element Method technique. The probe was modelled using an inner and outer conductor represented as a Perfect Electrical Conductor (PEC), with the insulator being made of (lossy) PTFE. The model was surrounded by a 25 cm³ block of air with the tip at its centre. Following the dimensions of the real probe, the inner conductor had a 0.1 mm diameter, the insulator had a 1.6 mm diameter, and the outer conductor had a 9.5mm diameter. The probe had a length of 150 mm. A load made from a semi-sphere droplet of pure water of 9.5 mm diameter circular base, was placed on the tip of the probe as seen in Figure 3.9.A to simulate the water drops measured.

When overlaying the simulation on a real image of the probe with a 200 µl sample of pure water in as seen in Figure 3.9.B, a few points can be noted. Firstly, while a semi-circle of water was used in the simulation, the real water droplet is in fact much flatter. While this will have had some effect when comparing to the simulation, as the majority of the volume was present, it is unlikely to have affected the comparison significantly. Secondly, while all field lines are shown to exist within the water droplet, as we know from the 'bump' in the data seen in section 3.4.1, this must not be the case. However, this simulation does show that a large proportion of the field lines are interacting with the fluid only, helping explain why the errors seen in section 3.4.4 later are so low.

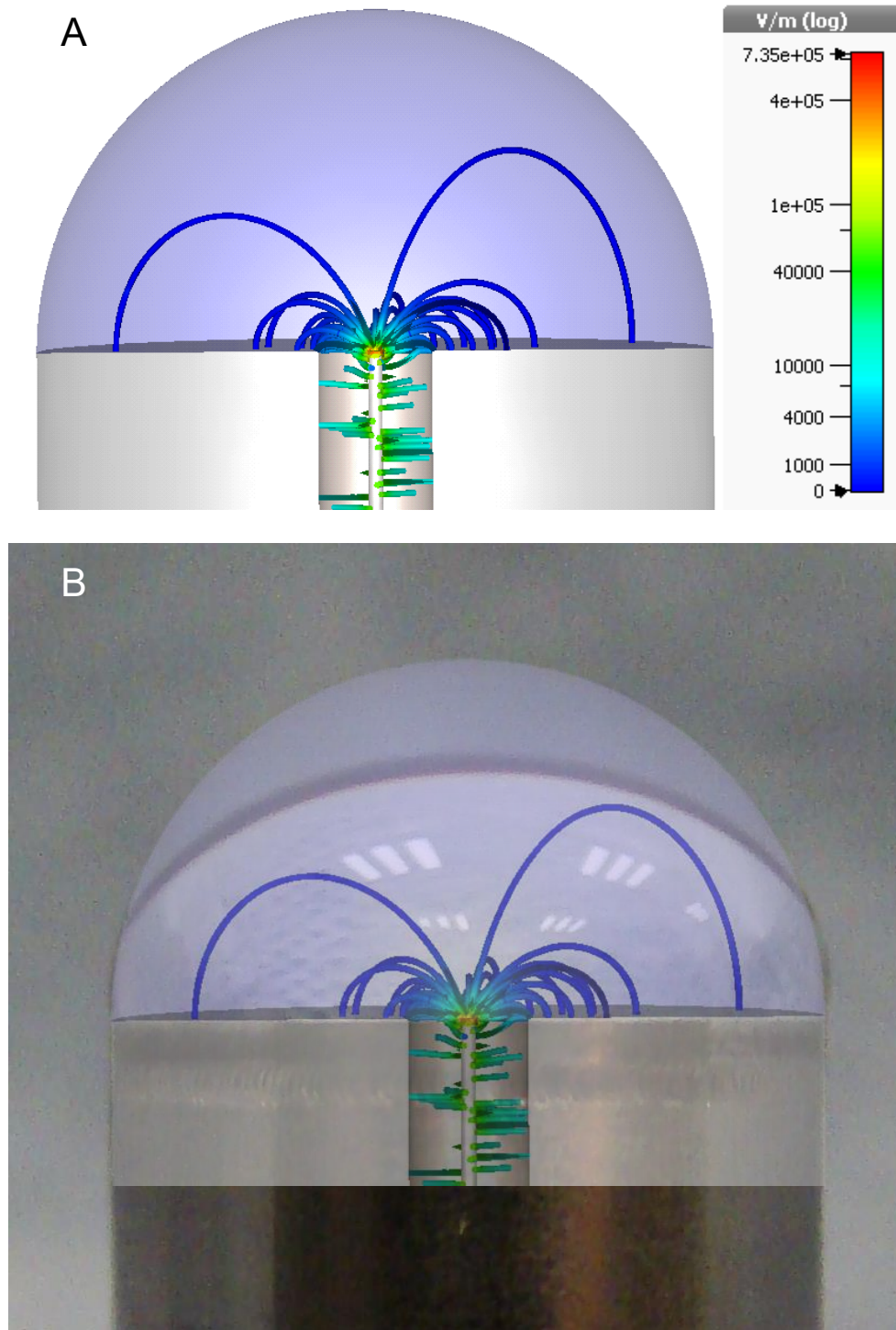


Figure 3.9: A) CST model of the tip of the dielectric probe (cross-section) with a droplet of water on top. The results show the electric field lines and strength at 0.5 GHz, with the electric field remaining within the sample at all frequencies measured (0.5-20 GHz). B) Overlay of the simulation on top of the probe with a 200 μl droplet of water.

3.4.3 Effect of time on the inverted microliter dielectric setup

In the measurement method for the inverted dielectric setup (section 3.3.3), it was mentioned that measurements were made within 5 seconds of the droplet being placed on the tip of the probe and that the probe was left for 3 minutes between each measurement. This stems from a second quirk of the inverted setup discovered during preliminary testing, which while time-dependent, is likely linked to temperature.

To demonstrate this, the probe was calibrated as normal, and a sample water drop was placed on the tip of the probe, with measurements made every 60 seconds for 10 minutes. When looking at Figure 3.10 A-B, the first thing to note is that as time increases, the dielectric properties respond as if the temperature of the sample is decreasing, as discussed in section 2.2.2. Secondly, when looking at Figure 3.10.C-D (a snapshot at 2 GHz which also holds true at all other frequencies) it can be seen that as time increases the rate of the change in the real permittivity decreases, until the dielectric properties measured levels of within the natural fluctuation of the system.

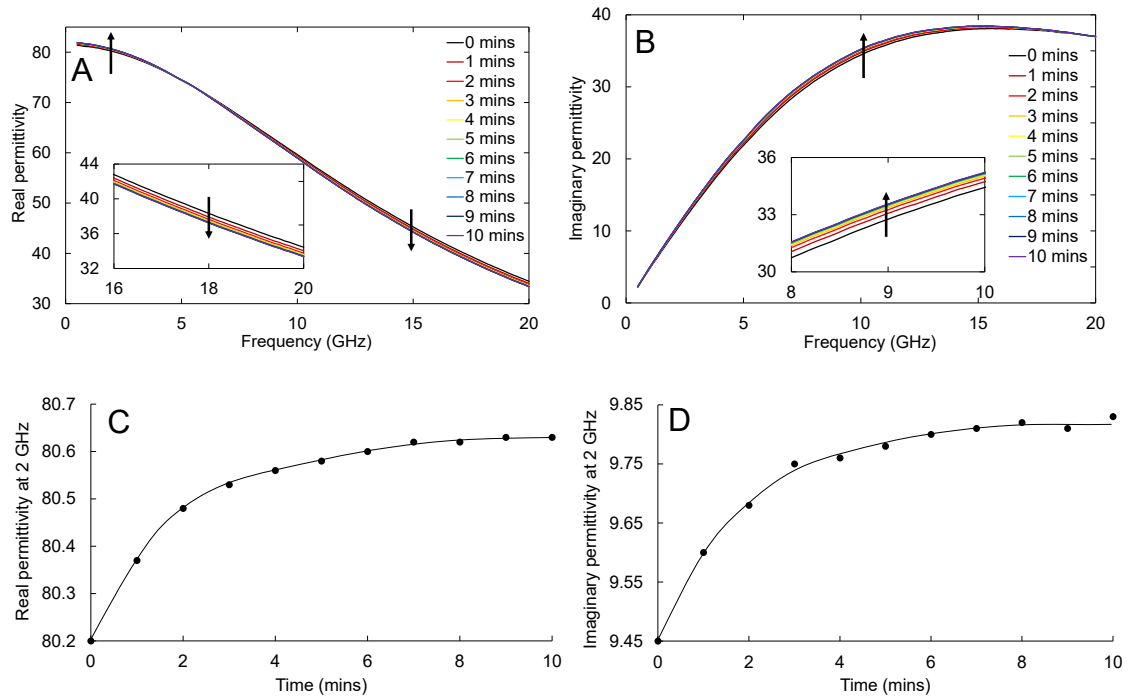


Figure 3.10: The broadband effect of time on the A) real permittivity and B) imaginary permittivity, of water samples left on the tip of a dielectric probe. The effect of time on the C) real permittivity and D) imaginary permittivity, of water samples left on the tip of a dielectric probe at 2GHz. Notice that the permittivity plateaus by 8 minutes.

While these changes are measured in the time domain, the author believes these effects are due to small discrepancies in the temperature of the probe (low specific heat capacity) and the water sample (high specific heat capacity). This stems from two reasons. Firstly, when using the normal dielectric setup, the volume of fluid is large, so any small discrepancies between the temperature of the probe and the sample would be absorbed by the whole sample, resulting in a minimal drop. By comparison, when using the inverted setup, any temperature difference between the probe and the sample would likely have a big impact on the sample, due to it having a significantly smaller volume relative to the probe. Secondly, the change in the dielectric properties measured against time levels off, showing that some sort of equilibrium was reached.

Unfortunately, due to the nature of the experiment, the temperature of the probe and sample could not be measured to confirm this. While this could be a cause for a large source of error, as will be shown within section 3.4.4, making the measurement within 5 seconds of the sample being placed on the tip of the probe still resulted in an acceptable repeatability rivalling that of the normal dielectric setup. Additionally, while not shown here, it was also found that a 3 minute cooldown period was needed between the removal of one sample and the placement of another on the tip of the probe for results to be repeatable, suggesting that the probe was returning to an equilibrium with room temperature. Attempts were made to try and control the temperature of the probe tip more closely using a resistive wire setup seen in Figure 3.11. This was however not taken forward, as it proved to destabilise the temperature of the probe further.

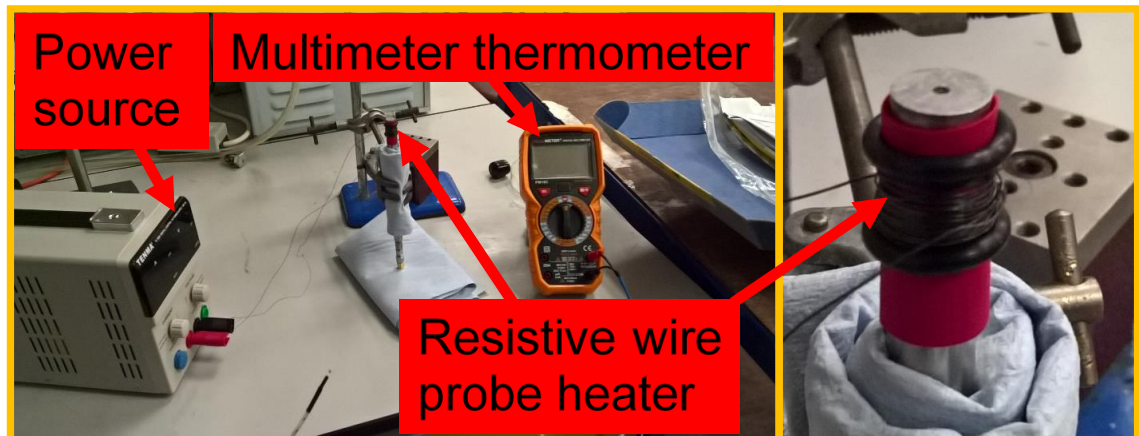


Figure 3.11: (L) Setup used to heat the probe tip to control its temperature. (R) Zoom in of the heat cuff made from heat shrink wire casing, resistive nichrome wire and 10mm O-rings.

One alternative option considered was to wait for all samples to reach equilibrium with the probe before taking a measurement. This, however, was not possible for two reasons. Firstly, it would have taken too long to conduct the experimental work, tripling the time taken to make measurements. Secondly, while not reported

in other works^{60,87}, it was found by the author that the permittivity of a blood mixture decreased with time as seen in Figure 3.12.A and Figure 3.12.B when a 40%HCT 288mOsmol/kg solution was left on the tip of the inverted dielectric probe for 60 minutes with measurements being made every 10 minutes. The author believes this was due to RBCs sinking due to gravity when left in a stationary fluid droplet (as RBCs have a higher density than the surrounding osmotic water), and was based on the increased presence of RBCs seen stuck to the probe tip with increased time. For our setup, this resulted in the decrease in both the real and imaginary permittivity as seen in Figure 3.12.A and Figure 3.12.B, and correlated well with an increase in %HCT. When looking at the change in permittivity with time at a specific frequency (9GHz) in Figure 3.12.C and Figure 3.12.D, there are two interesting points to note. Firstly, after 10 minutes, the decrease in permittivity relative to time is nearly linear, inferring that changes occurring within the fluid were occurring at a steady rate. Secondly, when examining the change between 0-10 minutes, it can be seen that there is a different rate of change relative to the rest of the experiment, with the real permittivity (Figure 3.12.C) having a sharper decrease, while the imaginary permittivity has a flatter decrease. The author believes this is likely a compounding of the temperature-dependent effects described above in Figure 3.10 A-B, with the time-dependent effects of gravity.

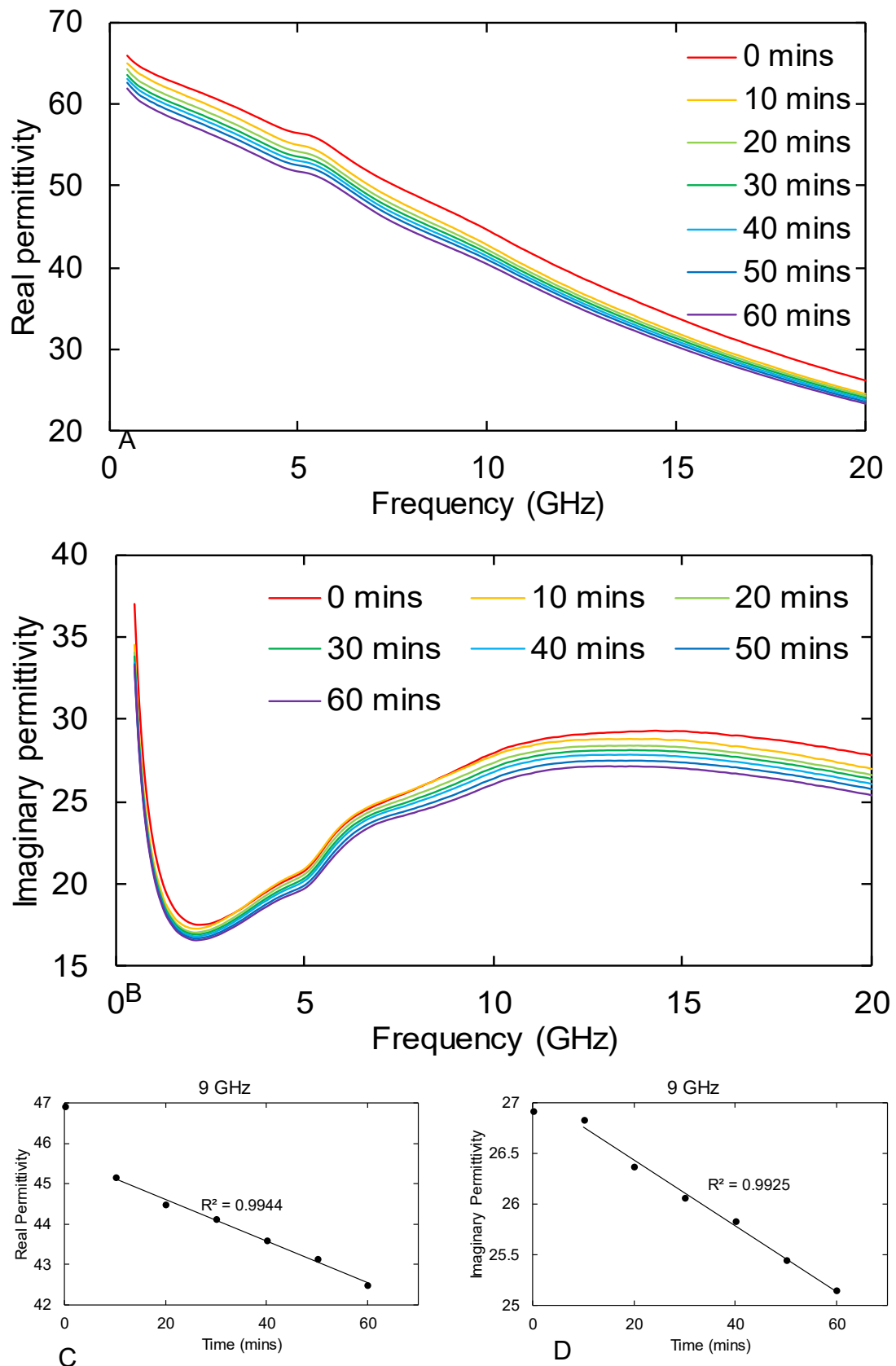


Figure 3.12: The effect of time and gravity on the A) real and B) imaginary permittivity of 40% HCT 288mOsmol/kg solution. The effect of time on a specific frequency (9 GHz) can be seen to impact the C) real and D) imaginary permittivity in a linear fashion, except between 0-10 minutes, where an additional temperature effect can be seen influencing the measurement.

3.4.4 Performance characteristics of the microliter dielectric setup

The performance of the dielectric probe was assessed using a 0.1M NaCl solution. While the general consensus is to use a traceable fluid significantly different from the calibration fluid (e.g. DMSO or ethanol) when characterising the dielectric system, the author found that such fluids did not possess the hydrostatic forces required to form a 200 μ l droplet on the tip of the probe.

Repeatability

The systems repeatability was measured by calibrating the system as described above in section 3.3.3, before making 6 replica measurements of a 0.1M NaCl solution which had been made using the processes described above in section 3.3.3. The results of this can be seen in Figure 3.13.

When averaged across all frequencies, it was determined that the real permittivity repeatability had a %3.S.D of 0.32%, while the imaginary permittivity repeatability had a %3.S.D of 0.33%. Overall, it was shown that the inverted dielectric setup possessed a very low variation when making replica measurement. This allowed the author to have confidence in incidences where only 1 measurement was made of a sample.

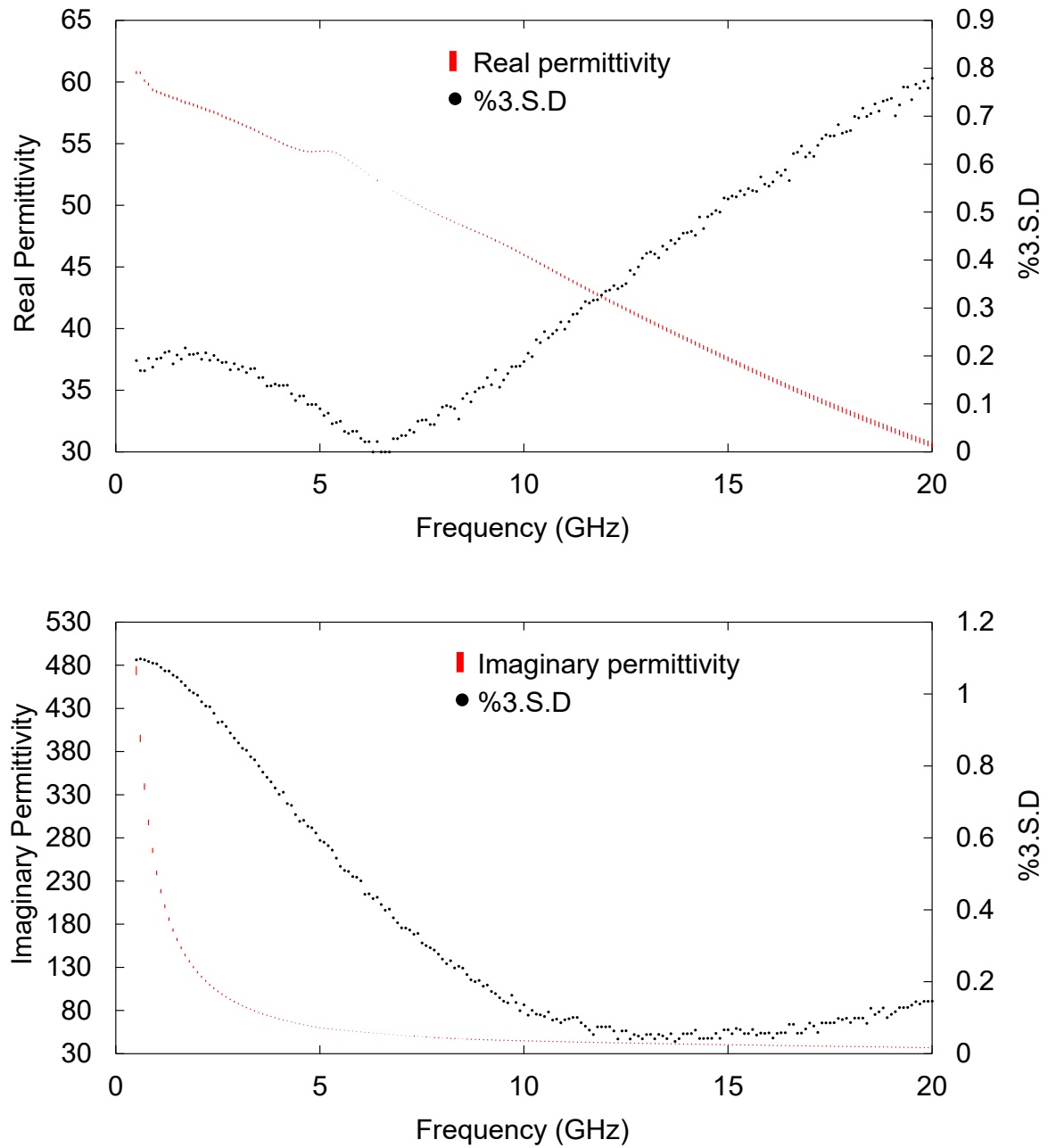


Figure 3.13: The repeatability of the A) real permittivity and B) Imaginary permittivity measured using the inverted dielectric setup when measuring using 0.1M NaCl ($n=6$). (Red) 3.S.D. error bars placed around the mean. (Black) %3.S.D.

Calibration error

The calibration error of the system was measured by conducting the repeatability test over five different calibrations. The results of this can be seen in Figure 3.14. When averaged across all frequencies, it was determined that the real permittivity had a %3.S.D calibration error of 1.31%, while the imaginary permittivity had a %3.S.D calibration error of 0.85%. While these values appear slightly larger than the ranges typically seen for the normal dielectric setup, this is not unexpected, as the quality of the calibration could not be readily checked (unlike the normal setup) due to the issues with the validating fluids not being able to hold droplets on the tip of the probe as discussed above.

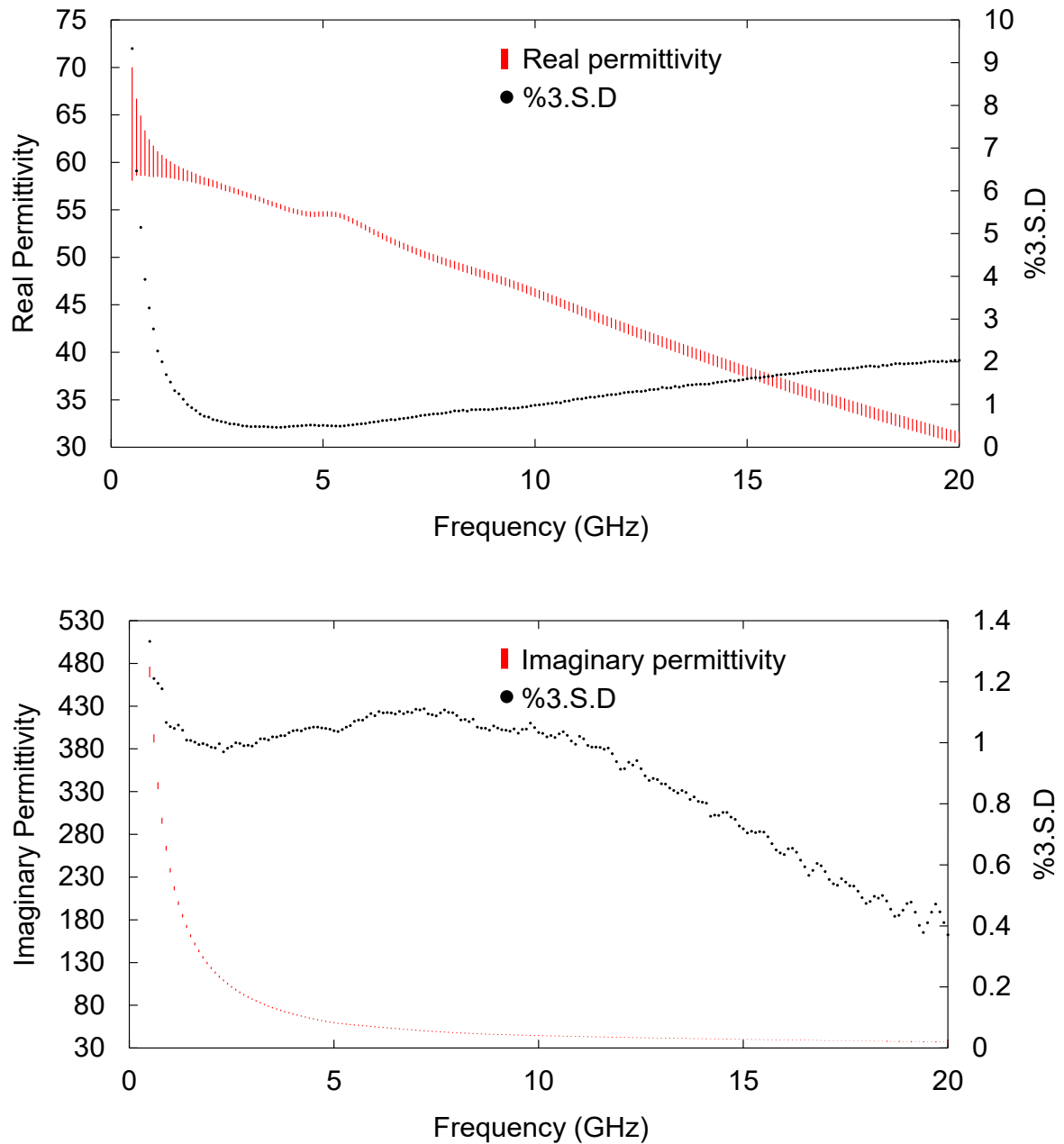


Figure 3.14: The calibration error ($n=5$) of the mean ($n=6$) A) real permittivity and B) Imaginary permittivity measured using the inverted dielectric setup when measuring using 0.1M NaCl ($n=5$). (Red) 3.S.D. error bars placed around the mean. (Black) %3.S.D.

Accuracy

The system's accuracy could not be determined in the traditional sense, due to the issues surrounding the validating fluids not being able to hold droplets on the tip of the probe as discussed above. Further, no accurate, traceable measurements exist for a 0.1M NaCl solution relative to the permittivity of free space.

As a result, the best gauge of the inverted dielectric systems accuracy was to compare the system's ability to mimic results obtained using the traceable normal dielectric setup. To do this the mean of 6 replica measurements of a 0.1M NaCl solution were made using the inverted dielectric setup and were compared against the mean of 6 replica measurements of a 0.1M NaCl solution made using the normal dielectric setup using a new calibration. This was repeated with 2 calibrations for each setup. The results of this can be seen in Figure 3.15 and Table 3.1.

In Figure 3.15 it can be seen that small differences exist in the permittivity measured using the normal and inverted dielectric setups used. For the real permittivity, this error was around 1.5%, while the error for the imaginary permittivity was around 2.3%. While these errors look large, they also have included in them two potential calibration errors, due to the two setups needing to be recalibrated between comparative measurements. As such, while the data produced won't be traceable, due to the small size of the error, it is unlikely to impact on the conclusions drawn from the comparative studies being conducted in this thesis.

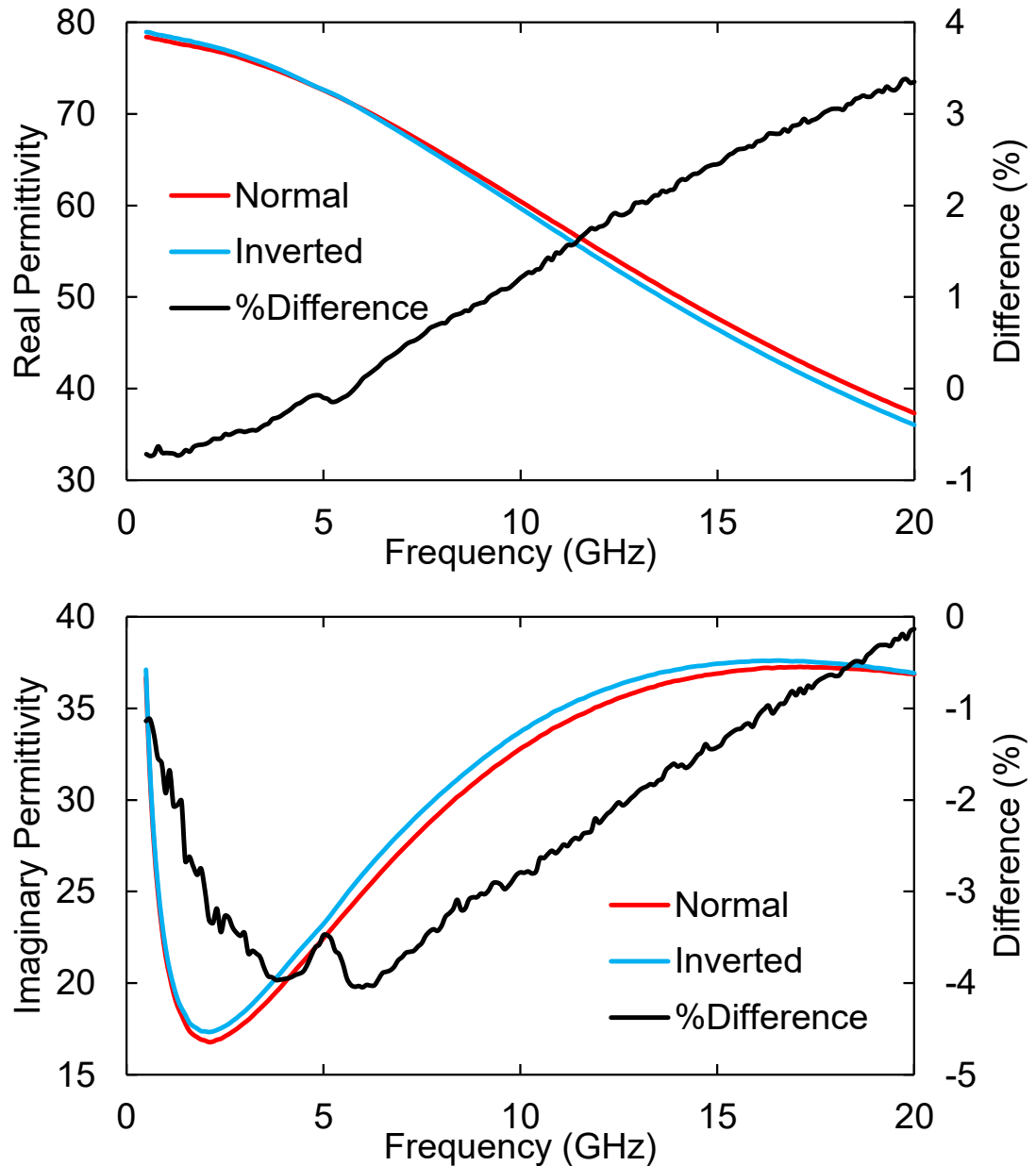


Figure 3.15: Example of the mean ($n=6$) % difference between a 0.1M NaCl solution measured using a dielectric probe in the normal setup vs the probe in the inverted setup. The mean absolute % difference across the frequency spectrum was 1.5% for the real permittivity and 2.3% for the imaginary permittivity.

Table 3.1: The min and max mean absolute % difference across the frequency spectrum of a 0.1M NaCl solution measured using a dielectric probe in the normal setup vs the probe in the inverted setup.

	Min mean % difference	Max mean % difference
Real permittivity	0.9	2.0
Imaginary permittivity	1.4	3.0

3.5 Summary of the microliter dielectric setup

The inverted setup offers a solution for measuring the broadband microwave dielectric properties of microliter sized samples for which large sample volumes could not be obtained. While the inverted setup offers advantages like allowing the instigator of the measurement to ensure no air bubbles were present during the measurement, the use of small sample volumes did have drawbacks.

Firstly, the introduction of 'bumps' in the data around 5.5GHz, caused by differences in the shape and volume of the calibration fluid relative to the shape of the sample. While this error can clearly be seen in Figure 3.3, as it is a known error, it could be modelled out by fitting to a Gaussian. Secondly, a susceptibility to variation in temperature due to the small sample size was identified. This effect was however minimised with a well-structured methodology, which resulted in a repeatability comparable to normal dielectric methodologies. Thirdly, there were found to be small difference in the permittivity measured between the inverted setup and the traceable normal dielectric system. While the inverted system is therefore not traceable / reproducible (using non-identical systems), the errors were small enough that they would be unlikely to impact on the conclusions drawn in this thesis which will be based around looking at the effect changes in composition have on the permittivity, at worst slightly muting some of the differences measured. Finally, while this work validated the probes using high permittivity solutions, there findings may not be applicable with low permittivity solutions, which were not tested.

As such, the author believes that while not ideal, the problems generated using the inverted setup, while valid, will not affect the overall discovers made throughout the rest of the works.

Chapter 4

Exercise induced dehydration causes changes in the permittivity of whole blood

4.1 Introduction

While there have been a range of studies examining the effect of individual blood components on the complex permittivity of blood, the author of this work believes that to date, no study has examined all major blood components together to see if these changes allow for hydration to be measured. This chapter presents pilot human trials looking at whether dehydration (induced through exercise) causes measurable changes in whole blood permittivity.

4.1.1 The effect of exercise induced dehydration on blood composition

The effects of individual blood components on the complex permittivity of blood has already been covered previously in section 2.2.2. This introduction aims to give the reader an informed understanding on the effects of exercise-induced dehydration on the body and blood.

There are a range of different mechanisms which can lead to dehydration, however, the two main ones are: being sedentary while withholding fluid over the course of days and strenuous exercise while withholding fluid over the course of hours, with the rest falling in between these two. Due to the time scales needed to dehydrate someone slowly over the course of days, along with the risks involved, these kinds of studies are rare. As such, this work will conduct and focus on short term exercise-induced dehydration.

In the study by S. M. Fortney. et al¹⁹, the participants cycled at 65-70% maximal aerobic power for 30 minutes at room temperature in 3 different states: Control – euhydrated, hypovolemia – induced via diuretic tablets and hypervolemia – induced via intravenous infusion (10% blood volume). This study showed that for

all condition's plasma volume decreased by 9.3-15.0 % after 30 minutes of exercise, %HCT increased by 2.4-3.2 %, osmolality increased by 6-10 mOsmol/kg and total protein increased by 0.7-1.0 g/dl.

In a similar study by C. T. Ungaro. et al³², participants cycled for 3 bouts in 29.5°C both while withholding fluid and while maintaining fluid, after which they rehydrated in 3 bouts while resting. This study showed that a 3 % loss of mass while restricting fluids resulted in an average increase in plasma osmolality of 5 mOsmol/kg from the baseline, decreasing by 5 mOsmol/kg from the baseline following fluid restoration. By comparison, when maintaining fluids, plasma osmolality decreased by 5 mOsmol/kg during exercise, levelling off during the second phase.

Up until now, the studies discussed have been short term. In an overnight study by N. Hamouti. et al⁸⁸, participants were first dehydrated in the evening to at least 3% body mass by cycling in a 32°C 46% RH environment at $\sim VO_{2peak}$ in 20 min bouts with 10 minute breaks. After dehydrating sufficiently, the participants were then asked to consume no more than 1% of the body mass lost and asked to return the following morning for measurements having consumed no additional food or fluid. This study found that on average serum osmolality increased by around 7 mOsmol/kg and plasma volume falling by 4 % at a 3 % dehydration, returning to baseline levels by the following morning, with no significant changes occurring within total serum protein levels. Further, while little change was observed in the extracellular fluid, the intercellular fluid saw continuous drops by up to 2% by the following morning.

One exercise study not involving cycling was conducted by D. B. Dill. et al⁸⁹. In their study, participants ran at 60-75 VO_{2max} in a 22°C 40-45% RH until a 4%

decrease in body mass was observed. They showed that on average %HCT increased by 1.6%, with blood volume decreasing by 9.6% with RBC volume decreasing by 6.3% and plasma volume decreasing by 12.2% over the 4 % body mass dehydration. Finally, plasma protein was found to increase by 0.59 g/dl.

In a study by D. L. Costill. et al¹⁸, participants were dehydrated until 5.8% of body mass was lost by cycling at ~ 70 % $\text{VO}_{2\text{max}}$ in a 39.5°C 25% RH environment. This study found that by 5.8% loss of body mass dehydration, on average plasma volume had reduced by 13.7%, plasma osmolality had increased by 20 mOsmol/kg, and plasma protein had increased by 1.3 g/dl. Further, it was shown that Interstitial volume had reduced on average by 14.5% with intracellular volume falling by 6.5%.

While the extent of the change in blood properties varies from study to study, due to the differences in methodology and individual variation, there is no mistaking the effect exercise-induced dehydration had. Across all studies, it was shown that exercise-induced dehydration caused a decrease in mass, total blood volume and blood plasma volume, while increasing %HCT, total blood protein, osmolality. Such changes are in line with the effects of other types of dehydration, allowing changes in whole blood permittivity collected during exercise-induced dehydration studies to apply to other forms of dehydration.

4.1.2 The effect of exercise induced dehydration on body metrics

Up until now, this work has focused on the effect of exercise-induced dehydration on blood composition. This section aims to give the reader an understanding of the effect of exercise-induced dehydration on the rest of the body.

When exercising with reduced / no fluid, it has been shown that increased levels of dehydration, result in increased heart rate^{90,91,92,93,94,95,96} and core body temperature^{90,91,93,94,95,96} relative to a euhydrated state. The increase in heart rate is complemented by a fall in cardiac output^{91,92,95,96}, stroke volume^{91,92,95,96} and atrial blood pressure^{95,96}. Further, as dehydration progresses it has been shown that sweat rates fall^{90,91} and become less salty⁹⁴, with blood flow in non-exercising tissues⁹⁶ decreasing.

4.2 Methods

4.2.1 Human trials ethics approvals, MTA's and volunteer criteria

Ethics approvals

Human blood was collected during exercise trials at St Mary's University (as Queen Mary University of London had no environmental chamber). These trials were approved by St Mary's University Ethics Sub-Committee under the ethics code: SMEC_2017-18_016 and were recognised by the Queen Mary Ethics Committee. These trials were further scrutinised and approved by the NPL ethics committee. The ethics approval letter can be seen in Appendix 1.

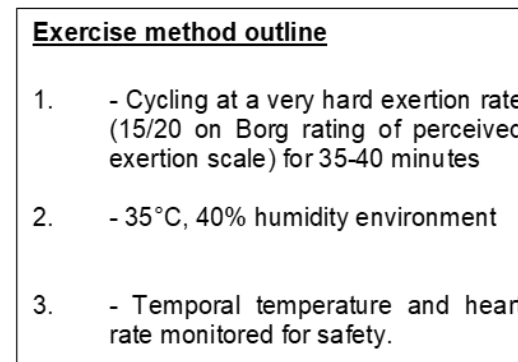
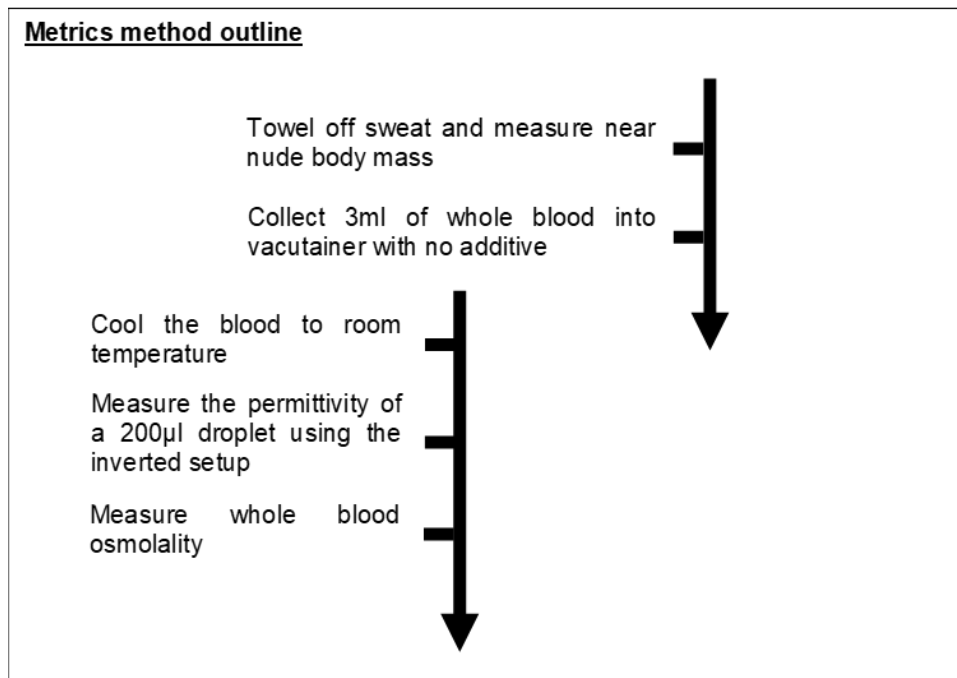
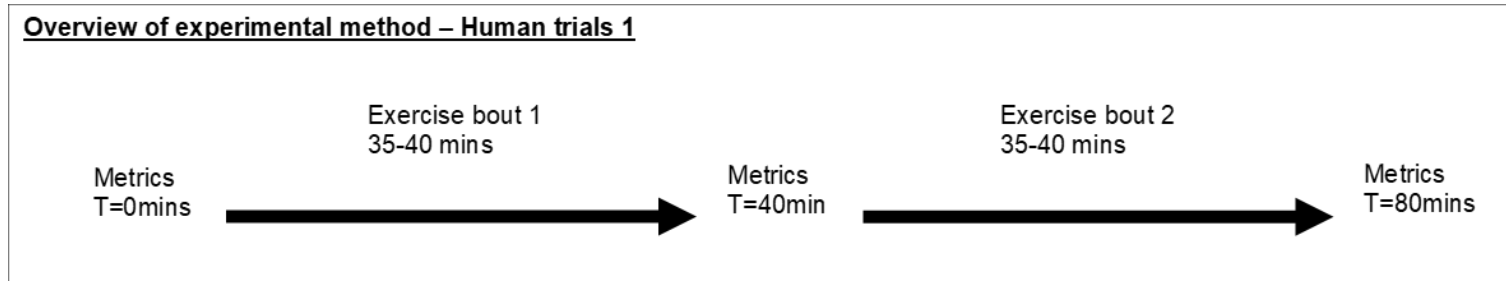
MTA

Blood samples were stored appropriately and were transported between St Mary's University and Queen Mary University of London under an MTA in accordance with the Human Tissue Act 2004, the law and local regulations. The signed document can be seen in Appendix 2.

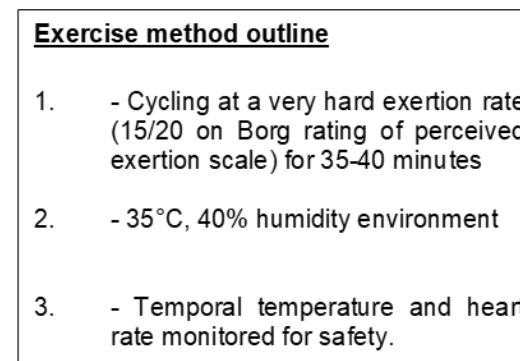
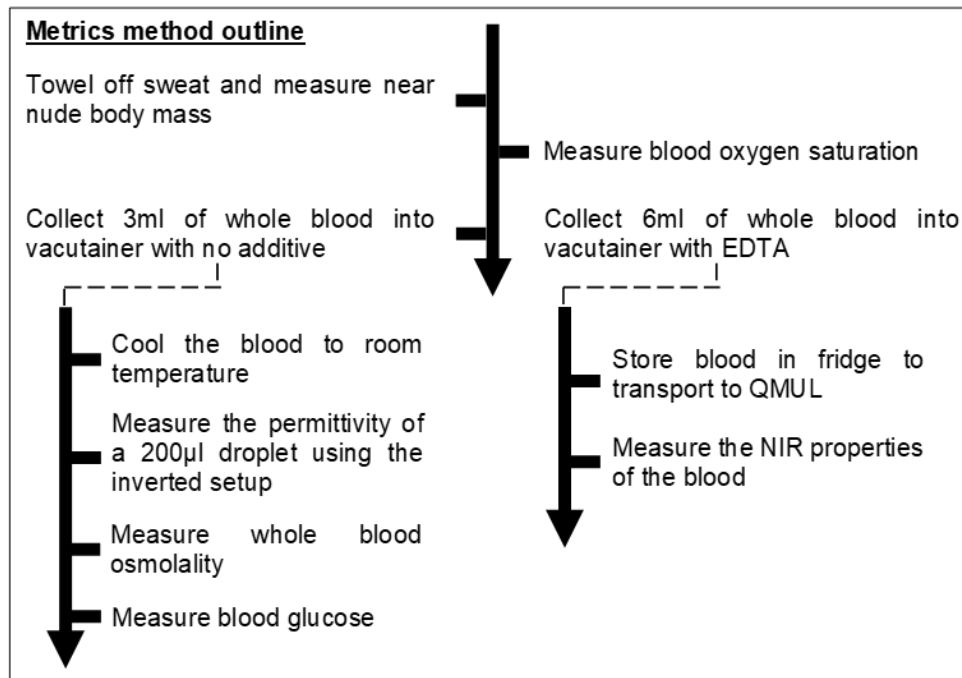
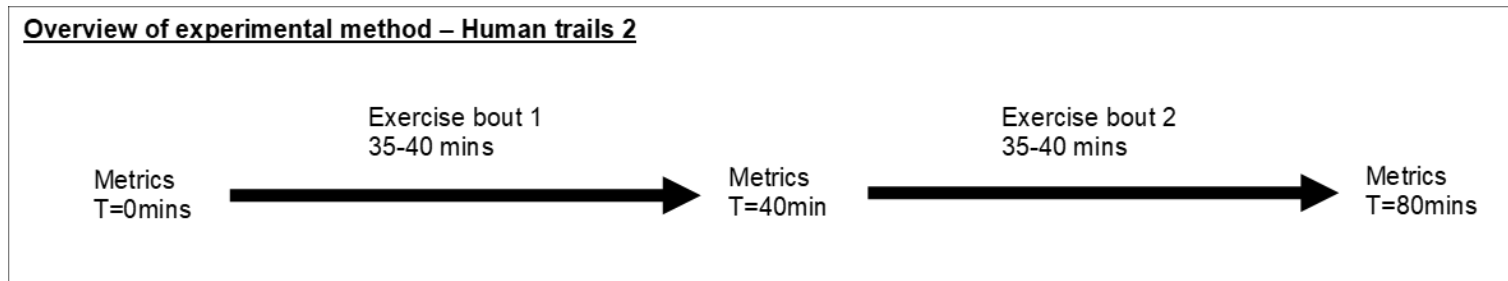
Volunteer criteria

Volunteers had to be fit (exercise roughly 2+ hours a day), healthy (no long-term or ongoing medical problems under GP supervision) and between the ages of 18 and 60, with no known blood born infections. Volunteers were also asked to be experienced blood givers. Volunteers were recruited from the local area via word of mouth, emails and posters. Before being able to take part, volunteers had to read and signed an information and consent form.

4.2.2 Experimental overview – Human trials 1



4.2.3 Experimental overview – Human trials 2



4.2.4 General Methodologies

Measuring height

The participant's height was recorded to 0.1 cm accuracy using a wall-mounted ruler prior to the first weighting session and whilst the participant had no shoes on.

Measuring body mass

Mass was measured using scales accurate to 0.1kg. Prior to weighing, participants were asked to void their bladder before being fitted with a chest ECG heart rate strap. Participants were then asked to strip to their underwear behind a screen (leaving the ECG strap on) and wipe off any sweat present. They were then asked to step onto the scales and read out their mass. Finally, they were asked to redress.

Measuring blood oxygen saturation

Whilst sitting on the medical examination couch prior to blood being collected, a pulse oximeter was placed on the middle finger of the arm blood was to be taken from. The blood oxygen saturation was then measured and recorded.

Blood collection

Blood was collected by an individual holding a recognised phlebotomy qualification, using the BD Vacutainer system. The blood taking apparatuses were prepared in advance by placing the needles and guard, blood collection tubes, and cotton wool ball onto a disposable cardboard tray.

Once the volunteer was lying relaxed on a medical examination couch, the blood collection sites was sought and cleaned. The needle was then inserted into the selected vein. Next, the blood was collected into the relevant tubes (1 X 3 ml no additive, 1 X 6ml EDTA). Finally, the needle was removed, and the cotton wool bud was placed over the needle site. The volunteer was then asked to hold the cotton wool bud there for 5 minutes while being monitored. The blood collected was then either processed and tested immediately or placed in a fridge to be transported and tested later.

Cooling the blood

Fresh blood samples have a temperature of $\sim 37.5^{\circ}\text{C}$. To prevent errors being generated by the above room temperature blood samples cooling when placed on the room temperature ($\sim 20.0^{\circ}\text{C}$) probe, the decision was taken to cool the blood to room temperature as quickly as possible, while preventing premature clotting. This was done by placing the blood sample in a Grant W6 water bath with a Grant C1G cooling unit set at 20°C ($\pm 0.1^{\circ}\text{C}$) or room temperature (whichever was lower) for 8 minutes. The sample was removed from the water bath every 50 seconds and was inverted gently for 10 seconds to prevent clotting. The temperature of the sample was measured just prior to the dielectric measurements being made using a temperature probe and was recorded alongside room temperature.

During preliminary studies involving water (which has a similar specific heat capacity to blood), it was found that water heated to the typical core body temperature ($\sim 37.5^{\circ}\text{C}$) and cooled using the above method, reached within 0.5°C of room temperature within 8 minutes. Hence this method was taken forward during the human trials.

Measuring permittivity

Permittivity was measured using the inverted dielectric setup previously described in section 3.3. Once the blood had been cooled to room temperature, up to three repeat measurements were made.

Measuring whole blood osmolality 20 μ l

Osmolality was measured using an Advanced Instruments Co., Ltd OsmoTECH single sample micro-osmometer which worked using freeze point depression.

The device was calibrated using an in-built calibration mode where the device measures a range of known references (100mOsmol/kg and 3000mOsmol/kg). Once the system was placed into calibration mode, the osmometer would display which of the standard fluids (brought from the supplier) it wished for the user to input. The osmometer would then measure the osmolality of the standard. Once the osmometer was happy it was calibrated to standard (± 2 mOsmol/kg), the device would switch back to normal measuring mode and was ready to make measurements.

After placing a fresh tip on the set volume pipette provided, a 20 μ l sample was drawn making sure to clean the edge of the tip where needed, to remove excess sample. The pipette was then placed into the sliding testbed and pushed up into the osmometers test chamber to start the measurement. Once the measurement was complete, the sliding testbed was pulled out of the osmometer, and the tip ejected into the appropriate bin. The test chamber was then cleaned by rotating a chamber cleaner left and right 6 times in the test chamber. Up to three repeat measurement were made per sample.

Measuring whole blood osmolality 200 µl

Osmolality was measured using an Advanced Instruments Co., Ltd 3250 single sample osmometer which worked using freeze point depression.

The device was calibrated using an in-built calibration mode and followed the same procedure described for the 20 µl osmometer.

Once the osmometer had been calibrated, a Gilson P200 mechanical pipette fitted with a clean tip was used to pipette 200 µl of the sample fluid into a disposable test vessel. The test vessel was then placed into the osmometer, and the start button pushed on the osmometer to start the measurement. Once the measurement was complete, the disposable test vessel was removed and disposed of, and the test head of the osmometer was cleaned and dried using lint-free paper without damaging the probes, such that no residue remained. Where biological samples were tested, the probe was cleaned first with the appropriate disinfectant, before being dried. Up to three repeat measurement were made per sample.

Measuring whole blood glucose

Once the whole blood sample with no additive had reached room temperature, a blood glucose measurement was made. After placing a fresh test strip into the GlucoRx Nexus blood glucose monitor, a small amount of blood was pipetted onto the test strip, and a measurement was made and recorded. Up to three repeat measurement were made per sample.

Measuring whole blood NIR spectrum

Infrared absorption spectroscopy was carried out using a PerkinElmer lambda 950 spectrometer at Queen Mary University of London within 7 days of drawing the sample at St Mary's University.

High-level calibrations checks were conducted monthly by internal technician staff. Prior to conducting a measurement, the controlling software was opened. The measurement parameters (gain, start and stop wavelengths, and wavelength intervals, sample path length) were then adjusted in accordance with the experiment being run. Next 2 empty cuvettes (PP 10 mm pathlength, PE 10 mm pathlength, Quart 10 mm pathlength with PTFE stopper or Quart 1 mm pathlength with PTFE stopper and acrylic supports) were placed into the spectrometer, with one being placed in the reference slot while the other was placed in the measurement slot. The spectrometer was then zeroed to the cuvettes used by performing a 100% transmission and absorption measurement across the entire frequency range set.

Once the system had been successfully calibrated, the cuvette in the measurement slot was removed and filled with the solution being tested using a pipette. The cuvette was then returned to the measurement slot of the spectrometer, and a measurement made. Once the sample had been measured, the pipette was then cleaned in a thorough (taking care not to scratch the walls) and appropriate (when biological samples were used) manner, before being finished off with a blast of pressurised air to remove any dust particles. This process was then repeated until the measurement parameters were changed and a new zeroing performed.

Exercise regime and safety protocol

Participants were asked to cycle at a very hard exertion rate (15/20 on Borg rating of perceived exertion scale) in an environmental chamber set at 35°C, 40% humidity environment for between 35 – 40 minutes. For safety, the participant's heart rate and temporal temperature were monitored every 10 minutes during exercise. Baseline temperature and heart rate measurements were made at rest in a room temperature environment prior to the first bout of exercise. The participant was asked to reduce their cycling intensity for 5 minutes if their heart rate exceeded 180BPM or 2.5 X resting heart rate (measured using the ECG test strap), or their tympanic temperature exceeded 30.0°C or increased more than 2.5°C starting temperature (measured using a handheld tympanic thermometer). If after 5 minutes they had not fallen within acceptable limits, they were pulled from the experiment and treated according to SOPs.

Experimental incidences

During the experiment, no major incidences occurred. 1 minor incident occurred where a participant became faint during the first blood collection session. The individual involved was immediately pulled from the study and received treatment at the time, before being deemed safe to go home. Following the incident, the participant requirements were updated to specify volunteers were experienced blood givers who had donated within the last 3 years.

4.3 Results: The effect of dehydration on bloods properties

4.3.1 Participant biometrics

Study 1 – Participants 1 – 4

Table 4.1 outlines the limited biometric data collected from the participants during the preliminary study. Note only 4 participants were recruited due to strenuous exercise requirements and blood collection regime.

Table 4.1: Biometrics of participants from study 1.

Participant number	Gender	Starting mass (kg)
1	Male	104.2
2	Male	68.5
3	Male	84.0
4	Female	57.5

Study 2 – Participants 5 – 8

Table 4.2 outlines the biometric data collected from the participants during the main study. Note again that only 4 participants were recruited because of the strenuous exercise requirements and blood collection regime.

Table 4.2: Biometrics of participants from study 2.

Participant number	Gender	Age (Years)	Starting mass (kg)	Height (m)	Starting whole blood osmolality (mOsmol/kg)	BMI
5	Male	54	75.0	1.830	287	22.4
6	Female	47	59.8	1.730	287	20.0
7	Male	38	84.1	1.831	287	25.1
8	Male	54	62.7	1.667	290	22.6
Mean		48	70.4	1.764	288	22.5

4.3.2 Real permittivity

Exercise-induced dehydration (determined by body mass lost) lead to a change in whole blood real permittivity for all 8 participants (Figure 4.1). For participants 3-7, a decrease in mass relative to 0% lead to a decrease in the real permittivity between 0.5-3.5 GHz, as highlighted by the insert. The sample shape calibration error can be seen in the data around 5 GHz, where a bump is present.

Decreases in body mass lead to weakly correlated ($r^2=0.44$) decreases in the % change in the real permittivity at 2 GHz when examining participants 1-8 (Figure 4.2.A). When outliers (participants 1, 2 and 8) were removed, this correlation improved ($r^2=0.84$) as seen in Figure 4.2.B.

Decreases in whole blood osmolality were strongly correlated ($r^2=0.97$) to decreases in the real permittivity at 2 GHz (Figure 4.2.C) for participants 5-7. This was comparable ($r^2=0.97$) to the correlation seen between the real permittivity at 2GHz and body mass loss when examined for the same set of participants (Figure 4.2.D).

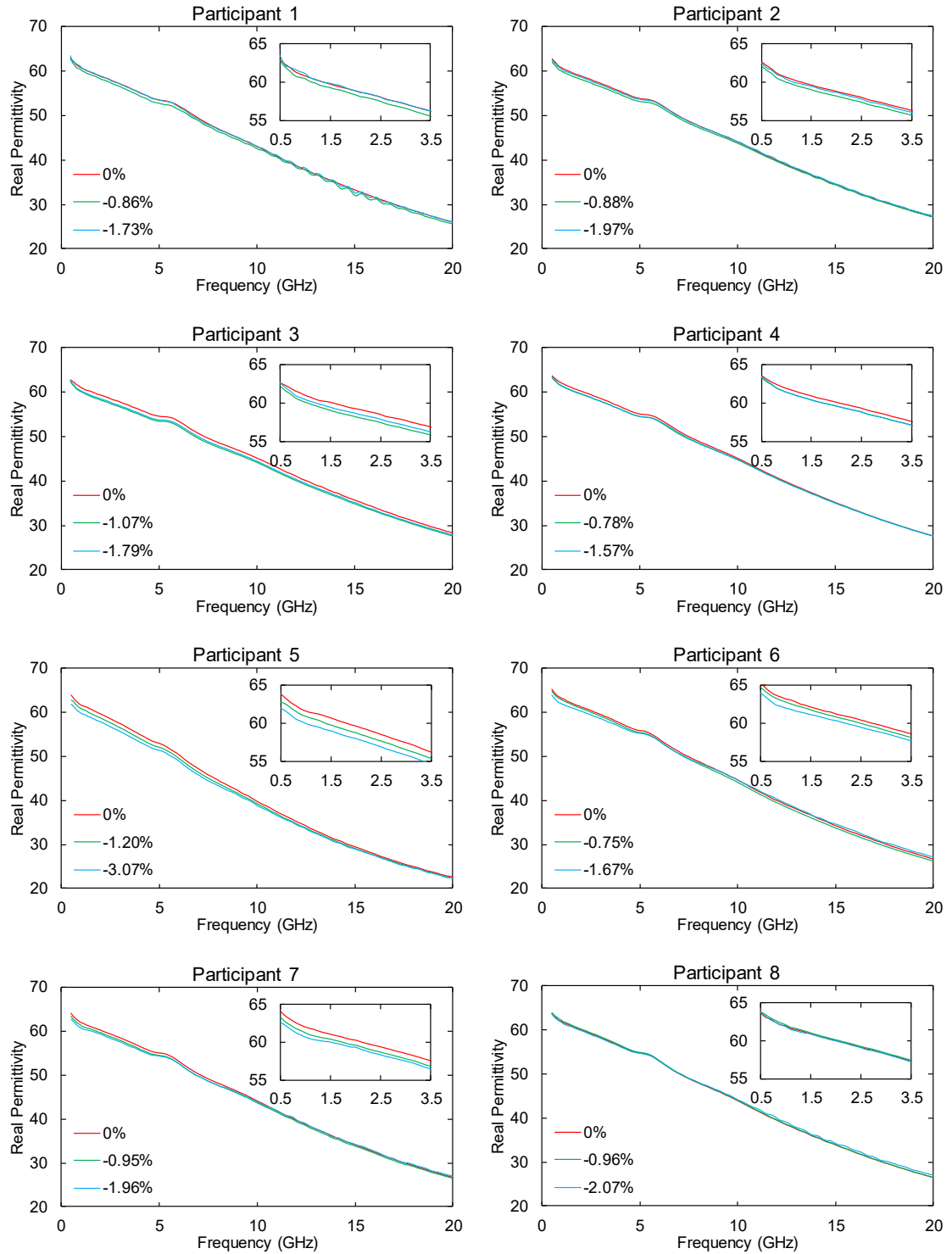


Figure 4.1: The effect of change in mass on the real permittivity of whole blood for participants 1-8. The insert shows frequencies between 0.5-3.5 GHz. Note that for participants 3-7, there is a clear trend where dehydration inferred through mass loss leads to a drop in the real permittivity.

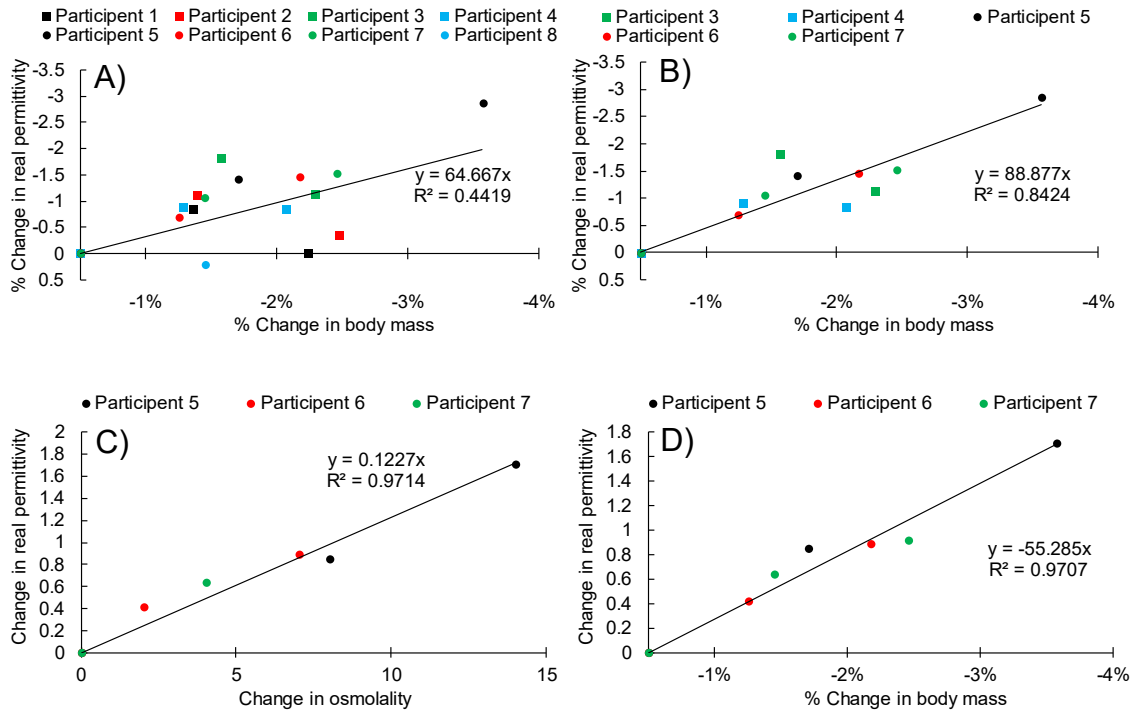


Figure 4.2: The effect of dehydration (tracked through loss in body mass) on the real permittivity of whole human blood at 2 GHz for A) participant 1-8, B) participant 3-7 and C) participant 5-7. D) The effect of dehydration (tracked through osmolality increases) on the real permittivity of whole human blood for participant 5-7.

4.3.3 Imaginary permittivity

Exercise-induced dehydration (determined by body mass lost) lead to a change in whole blood imaginary permittivity for all 8 participants (Figure 4.3). For participants 3-7, a decrease in mass relative to 0% lead to a decrease in the imaginary permittivity between 17.0-20.0 GHz, as highlighted by the insert. The sample shape calibration error can be seen in the data around 5 GHz, where a bump is present.

Decreases in body mass lead to weakly correlated ($r^2=0.24$) decreases in the % change in the imaginary permittivity at 18 GHz when examining participants 1-8 (Figure 4.4.A). When outliers (participants 1, 2 and 8) were removed, this correlation improved ($r^2=0.77$) as seen in Figure 4.4.B.

Decreases in whole blood osmolality were strongly correlated ($r^2=0.88$) to decreases in the imaginary permittivity at 18 GHz (Figure 4.4.C) for participants 5-7. This was comparable ($r^2=0.94$) to the correlation seen between the imaginary permittivity at 2GHz and body mass loss when examined for the same set of participants (Figure 4.4.D).

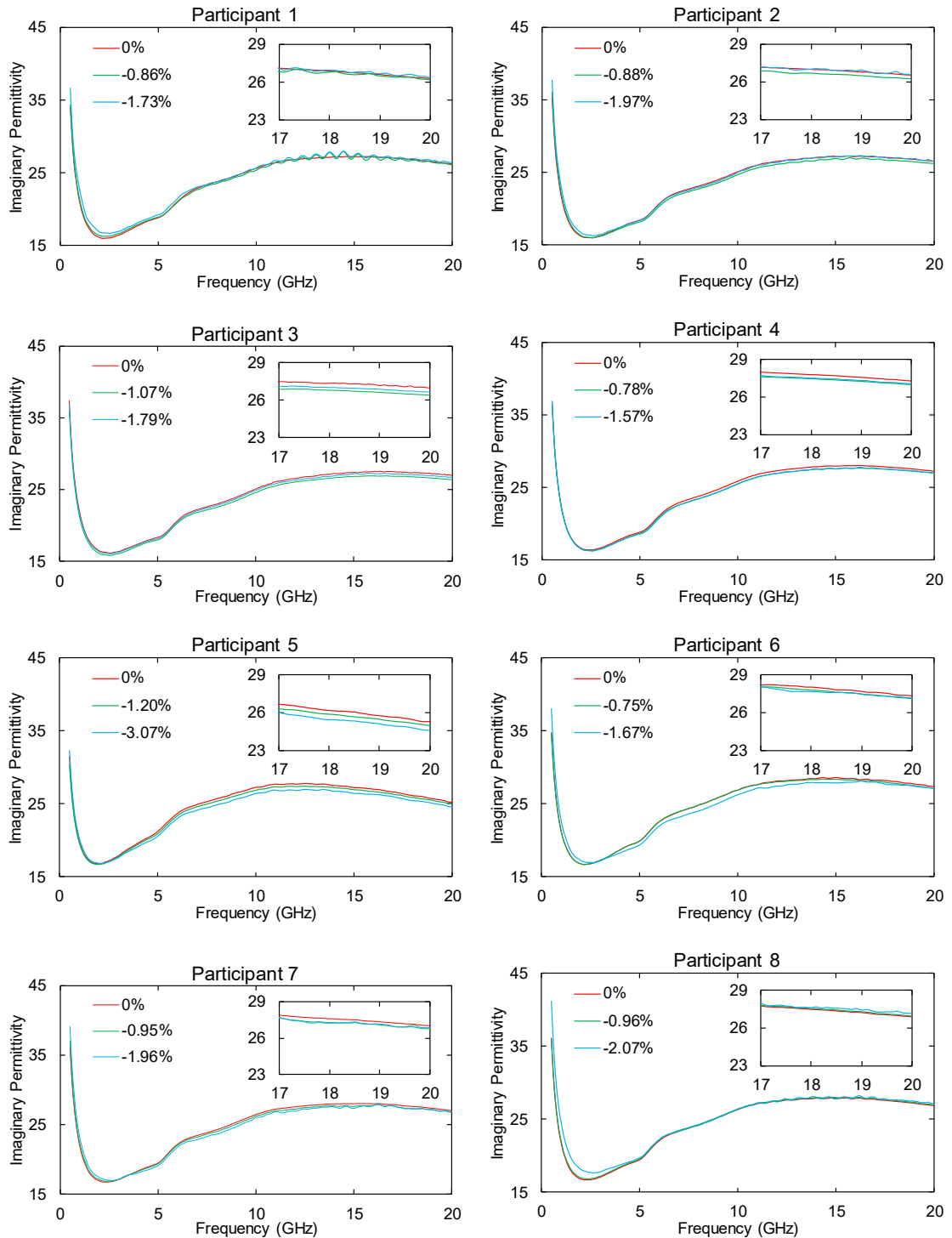


Figure 4.3: The effect of change in mass on the imaginary permittivity of whole blood for participants 1-8. The insert shows frequencies between 17.0-20.0 GHz. Note that for participants 3-7, there is a clear trend where dehydration inferred through mass loss leads to a drop in the imaginary permittivity.

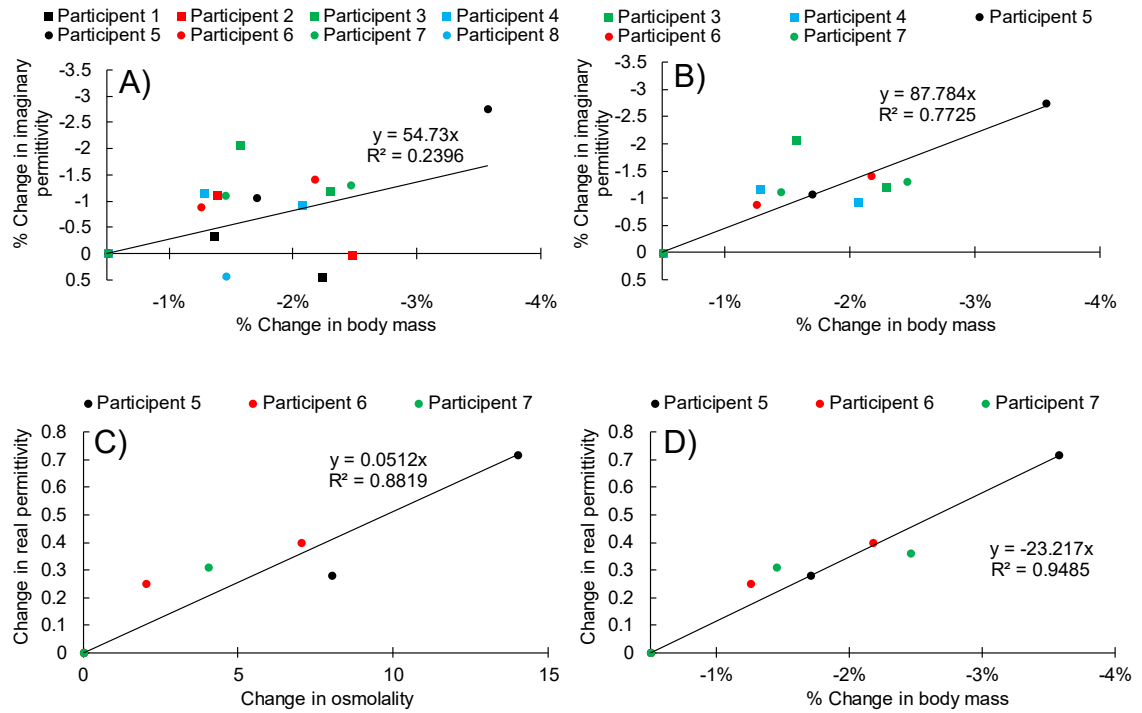


Figure 4.4: The effect of dehydration (tracked through loss in body mass) on the imaginary permittivity of whole human blood at 18 GHz for A) participant 1-8, B) participant 3-7 and C) participant 5-7. D) The effect of dehydration (tracked through osmolality increases) on the imaginary permittivity of whole human blood for participant 5-7.

4.3.4 Blood osmolality, glucose and oxygen

Exercise-induced dehydration (measured through body mass lost) was found to cause a small non-significant decrease in blood oxygen saturation (Figure 4.5.A) and results in no significant change in blood glucose (Figure 4.5.B). Decreases in body mass indicative of hydration were found to have a strong positive correlation ($r^2=0.92$) with % increase in whole blood osmolality when using a 200 μl sample size freeze point depression osmometer (Figure 4.5.C). Blood temperature was found to be no more than 3°C above room temperature just prior to measurements (Figure 4.5.D). Decreases in body mass indicative of hydration were found to have no correlation ($r^2=0.00$) with % change in whole blood osmolality (Figure 4.5.E) when using a 20 μl sample size freeze point depression osmometer.

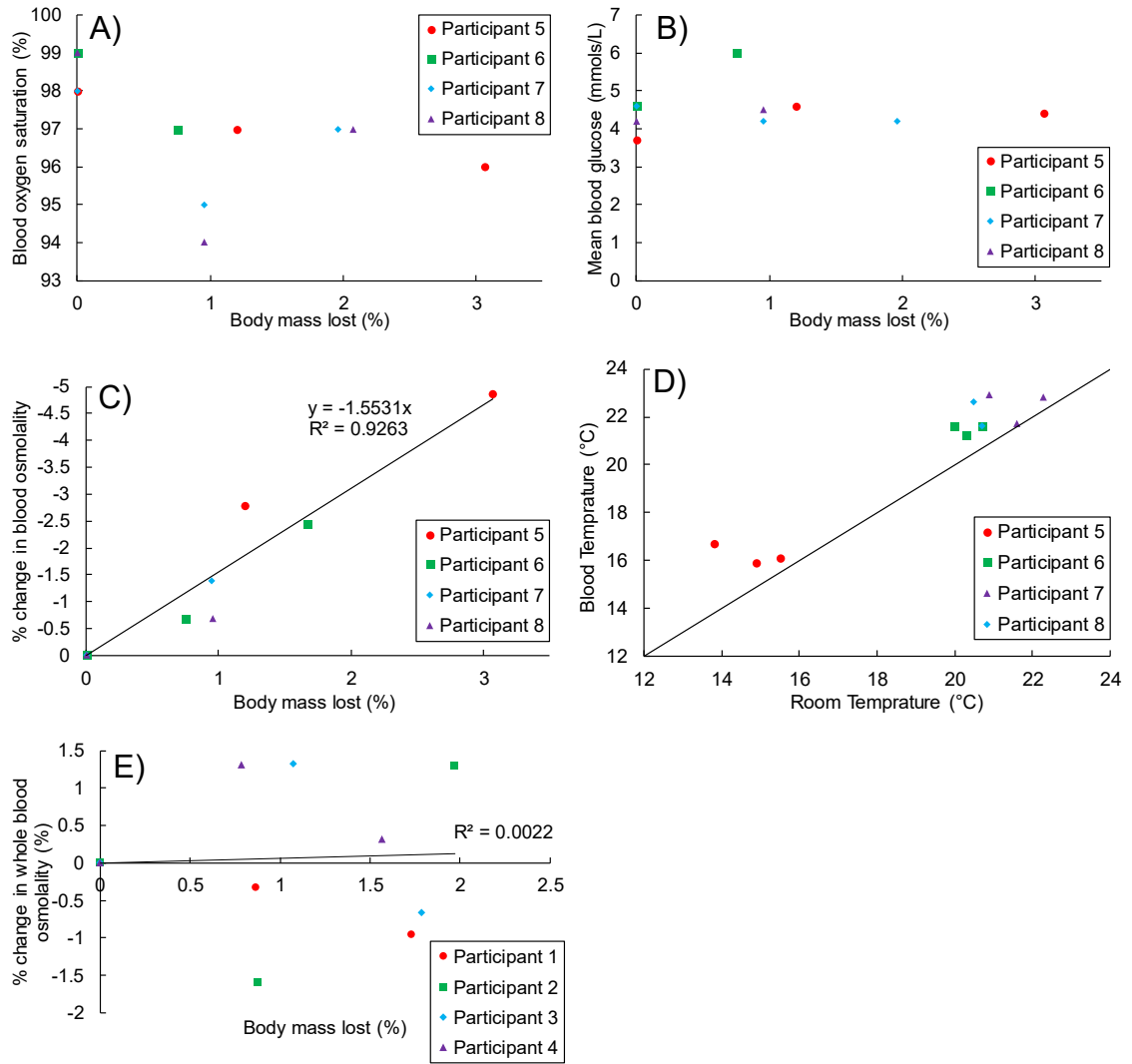


Figure 4.5: The relation between exercise induced dehydration via body mass loss and A) blood oxygen saturation, B) mean blood glucose ($n=1-3$) and C) % change in blood osmolality, for the second set of human trials. D) The temperature of the blood at the time of measurement relative to the temperature of the room. E) The relation between exercise induced dehydration via body mass loss and % change in whole blood osmolality, for the first set of human trials.

4.3.5 Infrared spectrum

The effect of dehydration on the VIS-NIR absorption spectra of whole blood diluted 1:9 in saline with a 1mm pathlength can be seen for participants 5-8 in Figure 4.6. Below 500 nm and above 1900 nm, a significant amount of noise can be seen, caused by the absorption being too large to measure. The blip in the data at 800 nm is caused by the machine changing from its optical source to with NIR source. The insert shows the absorption peaks between 510-590 nm. In these peaks, it can be seen that as mass lost increases (inferring worsening dehydration), the absorption of the peaks increases for all participants. Figure 4.7 displays the different absorption profiles for a range of fluids related to blood.

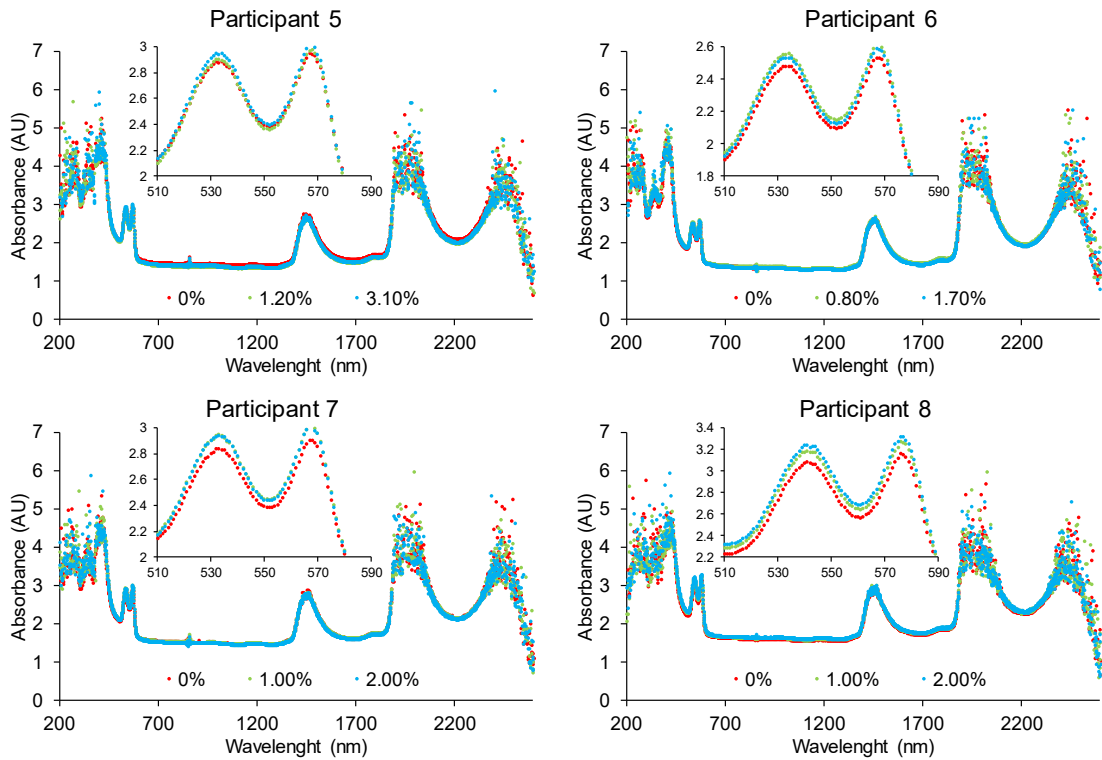


Figure 4.6: The effect of dehydration (shown by mass loss) on the VIS-NIR absorption spectra of whole blood diluted 1:9 in saline for participants 5-8 respectively measured with a 1mm path-length. The insert shows wavelengths between 510-590. Note that there is a general trend of dehydration resulting in an increase in the absorption at the peak around 535 and 570 nm.

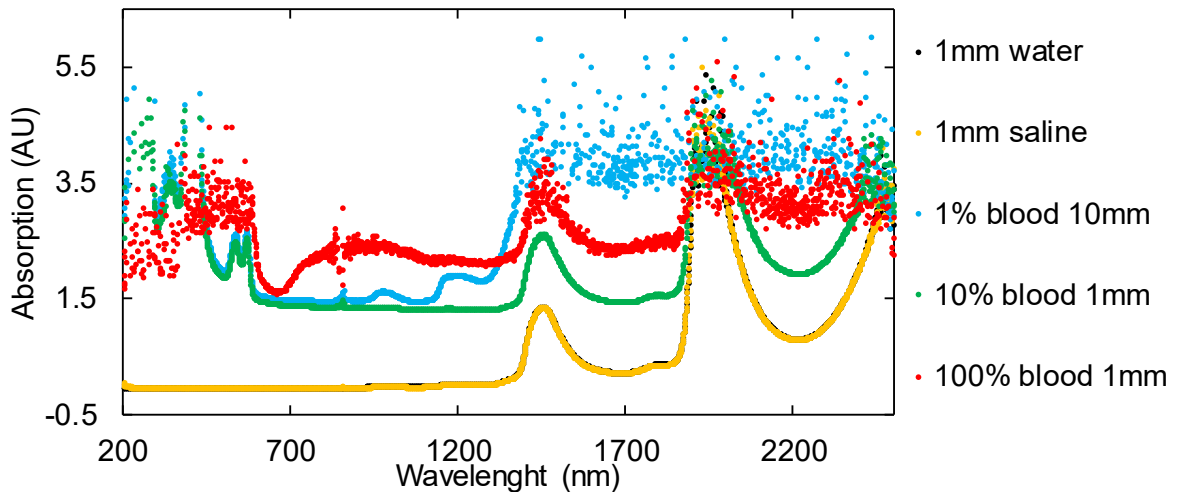


Figure 4.7: The VIS-NIR absorption spectra for a range of blood components dissolved in water measured with a 1mm path-length.

4.4 Discussion: The effect of dehydration on blood properties

This study set out to determine whether exercise-induced dehydration in a heated environment with no fluid intake lead to changes in whole human blood which could be measured using either broadband permittivity measurements in the microwave region (0.5-20 GHz) or VIS-NIR spectroscopy (200-2500 nm).

4.4.1 Real permittivity

When examining Figure 4.1 the measured broadband permittivity of whole blood changed with dehydration for all participants. For participants 3-7 between 0.5 and 3.5 GHz, as mass loss increased, permittivity decreased. When examining the correlation between permittivity and mass changes further at a specific frequency, 2 GHz (Figure 4.2.D)(2 GHz was selected as the frequency of interest as albumin, osmolality and %HCT are all known to experience large concentration dependent changes in their real permittivity at this frequency compared to higher frequencies), it can be seen that these changes process a high degree of linearity, suggesting that dehydration-induced mass loss causes changes in blood permittivity. This is not surprising, as dehydration has been shown to cause an increase in blood osmolality, blood protein and %HCT, all of which have been shown to affect blood permittivity. While we are unable to say which component caused which change due to limitations in the methodology (which will be discussed in section 6.1.2), this study was able to show that these changes were measurable and did not counteract each other. While participants 3-7 showed a high degree of linearity, this was not the case for the other participants (Figure 4.2.A). This was likely caused by both the changes measured being close to the error limit of the system, as well as the participants deviating

from the pre-trial consumption plan (with participant 8 admitting to having consumed 2L of water 2 hours prior to the study). This may explain why their results seemed to contradict the rest, with water still entering the bloodstream.

4.4.2 Imaginary permittivity

Much like with the real permittivity, the imaginary permittivity (Figure 4.3) behaved in a similar way, albeit with the area of correlation being between 17-20 GHz rather than 0.5-3.5 GHz. While the region around 2 GHz might be expected to be important (with this region being known to correlate well with changes in salt concentration), during the experiment the highest change on blood osmolality was ~15 mOsmol/kg, which is a change in concentration of ~8 mM. This is such a small change, that the effect was likely masked by other blood components. Further, much like with the real permittivity data, participant 1, 2 and 8 were again outliers. Going further, when comparing their real (Figure 4.1) and imaginary (Figure 4.3) profiles, it can be seen, that they behave in a similar way with respect to dehydration, with both the real and imaginary permittivity decreasing with a decrease in mass.

4.4.3 Infrared spectrum

When examining the effect of dehydration on the absorption spectra of diluted whole human blood (Figure 4.6), a few key features stand out. Firstly, when looking at the two absorption peaks at 535 and 570, as the participants were dehydrated (as inferred by the mass lost), the absorption peaks increased. Going further, by examining Figure 4.7, we can determine that this change was likely due to either the change in blood proteins or the change in %HCT, as

physiological salt levels were found to have no distinguishable difference for that of deionised water. As such, it could be theorised that red LEDs could be used to measure hydration in a wearable fashion (as is currently being attempted, as was discussed in section 1.4.3). There is however an argument against this conclusion, as ~600 nm is typically used by pulse oximeters to measure blood oxygen saturation and as seen in Figure 4.5.A, the participant's blood oxygen decreased as they dehydrated. However, this is unlikely to be the case due to the samples being exposed to the air during preparation, re-oxygenating any deoxygenated blood. Further, the presence of the double peak between 500-600 nm is a clear indicator that the blood was fully oxygenated.

While this work offers an argument for using red light to measure blood hydration, the author believes these results should be treated with caution. Firstly, only an $n=4$ was used, with participant 8 not being an outlier like they were with the dielectric data. This is most telling, as it would infer that participant 8's dielectric data was influenced almost entirely by osmolality, which would not be possible to the levels seen. Secondly, due to a 1:9 dilution being used, there is a chance that the pattern seen was a random occurrence created due to errors being introduced in the methodology.

The final features to note in Figure 4.6 are the random scatterings in the data below 350 nm and above 1800nm. This is a machine error, caused by the absorption reaching 100% (due to the low energy source being unable to penetrate the sample), while the light sensor still operates with baseline noise errors. From Figure 4.7, we can see that part of this high absorption is caused by RBCs, likely due to them scattering the light as their orientation in the fluid changes, with the other part being caused by water, which is known to have a high absorption in this region even when using a small path length.

In our experiments, we used a PerkinElmer lambda 950 spectrometer, which measured samples in a dark environment away from stray light beams with a (reasonably) high energy source. As such, it is unlikely that a wrist-mounted LED setup could make absorption measurements capturing the same level of detail. This along with some of the ideal frequencies for measuring hydration (1800nm+) existing outside the skins optical window further adds doubt over the viability of using VIS-NIR.

4.4.4 The effect of sample size on whole blood osmolality

During human trials 1, a 20 µl freeze point depression osmometer was used to measure whole blood osmolality. During this trial it was found that as there was no correlation between dehydration and osmolality as seen in Figure 4.5.C, contrary to the literature surrounding the link between hydration and osmolality. By comparison, when a 200 µl freeze point depression osmometer was used to measure whole blood osmolality during trial 2, a correlation was seen between dehydration and osmolality as seen in Figure 4.5.E. Upon further research, it was found that freezing point depression osmolality measurements made with 200 µl samples were no different to plasma samples^{97,98,99}, while 20 µl sample was found to have offset with a high degree of variability^{97,99}. While this phenomenon has been reported on, no reason for this difference existing has been found, however, it has been speculated that the freeze point depression methods for the smaller sample size might be creating ice crystals which rupture the cell membrane spilling its contents (which has a higher osmolality and lots of protein) out into the plasma, as RBCs themselves have been shown to have no impact on osmolality measurements^{98,99} when larger volumes were used.

4.5 Summary of findings

In this chapter we conducted invasive human trials to determine whether changes in human hydration, induced with intense cycling, resulted in detectable changes in whole blood when making broadband microwave permittivity and NIR measurements. We showed that at select frequencies, changes in blood permittivity correlated well with both osmolality and weight lost. However, the significance of the work was affected by the low n number, along with participants breaking pre-study protocol. While many companies are pursuing NIR technology for hydration monitoring, we found such devices would likely not be powerful enough to measure hydration due to the high absorption of water and the scattering caused by RBCs.

Key findings and novelty of the work:

- Changes in the real permittivity correlated well to changes in mass and whole blood osmolality at around 2GHz, while changes in the imaginary permittivity showed correlations around 2 and 18 GHz.
- We verified that 20 μ l freezing point depression osmolality of whole human blood was not suitable for tracing hydration, while shown that 200 μ l freezing point depression osmolality of whole human blood was acceptable.
- We demonstrated that it was unlikely that wearable NIR technology could be made for measuring changes in blood hydration.

Chapter 5

Microwave frequency dependent dielectric properties of blood as a potential technique to measure hydration

5.1 Introduction

This chapter takes a systematic approach examining the effect individual blood components have on the dielectric properties of whole blood and determines whether dielectric measurements of bovine blood can be used to measure hydration. When looking at early literature on the permittivity of blood, it can be seen that little thought was put into how individual blood components change in the blood, and how this might impact on the permittivity reported^{100,101}. This is despite the fact that blood composition is known to vary for a range of reasons^{88,19,102,103} and that numerous studies have shown that changes in individual blood components results in changes in bloods dielectric response. While newer studies are now no longer treating blood as a material with a fixed constant permittivity, they have yet to consider whether the change in concentration of key blood components allows for hydration to be measured. The chapter reports on a novel method for determining the viability of dielectric blood measurements to measure the hydration, tested with a bovine model, but applicable to other species.

5.1.1 The effect of %HCT, albumin and osmolality on the dielectric properties of blood

When an individual is dehydrated, their blood composition changes, including increases in osmolality, haematocrit (%HCT) and total blood protein (TBP)^{88,19,102,103}.

Changes in osmolality or salt concentration, have long been shown to cause a change in the permittivity of water-based solutions at microwave frequencies⁵⁶. Increases in salt concentration of 100mOsmol/kg are known to cause ~0.7 % decreases in the real permittivity between 0.5-20 GHz⁵⁶ and ~20 % increases in the imaginary permittivity below 3 GHz⁵⁶, reducing to negligible changes above 10 GHz⁶⁰.

More recently the effect of blood proteins, specifically albumin, have been examined. It was shown that increased concentrations of albumin resulted in a decrease in both the real and imaginary part of the complex permittivity at microwave frequencies⁶⁰ and that other proteins including lactoglobulins also have this effect⁶¹.

The contribution of proteins to the dielectric properties of blood is especially highlighted when looking at red blood cells (RBCs) typically presented as %HCT levels. While %HCT has long been shown to have a strong relationship with the permittivity of blood^{57,58,59}, recent studies by Basey-Fisher et al.⁶⁰ found that it is, in fact, the Hgb protein in RBCs which contribute to the blood's permittivity, with no significant difference being found between whole RBCs and an equivalent concentration of Hgb dissolved in osmotic water. Typically changes in %HCT have been shown to cause a linear decrease in both the real and imaginary part of the permittivity between 0.5-40 GHz. At 0.5 GHz, a ~11 % decrease in the dielectric constant can be seen over a change of 40 %HCT, decreasing to a negligible difference by 40 GHz⁶⁰. By contrast, the loss factor saw a ~21% decrease at 20 GHz, decreasing to a negligible difference by 0.5 GHz when conductivity was factored out⁶⁰.

5.1.2 The effect of other blood components and variables on the dielectric properties of blood

Aside from %HCT, osmolality and protein levels, a range of other chemicals and variables in the blood are constantly change. However, while some have been examined in some depth, others have been ignored. This section aims to cover the remaining blood components and variables to varying degrees.

Glucose is a monosaccharide mediating energy storage within the body and its concentration within the blood is continuously fluctuating¹⁰⁴. High, non-physiological concentrations of glucose dissolved in water have been shown to cause a small decrease in both the real and imaginary part of permittivity between 0.5-20GHz¹⁰⁵. However, at normal biological glucose levels, it was found that changes in glucose concentration caused no measurable change in the permittivity^{105,106}. The negligible effect of glucose on the permittivity of blood can therefore help justify the use of exercise-based dehydration studies when looking at the effect of dehydration on blood permittivity.

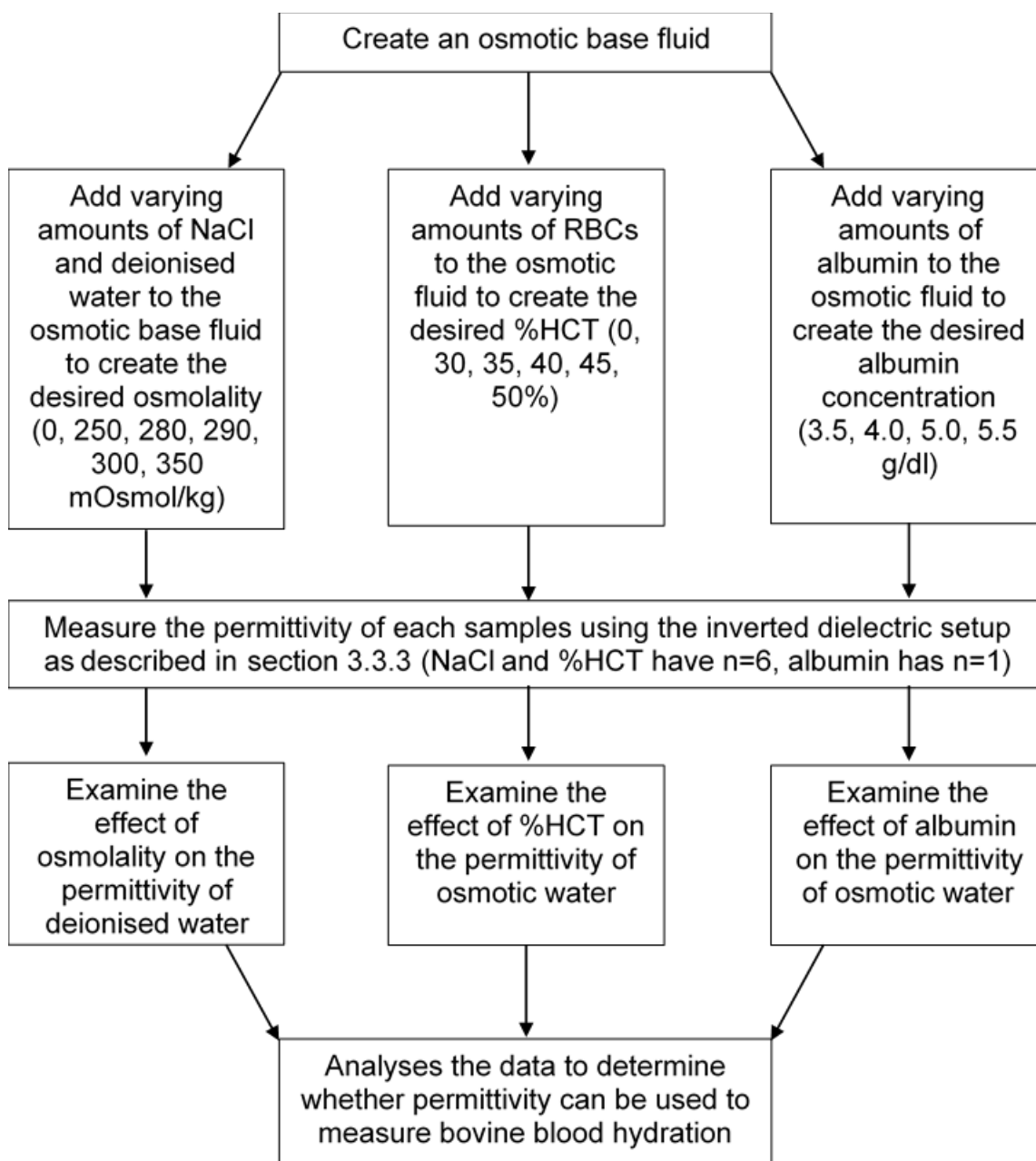
Humans typically maintain a core body temperature of around 36.8 ± 0.5 °C¹⁰⁷, however, this can increase by as much as +2 °C^{93,91,92} due to exercise or dehydration, which can be fatal. When it comes to permittivity measurements, the importance of temperature has long been understood¹⁰⁸, resulting in this variable being carefully controlled and measured in all dielectric studies. While the effects

of temperature on the dielectric properties of water are well understood and were covered in section 2.2.2, previous studies looking at the effect of temperature on the permittivity of blood have only gone up to 1 GHz^{57,58}. More importantly, these limited studies demonstrated that temperature had a complex frequency-dependent relation with blood permittivity, which needs more study if this variable is to be factored into future measurement systems appropriately.

There have been very few studies looking at the remaining blood components including WBCs, platelets and other biological chemicals most likely due to their low concentration and nature making them unlikely to have a significant impact on the permittivity. One solution proposed by Santorelli et al.⁸⁷ to characterises these biological components and chemicals involved using machine learning techniques. By measuring the concentration of Hgb, lymphocytes, platelets, sodium and creatinine from hundreds of patients and comparing them to broadband permittivity measurements of whole blood, the authors tried to determine the permittivity of different blood components. While the technique proved promising, the key results of the study were brought into disrepute due to the authors' failure to include key blood components known to affect blood's permittivity such as albumin in their study, resulting in inaccurate estimation and non-significant p-values for substances such as platelets.

5.2 Methods

5.2.1 Experimental overview



5.2.2 Materials and equipment

Biological components

Following internal advice, it was determined ethics approval would not be required to work with blood from healthy animals, which had been purchased from a supplier, as the suppliers would be collecting the blood while complying with animal welfare regulations. Bovine RBCs suspended 50:50 in Alsever's solution (Lot: BOV6231), was purchased from BioIVT LLC and was delivered and stored at 2-4°C. Bovine serum albumin obtained by heat shock fractionation by the manufacturer (Product number: A7906, Lot: SLBB8468V) was purchased from Sigma-Aldrich Co Ltd and was delivered and stored at 2-4°C.

Other components

99.9% pure NaCl (S-5889, Lot: 96H0675) was purchased from Sigma-Aldrich and was stored and delivered at room temperature. Fresh deionised water was generated in-house using a deionizer (ELGA Maxima).

Other equipment used

Weight was determined using either a 2.D.P. scale (Mettler Toledo, Model: MS4002S/01) or a 4.D.P. (Mettler AJ100). Microliter fluid samples were pipetted using either a Gilson P1000 pipette or a Gilson P200 pipette. Samples were separated using a Thermo IEC CL31 multispeed centrifuge. Activates involving biological substances were performed in an Astec microflow advanced biosafety cabinet class 2.

5.2.3 Making fluids with known osmolality

Making osmotic stock fluid

To ensure biological components remain viable when diluted, an osmotic base fluid first needed to be made. A stock bottle of the osmotic base fluid was made by first weighing out a known weight of deionised water (m_{H_2O}) out into a 1 L glass bottle using 2.D.P. scales. Next, the appropriate weight of sodium chloride salt (m_{NaCl}) was added (weighed out using a 4.D.P. scale and a plastic weighing

boat) to create the desired osmolality (~290mOsmol/kg) using *Equation 12*:

$$\ell_s = \frac{m_{NaCl}\varphi_{NaCl}}{m_{H_2O} \frac{M_{NaCl}}{2}} \quad \text{Equation 12}$$

where (ℓ_s) is stock osmolality, (φ_{NaCl}) is the osmotic coefficient of NaCl which is 0.93^{109,109}, and (M_{NaCl}) is the molar mass of NaCl which is 0.05844kg/mol. Once made, the osmolality of the stock was validated by measuring its osmolality using the method outlined in section 4.2.4.

Making osmotic fluid for reconstituted blood

When making a fluid with a known osmolality, osmotic stock fluid was first aliquoted into a smaller vessel where the osmolality was then adjusted. The osmolality was decreased by adding deionised water using *Equation 13*, while osmolality was increased by adding NaCl using *Equation 14*,

$$\ell_n = \frac{(\ell_s \times m_s) + (\ell_d \times m_d)}{m_s + m_d} \quad \text{Equation 13}$$

$$\ell_n = \ell_s + \frac{m_{NaCl}\varphi_{NaCl}}{m_s \frac{M_{NaCl}}{2}} \quad \text{Equation 14}$$

where (ℓ_n) is the new osmolality of aliquoted fluid, (m_s) is the mass of the stock fluid aliquoted, (ℓ_d) is the osmolality of deionised water added, (m_d) is the mass of deionised water added.

5.2.4 Making fluids with known albumin concentrations

When making a sample with a known albumin level, an appropriate volume of an appropriate osmotic fluid was aliquoted out. Next, the appropriate weight of BSA was weighed out using 4.D.P. scale and a plastic weighing boat and was added to the osmotic fluid such that the concentration can be determined by *Equation 15*, where (ρ_A) is the concentration of albumin in the fluid, (V_{OW}) is the volume of osmotic water and (m_A) is the mass of albumin added to the osmotic

water. The BSA mixture was then placed on roller mixer in a cold storage room (2-6°C) until the albumin had fully dissolved. The solution was then placed in the fridge until it was used.

$$\rho_A = \frac{m_A}{V_{OW}} \quad \text{Equation 15}$$

Adjusting for the effect of albumin on the osmotic properties of the fluid

During preliminary studies, it was found that adding albumin to an osmotic fluid increased the osmolality. This effect was quantified by adding known quantities of albumin into known concentrations of osmotic water, with the results seen in Figure 5.1.

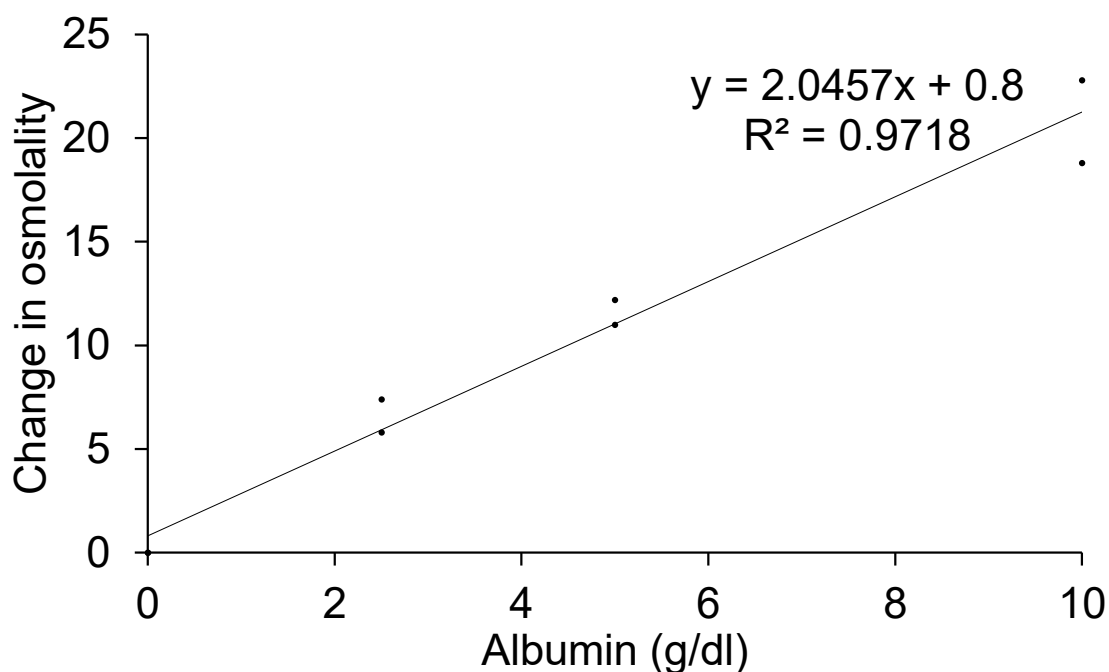


Figure 5.1: The change in osmolality caused by increasing albumin concentrations.

From research, it was determined that albumin should not impact osmolality. As a result, the author theorised that the salt present may be residue leftover from the manufacturing process, however, the manufacturer was unable to comment on this as they did not test the osmolality of the product themselves. From this preliminary study, the effect of albumins concentration on the osmolality of the osmotic base fluid was determined, as seen in Equation 16, where ($\Delta\ell$) is the change in osmolality (mOsmol/kg) due to the addition of albumin, with all masses being in kg. The effect of albumin on osmolality means

that when aiming to make a reconstituted blood sample with a given osmolality, the initial fluid osmolality needs to be adjusted (lowered) accordingly.

$$\Delta\ell = 0.8 + 205 \left(\frac{m_{NaCl}}{m_{H_2O}} \right) \quad \text{Equation 16}$$

5.2.5 Making fluids with known %HCT

When making a sample with a known %HCT, stock bottle of whole blood or RBCs suspensions were treated in a similar fashion. The stock bottles were left for 3 days in a fridge causing the separation of RBCs from the rest of the blood or suspension. ~12 ml of RBCs were then aliquoted out using a pipette and were spun in a centrifuge at 500G for 5 minutes. Any excess plasma or cell suspension fluid was then pipetted out. To generate the desired %HCT, the appropriate volume of RBC's was added to an appropriate volume of previously aliquoted osmotic fluid as described by *Equation 17* using a pipette, where (V_{RBC}) was the volume of RBCs present.

$$\%HCT = \frac{V_{RBC}}{V_{RBC} + V_{OW}} \times 100\% \quad \text{Equation 17}$$

As a pure RBC volume had a tendency to stick to the inside of pipettes, the final %HCT had to be determined. This was done by spinning the blood in a centrifuge at 500G for 5 minutes, before measuring the volumes by eye using the scales provided on the container. The reconstituted blood was then re-mixed and placed in the fridge until it was used.

5.2.6 Making fluids with known glucose concentration

To make a solution with a known glucose concentration (ρ_G), the appropriate volume of deionised water (V_{H_2O}) was first aliquoted using a pipette. The appropriate weight of glucose (m_G) was the weight out using a 4.D.P. scale and plastic weighing boat, following *Equation 18*, before being added to the deionised water.

$$\rho_G = \frac{m_G}{V_{H_2O}} \quad \text{Equation 18}$$

5.3 Results: The effect of blood components on the permittivity of water

5.3.1 %HCT

Increasing the physiological concentration of RBCs (35 % - 50 %, n=6) in osmotic water (288 mOsmol/kg) led to decrease in both the real (Figure 5.2.A) and imaginary (Figure 5.2.C) permittivity at all frequencies measured (0.5-20 GHz, 0.1 GHz intervals). Further, it was demonstrated that the change in permittivity relative to change in %HCT was highly linear for both the real (Figure 5.2.B) and imaginary (Figure 5.2.D) permittivity, with $R^2 > 0.999$ at all frequencies shown, which held true at all other frequencies measured.

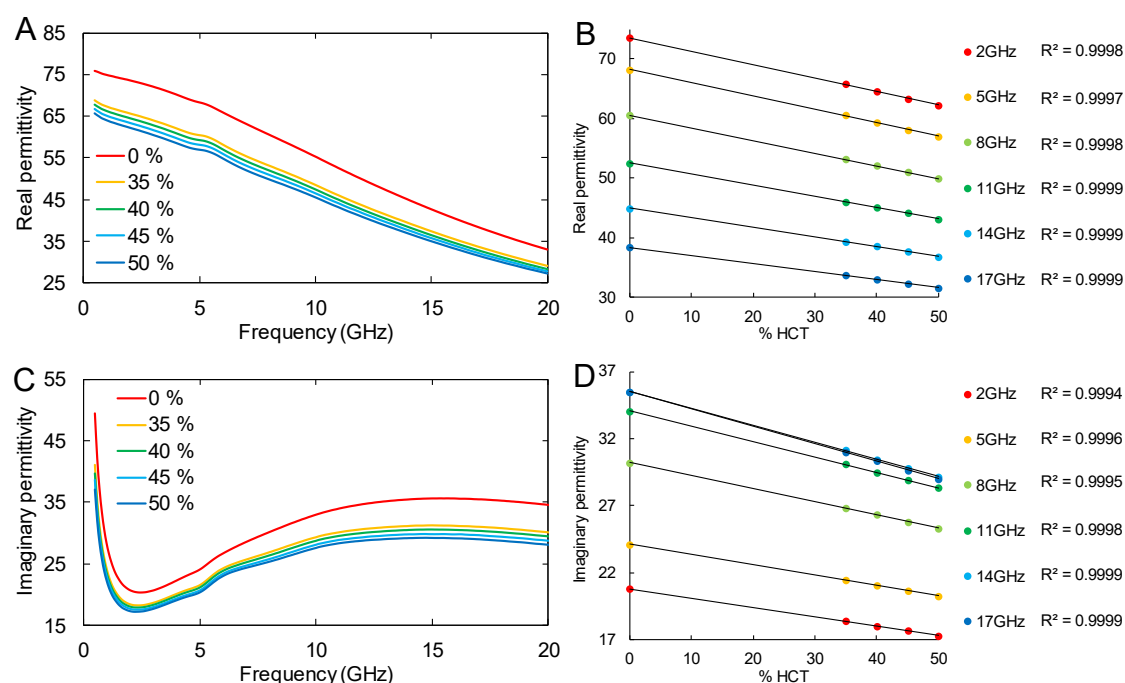


Figure 5.2: The mean (n=6) A) real and C) imaginary permittivity of physiological concentrations of %HCT (35 % - 50 %) diluted in osmotic water (288mOsmol/kg) measured between 0.5 -20 GHz at 0.1 GHz intervals. The mean (n=6) B) real and D) imaginary permittivity plotted against %HCT at a range of frequencies demonstrated the highly linear relation between the two, with $R^2 > 0.999$ across all frequencies measured, not just the sample shown.

5.3.2 Albumin

Increasing the physiological concentration of albumin (3.5 – 5.5 g/dl, n=6) in osmotic water (288 mOsmol/kg) led to a decrease in both the real (Figure 5.3.A) and imaginary (Figure 5.3.C) permittivity at all frequencies measured (0.5-20 GHz, 0.1 GHz intervals). Further, it was demonstrated that the change in permittivity relative to change in albumin was highly linear for both the real (Figure 5.3.B) and imaginary (Figure 5.3.D) permittivity, with $R^2 > 0.98$ at all frequencies shown, which held true at all other frequencies measured.

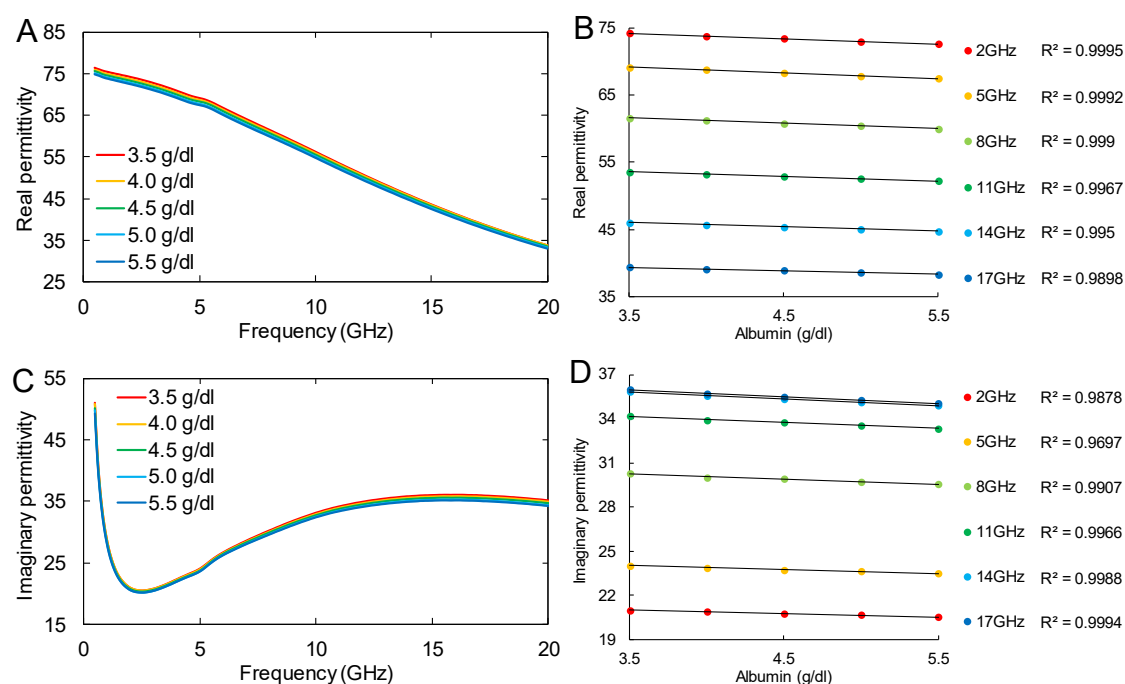


Figure 5.3: The A) real and C) imaginary permittivity (n=1) of physiological concentrations of albumin (3.5 – 5.5 g/dl) diluted in osmotic water (288mOsmol/kg) measured between 0.5 -20 GHz at 0.1 GHz intervals. The B) real and D) imaginary permittivity (n=1) plotted against albumin at a range of frequencies demonstrated the highly linear relation between the two, with $R^2 > 0.98$ across all frequencies measured, not just the sample shown.

5.3.3 NaCl

Increasing the concentration of NaCl to create increased physiological osmolality's (250 – 350 mOsmol/kg, 0.134 - 0.188 M, n=6) in deionised water led to a decrease in the real permittivity (Figure 5.4.A) at all frequencies measured (0.5-20 GHz, 0.1 GHz intervals), which became negligible by 20 GHz. By comparison, the imaginary permittivity (Figure 5.4.C) saw an increase at all frequencies measured (0.5-20 GHz, 0.1 GHz intervals), which became negligible by 20 GHz. Further, it was demonstrated that the change in permittivity relative to change in osmolality was highly linear for both the real (Figure 5.4.B) and imaginary (Figure 5.4.D) permittivity, with $R^2 > 0.80$ at all frequencies shown, which held true at all other frequencies measured.

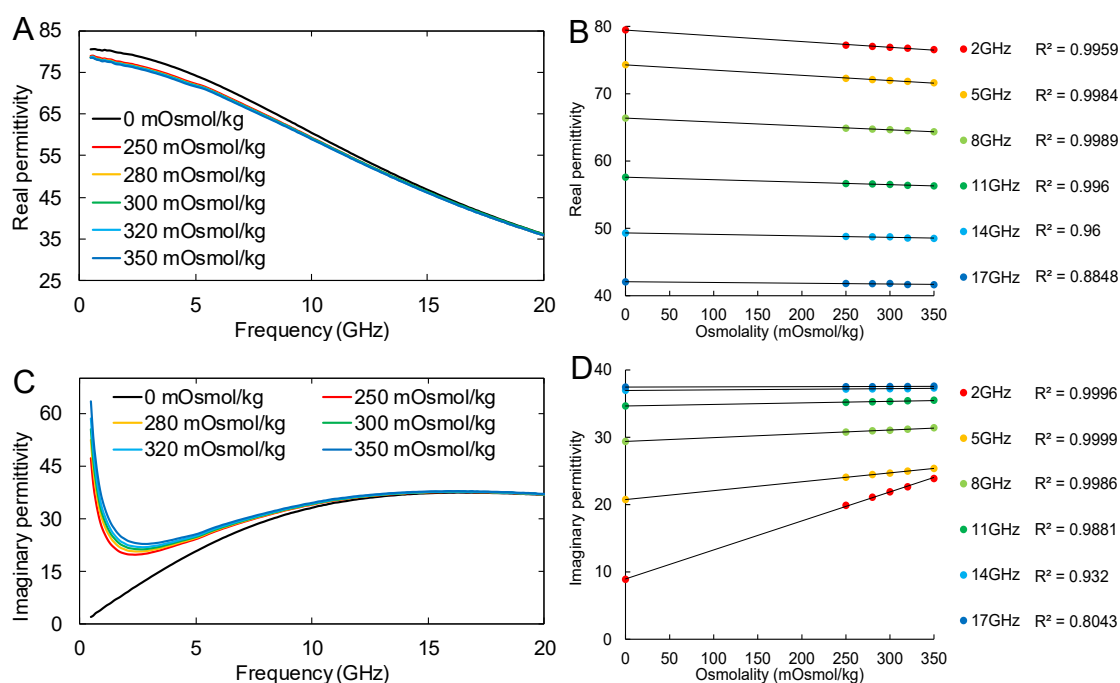


Figure 5.4: The mean (n=6) A) real and C) imaginary permittivity of physiological osmolality's (250 - 350 mOsmol/kg, 0.134 - 0.188 M) diluted in osmotic water (288mOsmol/kg) measured between 0.5 -20 GHz at 0.1 GHz intervals. The mean (n=6) B) real and D) imaginary permittivity plotted against osmolality at a range of frequencies demonstrated the highly linear relation between the two, with $R^2 > 0.80$ across all frequencies measured, not just the sample shown.

5.3.4 Glucose

Adding a high physiological concentration of glucose (200 mg/dl, $n=5$) to deionised water lead to no significant change in the real (Figure 5.5.A) and imaginary (Figure 5.5.B) permittivity of deionised water ($n=5$) measured between 0.5 and 20 GHz. The absolute % difference of the real permittivity was 0.056%, while the imaginary permittivity absolute % difference was 0.119%.

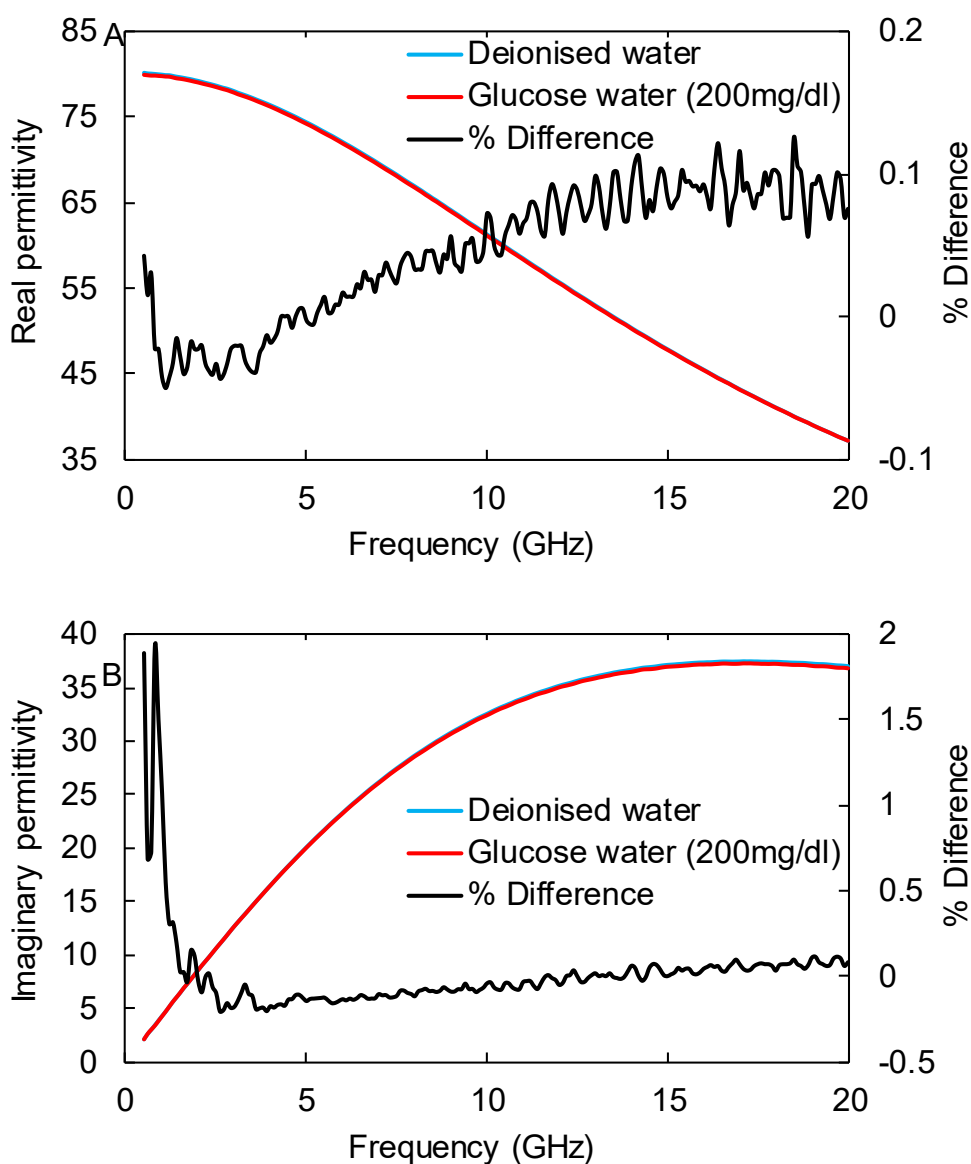


Figure 5.5: The mean ($n=5$) A) real and B) imaginary permittivity of a (red) high physiological concentration of glucose (200 mg/dl) diluted in deionised water, compared against the permittivity of (blue) deionised water. The (black) % difference between the two can also be seen, with the absolute % difference for the real permittivity being 0.056%, with the absolute % difference for the imaginary permittivity being 0.119%.

5.3.5 The effect of blood components on osmotic waters permittivity

The effect increasing (red) %HCT by 5 %, (green) albumin by 1 g/dl and (blue) osmolality by 10 mOsmol/kg on the real (Figure 5.6.A) and imaginary (Figure 5.6.C) permittivity of osmotic water (288 mOsmol/kg) can be seen. %HCT, albumin and osmolality all cause a decrease in the real permittivity with increased concentration, with %HCT and albumin sharing very similar profiles (Figure 5.6.B), with small differences appearing at changes associated with a high level of dehydration. Changes in the real permittivity with respect to osmolality tended to zero at 0 and 20 GHz, offering a window for %HCT and albumin to be measured independent of osmolality. By comparison, osmolality resulted in an increase in the imaginary permittivity, with the %HCT and albumin again sharing very similar profiles (Figure 5.6.D) with minimal differences appearing at changes associated with a high level of dehydration. Changes in the imaginary permittivity with respect to osmolality tended to zero at 20 GHz, offering a window for %HCT and albumin to be measured independent of osmolality.

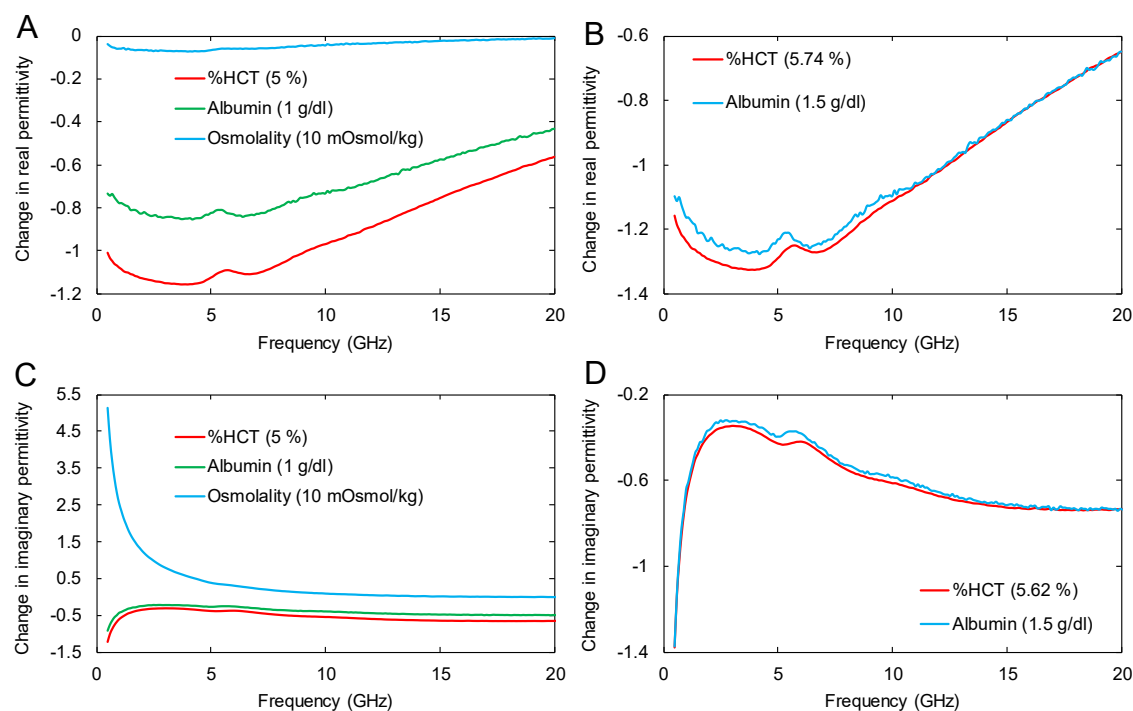


Figure 5.6: The change in A) real and C) imaginary permittivity (calculated from the gradients of permittivity values with respect to changes in blood component concentration seen in Figure 5.2-4) for an increase in (Red) %HCT by 5 %, (green) albumin by 1 g/dl and (blue) osmolality by 10 mOsmol/kg, plotted between 0.5 -20 GHz at 0.1 GHz intervals. The similarities between the B) real and D) imaginary permittivity profile of (blue) albumin and (Red) %HCT are highlighted.

5.4 Discussion: The effect of blood components on the permittivity of water

This study set out to develop a method to determine whether broadband microwave permittivity measurements of blood could be used to measure hydration for a specific species using a bovine model. This was done by examining the permittivity profile of key blood components: RBC's, Albumin and osmolality, calculated from permittivity measurements made across a range of physiological concentration.

5.4.1 %HCT

When examining the effect increasing %HCT has on the real and imaginary permittivity of osmotic water (Figure 5.2.A,C), it can be seen that there was a measurable decrease in both across all frequencies measured, in line with the current literature⁶⁰. Further as demonstrated in Figure 5.2.B,D, the response of the permittivity to change in concentration was linear at all frequencies. The decrease seen in the permittivity is caused by the low permittivity haemoglobin (large protein with few electrostatic interactions) occupying volume previously occupied by the high permittivity (from the H-bonds) water and is typically modelled using Maxwell-Garnett effective medium theory¹¹⁰.

5.4.2 Albumin

When examining the effect increasing albumin has on the real and imaginary permittivity of osmotic water (Figure 5.3.A,C), it can be seen that there was a measurable decrease in both across all frequencies measured, in line with the current literature^{60,111}. One exception to this was in a study by Basey-Fisher, 2011¹¹², who showed similar behaviours in the permittivity with increased protein content, except below 4GHz, where the imaginary permittivity increased. The author of this work believes that Basey-Fisher likely had the same issue as the author of this thesis, in that the protein had a small salt impurity as discussed in section 5.2.4 (which Basey-Fisher did not test for), which was amplified by his use of a pure water base solvent, resulting in this recorded increase. Further as demonstrated in Figure 5.3.B,D, the response of the permittivity to change in concentration was linear at all frequencies. Like with haemoglobin, the decrease

seen in the permittivity is caused by the low permittivity albumin protein occupying volume previously occupied by the high permittivity water.

5.4.3 NaCl

Increasing the concentration of NaCl in deionised water lead to differing responses in the real and imaginary permittivity, with the real permittivity (Figure 5.4.A) decreasing while the imaginary permittivity (Figure 5.4.C) increasing, in line with current findings^{60,113,114}. The decrease seen in the real permittivity follows a similar mechanism to that described above for the proteins, with the NaCl occupying some of the volume previously occupied by water dipolar interactions between $H^{\delta+}$ and $O^{\delta-}$ ¹¹⁵. Further, the ions reserve some of the surrounding water to form a hydration layer of bound water, further impacting on the dielectric response. The decrease in the real permittivity seen for NaCl is however considerably smaller compared to %HCT and albumin and is due to physiological concentrations of NaCl occupy less volume in the solvent. The increase seen in the imaginary permittivity with increased concentration of NaCl (Figure 5.4.C) can be explained by examining the interactions of dissolved Na⁺ and Cl⁻ ions in an electric field as discussed earlier. When the NaCl solution is placed in an oscillating electric field, the induced ionic motions absorb the field energy and dissipate it as heat, resulting in an increase in the loss factor. The effect of NaCl is frequency-dependent with higher loss at lower frequencies. However, over a frequency of ~10 GHz, this effect can be deemed to have a negligible impact on the loss factor within physiological limits^{60,73}. This effect can be examined using a Debye model¹¹⁶. When examining Figure 5.4.D, a minimum in the loss factor can be observed around 2 GHz. As all blood components were measured in osmotic fluid (created using NaCl), ionic dielectric polarisation also plays a role in the loss factor measured. The change in the loss factor observed is caused by the transition from dipole polarization loss mechanisms below 2 GHz, to ionic losses mechanism above 2GHz and is well documented¹¹⁷. Finally, much like %HCT and albumin, changes in NaCl concentration lead to a linear permittivity response at all frequencies measured (Figure 5.4.B,D).

5.4.4 Glucose

When examining the effect adding a high concentration of glucose to deionised water had on its real and imaginary permittivity (Figure 5.5), it can be seen that there was no significant change in the permittivity with average % differences being $> 0.12\%$. This is in line with current literature^{105,106}, and is explainable when looking at the structure of glucose. Glucose is a relatively small molecule processing a range of $-H$, $-OH$ and $=O$ groups. As such, it behaves in a similar fashion to the water it is dissolved in when it comes to its dielectric response, all-be-it at a lesser extent per volume. This is mirrored by the data, where it can be seen that the addition of glucose did in fact lead to a small decrease in permittivity, showing it lower H-bond density.

5.4.5 Effect of %HCT, albumin and osmolality on the real permittivity

When increasing the concentration of RBCs, albumin and NaCl in water (Figure 2.A, Figure 3.A and Figure 4.A respectively), a decrease in the real permittivity was seen at all frequencies measured to varying degrees. As the change in permittivity was linear with respect to concentration, the broadband change in permittivity with respect to different concentrations could be analysed as shown in Figure 5.6.A. When examining this figure, a few observations can be made. Firstly, albumin and %HCT share very similar plot profiles. When comparing the profiles further (Figure 5.6.B) it can be seen that there is little difference between the two over 10GHz, with only small differences occurring below 10 GHz, despite the figure depicting concentration changes coinciding with a high level of dehydration. This is not surprising considering the protein haemoglobin makes a big part of RBCs, with few other cell elements affecting the microwave permittivity. This could lend weight to the idea, that from a bovine hydration measurement perspective, there is little difference between RBC's and albumin. While this could make it difficult to isolate which variable is changing in a mixture, as broadband measurements were made, small changes in the profile could likely be picked out when larger changes in hydration occur. Secondly, when examining the plot profile of changing osmolality on Figure 5.6.A, it can be seen that osmolality had a very small contribution to the real permittivity which tends to zero at 0 and 20 GHz. This provides a window where other blood components could

be examined independently of osmolality which could help with the deduction of blood overall composition. Finally, when comparing the plot profiles of albumin and %HCT with a scaled-up osmolality it was found that there is a significant difference over the frequency spectrum, making osmolality easily identifiable from albumin and %HCT. However, over the normal osmolality changes observed due to dehydration, the changes in osmolality would likely merge with albumin and %HCT as noise. Overall, broadband real permittivity measurements would allow for the distinction of albumin and %HCT at high enough dehydrations, with osmolality having little impact.

5.4.6 Effect of %HCT, albumin and osmolality on the imaginary permittivity

When increasing the concentration of RBCs, albumin and NaCl in water (Figure 2.C, Figure 3.C and Figure 4.C respectively), it can be seen that while RBCs and albumin cause a decrease in the imaginary permittivity, while NaCl caused an increase. As the change in permittivity was linear with respect to concentration, the broadband change in permittivity with respect to different concentrations could be analysed as shown in Figure 5.6.C. When examining this figure, a few observations can be made. Firstly, much like with the real permittivity, albumin and %HCT share very similar plot profiles (Figure 5.6.D). The key difference being that the difference seen in their distribution occurring around 2-18 GHz. This again means it could be problematic to distinguish between the two without a large dehydration occurring. However, this similarity further adds to the idea that for bovine hydration measurement, there is little difference between RBC's and albumin. Secondly, when examining Figure 5.6.C., it is clear that NaCl has a significantly different plot profile. Further, at low frequencies tested, small changes in the osmolality cause a large measurable change in the imaginary permittivity, unlike in the real permittivity. Finally, when looking at osmolality, it can be seen that over 10GHz, the effect of osmolality tends to 0. This again offers a window in the data where other blood components could be examined independently of osmolality. In summary broadband imaginary permittivity measurements would struggle to distinguish between albumin and %HCT at all but the highest levels of dehydrations, while small changes in osmolality would be readily measurable around 0.5 GHz.

5.4.7 Limitation of the work

Previously in section 3.4.3, it was shown that the system had a mean 3.S.D repeatability of 0.32% for the real permittivity and mean 3.S.D repeatability of 0.33% for the imaginary permittivity. This translated to the system being sensitive to changes in permittivity of $\sim\pm 0.1$. While this may seem small, as demonstrated when measuring osmolality, this is rather large when measuring changes of ± 0.065 per ± 10 mOsmol/kg, as seen in Figure 5.4. However as demonstrated, with enough repeats, and due to the linear response to changes in concentration (Figure 5.4.B), small changes can be detected over a large enough change in osmolality.

When examining Figure 5.2, Figure 5.3 and Figure 5.4, it can be seen that the characteristic bumps described in section 3.4.1 in the data can be seen. However, as predicted, due to the main premise of the thesis focusing on the effect of change in physiological concentration of blood components on the permittivity, the effect of the bump carries across all the data for each individual blood component, making it a fixed constant error. While this leads to a distortion in the data in Figure 5.6.A and Figure 5.6.C, adding a bump, this could be modelled out by fitting to a Gaussian.

One of the main limitations relates to the experimental protocol. For albumin and %HCT measurements, osmolality was controlled and set at 288 mOsmol/kg. 288 mOsmol/kg was chosen as it is a hydrated physiological osmolality. As such, the corrective curves seen in Figure 5.6.A and Figure 5.6.C will only hold true at 288 mOsmol/kg. Further, as no measurement was taken with all 3 variables present, the effects of masking could not be assessed. However, the author believes that using the methods presented in the thesis, such data could be obtained in the future.

While this study examined the key blood components albumin, %HCT and osmolality, it omitted to fully analyse the effect of other blood components including glucose, white blood cells, clotting factors, or the blood protein globulin group, which could introduce a small amount of error. In Figure 5.5 it was shown that at high physiological concentrations of glucose had little to no impact on the permittivity, in line with others findings^{105,106}, suggesting that it could be treated as a small fixed constant error. White blood cells and clotting components typically make up <1% volume fraction of blood¹⁵. While their volume fraction

would increase during dehydration, it would only see a small increase in its volume fraction due to its initial low composition in the blood (and can instead be thought of as a small ever-present constant during measurement), resulting in a negligible change in the dielectric properties of blood and therefore error. The biggest source of error would likely come from not including the effect of the group of plasma proteins known as globulins, the second most prevalent blood protein. This protein was not measured in this work due to time constraints (consisting of 4 sub-groups and over 100 unique proteins¹¹⁸), but its effect on blood dielectrics could be quantified in future works following the same method used for albumin described above. Overall, the exclusion of glucose, white blood cells and other clotting components will have had little impact on the model's ability to determine changes in hydration, with only globulins exclusion being a potential source of error.

5.5 Summary of findings

Overall, this chapter laid the groundwork for the use of dielectric analysis to measure hydration using blood samples. It has shown that while increasing the concentration of NaCl, albumin and RBCs all cause a decrease in the dielectric constant of water = blood component mixtures, they affect the dielectric constant at different rates with respect to frequency, opening up the opportunity to determine changes in blood composition using either broadband or multi-frequency measurements. While NaCl, had the unique property of increasing the loss factor with increased concentration, the similarities between increasing RBC and albumin concentrations on the decrease of the loss factor with respect to frequency, makes them a less suitable measurement option for hydration.

Key findings and novelty of the work:

- Brought together dielectric measurement data for albumin, %HCT and osmolality for the purposes of analysing hydration measurement and explained why other blood components other than globulin were unlikely to impact the measurement of hydration.
- Proposed a method to analyse the feasibility of using blood to track the hydration of a specific species. This was demonstrated with a bovine model and could be applied to other species including humans.
- Demonstrated that within a bovine blood model, broadband microwave spectroscopy between 0.5-20.0 GHz could be used to measure the hydration.
- That a window exists above 18 GHz where %HCT and albumin can be measured independent of osmolality for both the dielectric constant and loss factor.
- Showed that while %HCT and albumin cause similar dielectric responses, there is a ~4.5 % difference in their concentration correction equations below 5 GHz allowing for distinction between the two.

Chapter 6

Final discussion and future work

6.1 Final discussion on the key findings

This PhD was initially funded on the premise of trying to help develop a non-invasive real-time wearable hydration monitor for use by sport and healthcare professionals. While this project was unable to fully reach this goal due to the time constraints of a PhD, we were able to make some significant contributions to the field by laying the ground works, showing that microwave dielectric measurements of blood could be used to measure hydration. This will help inform future research how best to realise this goal.

6.1.1 Inverted dielectric probe work

We developed a novel method for measuring the broadband permittivity of microliter samples while only introducing a small amount of error. This was done by repurposing a traditional dielectric probe by placing it upside down, using a pipette to place samples on the tip.

While characterising the setup, we found small “bumps” occurred in the data due to differences between the shape of the calibration fluid and the sample. However, we demonstrated that this error was negligible, and could be modelled out using Gaussians.

Later we found that the system had a time-dependent measurement characteristic which was likely caused by temperature variations between the sample and the probe, based on the fact it quickly reached equilibrium. While this could not be verified experimentally, it was found that the system had a repeatability equivalent to normal dielectric setups if the measurement was done quickly enough.

During the study, we were first to report that when making permittivity measurements of RBCs, there is a necessity to mix the sample well and making the measurement of the sample as quickly as possible. This is believed to be due to the effect of gravity pulling the denser RBCs to the bottom of the fluid and caused a drop in the permittivity measured.

Finally, while we were unable to determine the setups accuracy using a traceable fluid (due to no traceable fluid processing sufficient hydrostatic forces), by comparing the results of a permittivity measurement of a 0.1M NaCl solution

made using a normal dielectric setup with our inverted setup, we showed our system resulted in a muted permittivity response of ~3%.

6.1.2 Human blood measurement work

We conducted human dehydration trials where we measured whole blood permittivity alongside osmolality, weight and a range of other biometrics at three points between two high-intensity cycling phases in a heated room.

We validated that freezing point depression osmolality was not an accurate measure of hydration when using 20 μl of whole blood but worked appropriately when using 200 μl of whole blood.

We also showed that dehydration caused a measurable change in both the real and imaginary permittivity of blood, with some correlations being seen with osmolality and temperature at set frequencies.

Finally, we demonstrated that blood hydration could not be measured in the vis-IR region, due to both the RBCs creating scattering and water processing a very high absorption in this region. Further, it was shown that saline at a physiological osmolality caused no measurable difference when compared to deionised water.

6.1.3 Assessing the potential to measure hydration in bovine blood

In our published work, we produced a method for determining whether broadband microwave permittivity measurements of a species blood could be used to measure changes in hydration through determining composition. This was done by analysing the frequency-permittivity profiles of %HCT, albumin and NaCl dissolved individually in osmotic water. For our study we used a bovine model and were able to show that distinct changes occurred in the frequency-permittivity spectra for %HCT, albumin and NaCl, inferring that for bovine samples, blood hydration changes could be tracked.

We also showed that both RBCs and albumin caused decreases in both the real and imaginary permittivity at all frequencies. Further, we showed that until large decreases in either occurs, it was difficult to distinguish between there frequency-permittivity profile.

Finally, we showed increases in NaCl caused small decreased in the real permittivity which tended to zero at 20 GHz, with large increases occurring in the

imaginary permittivity tending to zero after 10 GHz. As a result, it was postulated that frequencies around 20 GHz would offer windows where other blood components (RBCs or proteins) could be measured independent of osmolality.

6.2 Analysis of the methodologies used and thoughts on the direction of future work

The author of this thesis understands that there are some rather glaring limitations with the work produced, be it due to equipment or methodology limitations. This section aims to discuss some of these issues and go over how future works may wish to approach these experiments. Later sections then go on to discuss other areas which need researching to fully develop this field.

6.2.1 Inverted dielectric probe work

During the initial characterisation of the probe, a whole host of issues occurred which ultimately led to issues with the system not being traceable as discussed in chapter 3.

While this work showed a fairly accurate method for making broadband permittivity measurements of microliter fluid samples, the main flaws in this study were introduced due to not enough fluid being measured. One solution to this issue would be to have a low permittivity cup placed around the tip of the probe, allowing for the use of more fluid, as seen in Figure 6.1. While this would not be possible for all samples, this could be done for blood, with ml's worth typically collected. However, the inverted probe setup would still be favourable, as it prevents the risk of air bubbles occurring.

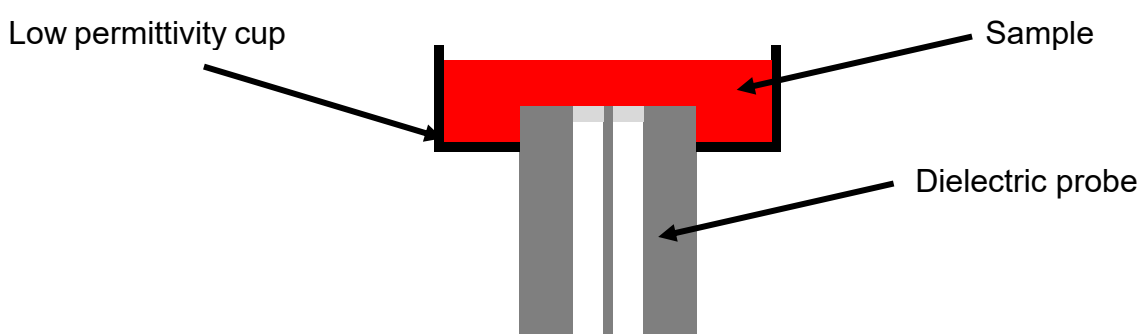


Figure 6.1: Proposed inverted dielectric probe setup with a low permittivity cup to measure larger sample volumes.

Using such a cup to hold fluids would likely help fix some of the other issues previously mentioned. With a large volume of sample, “bumps in the data” would be less likely to have occurred. Further, traceable fluids which had low electrostatic forces (so could not be pipetted onto the probe tip) could now be

used to accurately measure system accuracy and validate calibrations. Using such a cup would however have drawbacks, taking longer to clean, and being susceptible to cells sinking if it took too long to set up.

For this thesis, the probe and VNA used were limited to a working range of 0.5-20GHz. Future works may wish to use newer models which operate between 0.2-50GHz¹¹⁹, especially for blood measurements, as the permittivity properties described in this thesis have been shown to continue on to 40GHz¹²⁰.

6.2.2 Human blood measurement work

In hindsight, there is no denying that there were numerous flaws within the human trial, which prevented the experiment reaching its full potential. Through the use of an enhanced methodology, the author believes it should be possible to determine how each of %HCT, albumin, globulin and osmolality affect the permittivity of blood, and with enough data, be able to determine blood's composition (and therefore hydration) using an invasive blood permittivity measurement alone.

One of the biggest issues facing the author was the low "n" number. This was due to 3 main factors: the length of time needed for the study (within the working week), the harsh exercise regime involved and the blood collection requirement. All three factors resulted in poor recruitment. Unfortunately, there is little which can be done to improve the experimental regime as blood has to be collected and reducing the intensity of the exercise regime would increase the time requirement. As such, future studies should ideally advertise over a wider audience, and not set a date for experimental completion.

There were clear iterations occurring within the protocol between the first and second set of human trials with the addition of a range of additional biometrics being collected including age, height, blood oxygen and blood glucose. However, as shown in chapter 6, they did not go far enough, as we later learned protein concentration significantly affected the dielectric response of blood¹²⁰. As such, future work should at the very least aim to measure total protein content using a refractometer, or better still, use gel electrophoresis to determine the change in concentration of the different types of albumin and globulin. Measuring protein content accurately alongside %HCT and osmolality could allow for a more

accurate correlation between these blood composition and changes in permittivity measured.

During the second set of trials, blood glucose was additionally measured. However, this variable can be dropped having been shown to have little to no impact within the region tested. Blood oxygen saturation was also collected. However, due to how the samples were collected and tested, they were fully oxygenated. As such future experiments should examine the effect oxygen molecules have on the permittivity of the haemoglobin protein, so a better understanding of the effects of low blood oxygen on blood's permittivity can be made.

While %HCT was used as the main gauge for changes in RBC concentration, future works may wish to go further, and additionally quantify both cell density and haemoglobin levels. However, it should be noted that when measuring cell density, a machine should be used, as a haemocytometer method was found to be too inaccurate for the small changes in blood cell density, requiring a 1/200 dilution¹²¹. Measuring the haemoglobin protein may prove most beneficial, having been proved to be the main source of RBCs permittivity response. Further, when trying to standardise for the general population, measuring both haemoglobin and %HCT may prove vital to avoiding a potentially large source of error, with the concentration of haemoglobin in RBCs varying by over 5% within an individual^{122,123,124} alone.

Between studies, it was found that the additive lithium heparin had little impact on the dielectric properties of blood¹²⁵ unlike other more common additives¹²⁶, which was verified by the author. The decision was made not to change from the no additive tubes to the lithium heparin tubes to allow for the most accurate comparison of data from the two set of experiments. However, future works should use lithium heparin, as even though it only preserves the blood for 6-72 hours^{127,128} (depending on storage condition and component being measured), this is more than enough time to cool the samples to room temperature and measure their properties. This would also help eliminate the risk of the blood clotting prematurely (which occurred on multiple occasions when using the no additive tubes) preventing measurements and repeats being made. Further, as the samples could reach a truer room temperature, there would be less temperature variability in the permittivity measurement.

The temperature the sample was measured at could also be a source of error when it comes to transitioning data from room temperature blood permittivity measurements to body temperature measurements, as blood permittivity is known to have a complex relationship with temperature^{129,58}. During the planning phase, it was determined that the VNA would be outside its internal calibration window, if measurements were made in a body temperature room, hence measurements were made at room temperature. As such, future work should aim to use a VNA calibrated for use in a body temperature room, so blood measurements can be made at body temperature.

In summary, with a large enough study using the enhanced methodology described above, the author believes that changes in blood permittivity could be correlated to changes in %HCT, albumin, globulin and osmolality. The final validation test needing to be conducted would be a blind trial to determine whether broadband microwave permittivity measurements of blood could be used to accurately predict blood's composition, and therefore hydration.

6.2.3 Assessing the potential to measure hydration in bovine blood

Chapter 5 showed a novel approach to assessing whether a species blood could be used to track changes in hydration using broadband microwave permittivity. However, there were some parts of the methodology which did not go far enough, which future work may wish to build upon.

Within the experiment, each of the blood components albumin and %HCT were diluted in NaCl independent of each other. Future experiments should aim to make permittivity measurements while varying the concentration of the two in the same mixture to confirm that no masking effects take place between the two.

To reduce the experimental workload, the decision was made to have the osmolality of the albumin and %HCT experiments remain constant at 288 mOsmol/kg. While osmolality is unlikely to impact on the data generated for the real permittivity (only causing small changes), due to how sensitive the imaginary permittivity is to osmolality (change in salt concentration) at low frequencies below 10GHz, there is likely to be a small degree of variability in the data which should be explored.

During the experiment, RBCs were suspended in an osmotic solution contain only NaCl. This was done to reduce the complexity of the experiment, and because

RBCs are not damaged in such a solution. However, blood typically contains other salts like K^+ and Cl^- , which can process slightly different permittivity properties due to the differences in their size. As such future work should aim to quantify their effect.

6.2.4 Other areas of research

So far, the future works topics discussed have been related directly to topics discussed in this thesis. This section will cover areas slightly further afield both in topic and research applicability.

Effect of RBC shape and sickle cell anaemia detection

In patients with sickle cell anaemia a single amino acid in the haemoglobin protein is different compared to a health individual. This results in an additional hydrophobic binding site being present when the haemoglobin is deoxygenated. The hydrophobic spots on individual haemoglobin proteins stick together, resulting in long chains of haemoglobin molecules forming, rather than the typical homogeneous distribution of the haemoglobin^{130,131}. This in turn leads to the cell having a sickle shaped morphology¹³² as seen in Figure 6.2.A-B. While the change in the cell membrane shape and one different amino acid group on the haemoglobin molecule are in themselves unlikely to have an impact on the dielectric response at microwave frequencies as discussed earlier, the shape and distribution of the haemoglobin protein would. Numerous studies have shown that the shape of a dielectric object can affect its measured permittivity^{133,134,135,136}. This applies to the detection of sickle cell anaemia, as it is not unreasonable to believe that long fibres of haemoglobin stuck together which occur in sickle cell sufferers (Figure 6.2.C) would produce a significantly different permittivity profile compared to normal homogeneously distributed spherical haemoglobin proteins. Future work may want to examine this possibility using methodologies explored in this thesis.

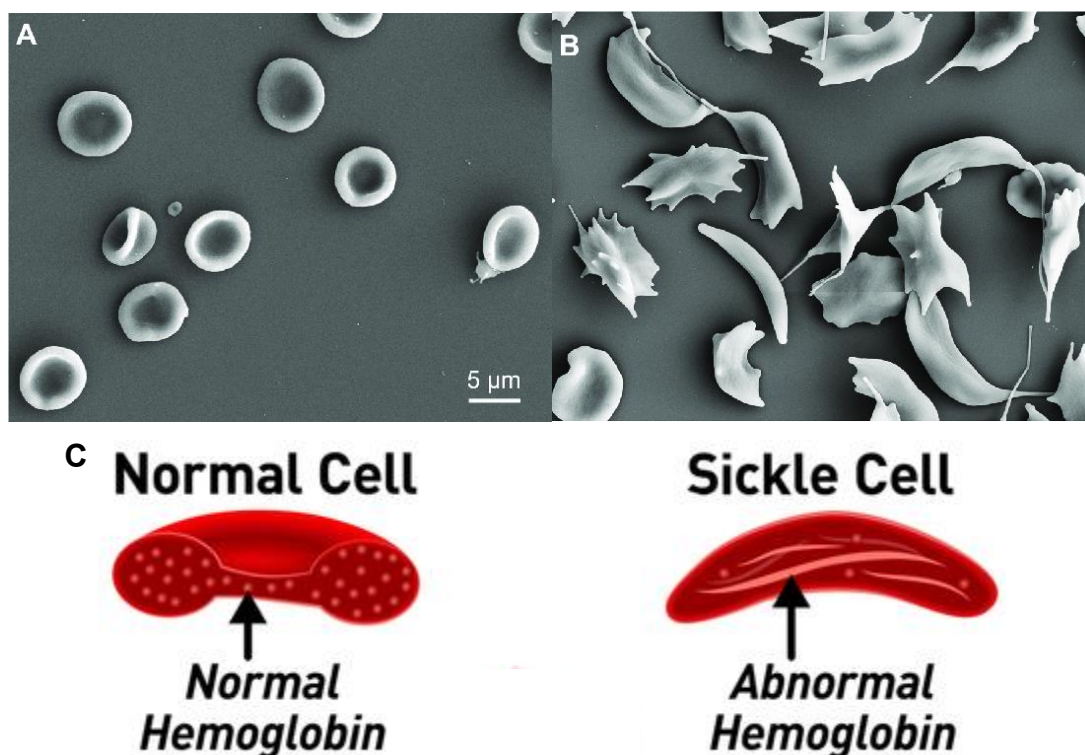


Figure 6.2: Scanning electron microscopy (SEM) image of sickle RBCs in a A) oxygenated and B) Deoxygenated state. Image adapted from (A.Abay,2019)¹³⁷. C) Shape of haemoglobin in normal and sickle cell anaemia (adapted from¹³⁸)

Invasive hydration monitoring device

As discussed above, the author believes there is a very high possibility that a database could be made showing the effect of %HCT, albumin, globulin and osmolality on the permittivity of blood. Were such a database to be made, the first area we could see hydration monitoring used relates to where blood is already being accessed invasively. As such, the first invasive devices are likely to be within hospital theatres to inform the surgeon on the hydration of the unconscious patient. Such a device will likely use broadband spectroscopy measurements. These devices could be taken further, acting as a sensor for a feedback loop controlling the mix of salt and water being put in a patient through an IV drip.

Multi frequency wearable non-invasive hydration monitoring device

As has been discussed, broadband spectroscopy will likely be able to detect changes in blood composition. However, to drive this technology forward into the wearable market, this is not going to be an option (unless nanoVNAs really jump forward¹³⁹). The alternative is to measure the permittivity at multiple frequencies

using at least 4 patch antennas operating at different frequencies (1 for each of the variables known to impact blood permittivity: %HCT, albumin, globulin and osmolality), and solving the simultaneous equations based on the change in permittivity to determine composition. This also comes with multiple challenges, namely building a small enough patch system, being able to measure blood through the skin, and accounting for the pressure fluctuations caused by the heart beating. However, this remains for future work.

Single frequency wearable non-invasive hydration monitoring device

During the human trials no visible correlation was seen between the imaginary permittivity and change in bodyweight Figure 4.3 or blood osmolality at lower frequencies (around 2 GHz). This is surprising considering that we later validated that the imaginary permittivity was highly sensitive to changes in NaCl within physiological osmolalities around this frequency. The lack of a correlation was likely due to the limitations with the experiment as described above, as well as participants deviating from the protocol. During future human trials, were, this correlation to be found, it could open up the option of a single frequency hydration monitoring device in the form of a dielectric resonator operating around 2 GHz. Such a device would however have the limitation of only informing on changes in blood osmolality and protein level, however, this would still give enough information to inform on hydration in a non-clinical setting.

List of publications

Dawsmith, W., Ohtani, N., Donnan, R., Naftaly, M., Dudley, R. A., Chowdhury, T. T. (2020). Microwave Frequency Dependent Dielectric Properties of Blood as a Potential Technique to Measure Hydration. *IEEE Access*. [10.1109/ACCESS.2020.2977432](https://doi.org/10.1109/ACCESS.2020.2977432)
<https://ieeexplore.ieee.org/document/9019690>

Conference and symposium contributions

Oral presentations

Dawsmith, W., Ohtani, N., Donnan, R., Dudley, R. A., & Chowdhury, T. T. *Monitoring Dehydration with Osmolality in Whole-Blood Specimens Collected from Cycling Athletes*. BioMedEng18. Imperial Collage, London.

Date: Friday 7th September 2018.

Dawsmith, W., Ohtani, N., Donnan, R., Dudley, R. A., & Chowdhury, T. T. *Microwave dielectric measurements of bovine blood for the creation of a predictive computational model*. 2nd Russell Binions PhD Symposium. Queen Mary University of London, London.

Date: Tuesday 23rd April 2019.

Dawsmith, W., Ohtani, N., Donnan, R., Dudley, R. A., & Chowdhury, T. T. *Examining the Potential of Microwave Dielectric Measurements to Track Hydration Status using a Bovine Blood Model*. Biology Meets Physics Symposium. Queen Mary University of London, London.

Date: Friday 20th September 2019.

Poster presentations

NPL PGI Conference

Non-Invasive Human Hydration Monitor. NPL, London.

Date: Friday 30th September 2016.

The Industrial Liaison Forum

Characterisation of a dielectric probe to monitoring hydration levels in vitro.

Queen Mary University of London, London.

Date: Wednesday 22nd November 2017.

The Industrial Liaison Forum

Measuring the dehydration of whole blood collected from exercising athletes using a dielectric system. Queen Mary University of London, London.

Date: Wednesday 14th November 2018.

BioMedEng19

Microwave dielectric measurements of bovine blood for the creation of a predictive computational model. Imperial Collage, London.

Date: Thursday 5th September 2019.

Stand presentation

Wearable Technology Show 2018

NPL HydarSense on behalf of Innovation UK

ExCel London

Date: Tuesday 13th March 2018 – Wednesday 14th March 2018.

References

1. Campbell, N. Dehydration: why is it still a problem? *Nurs. Times* **107**, 12–15 (2011).
2. NHS England. *Guidance – Commissioning Excellent Nutrition and Hydration 2015 – 2018*. (2015).
3. Bar-david, Y., Urkin, J. & Kozminsky, E. The effect of voluntary dehydration on cognitive functions of elementary school children. *Acta Paediatr.* **94**, 1667–1673 (2005).
4. Masento, N. A., Golightly, M., Field, D. T., Butler, L. T. & van Reekum, C. M. Effects of hydration status on cognitive performance and mood. *Br. J. Nutr.* **111**, 1841–1852 (2014).
5. Pawson, C. *et al.* Drink availability is associated with enhanced examination performance in adults. **19**, 57–66 (2013).
6. Montain, S. J. Hydration recommendations for sport 2008. *Curr. Sports Med. Rep.* **7**, 187–192 (2008).
7. Maughan, R. J. & Shirreffs, S. M. Dehydration and rehydration in competitive sport. *Scand. J. Med. Sci. Sport.* **20**, 40–47 (2010).
8. NHS. *Medicines and Dehydration Patient Information*. (NHS).
9. Dr Richard K. Bernstein. *Dr Bernstein's Diabetes Solution: A Complete Guide To Achieving Normal Blood Sugars*. (Little, Brown US, 2011).
10. Tomson, C. R. V. Advising dialysis patients to restrict fluid intake without restricting sodium intake is not based on evidence and is a waste of time. *Nephrol. Dial. Transplant.* **16**, 1538–1542 (2001).
11. Office for National Statistics. *Deaths from dehydration and malnutrition, by place of death, England and Wales, 2014-2015*. (2016).
12. O'Donoghue, D. Flawed NHS care 'leads to 12,000 kidney deaths a year'. *British Broadcasting Corporation* (2013).
13. Shepherd, A. Measuring and managing fluid balance. *Nurs. Times* **107**, 12–16 (2011).
14. John McMurry, M. E. C. *Fundamentals of General, Organic, and Biological Chemistry*. (Prentice Hall, 2002).
15. G.J.Tortora, B. D. *Principles of Anatomy & Physiology*. (Wiley, 2011).
16. Yawn, D. H. Plasma. *Encyclopædia Britannica* (2020). Available at: <https://www.britannica.com/science/plasma-biology>.
17. Thornton, S. N. Thirst and hydration: Physiology and consequences of dysfunction. *Physiol. Behav.* **100**, 15–21 (2010).
18. Costill, D. L., Coté, R. & Fink, W. Muscle water and electrolytes following varied levels of dehydration in man. *J. Appl. Physiol.* **40**, 6–11 (1976).
19. Fortney, S. M., Nadel, E. R., Wenger, C. B. & Bove, J. R. Effect of blood volume on sweating rate and body fluids in exercising humans. *J. Appl. Physiol.* **51**, 1594–1600 (1981).
20. Armstrong, L. E. Hydration assessment techniques. *Nutr. Rev.* **63**, 40–54 (2005).
21. Shirreffs, S. M. Markers of hydration status. *Eur. J. Clin. Nutr.* **40**, 6–9 (2003).
22. Bak, A., Tsiami, A. & Greene, C. Methods of Assessment of Hydration Status and their Usefulness in Detecting Dehydration in the Elderly. *Curr. Res. Nutr. Food Sci.* **5**, 43–54 (2017).
23. Armstrong, L. E. Assessing hydration status: the elusive gold standard. *J. Am. Coll. Nutr.* **26**, 575–584 (2007).
24. Hughes, F., Mythen, M. & Montgomery, H. The sensitivity of the human thirst response to changes in plasma osmolality: a systematic review. *Perioper. Med.* **7**, 1–11 (2018).
25. McKenzie, A. L. & Armstrong, L. E. Monitoring Body Water Balance in Pregnant and Nursing Women: The Validity of Urine Color. *Ann. Nutr. Metab.* **70**, 18–22 (2017).
26. Tucker, M. A. *et al.* Spot Sample Urine Specific Gravity Does Not Accurately Represent Small Decreases in Plasma Volume in Resting Healthy Males. *J. Am. Coll. Nutr.* **37**, 17–23 (2018).
27. Hustrini, N. M., Siregar, P., Nainggolan, G. & Harimurti, K. Diagnostic Performance of Afternoon Urine Osmolality to Assess Optimal Hydration Status in an Adult Healthy Population. *Acta Med. Indones.* **49**, 112–117 (2017).
28. Maughan, R. J., Shirreffs, S. M. & Leiper, J. B. Errors in the estimation of hydration status from changes in body mass. *J. Sports Sci.* **25**, 797–804 (2007).
29. Ely, B. R. *et al.* Assessment of extracellular dehydration using saliva osmolality. *Eur. J. Appl. Physiol.* **114**, 85–92 (2014).
30. Ely, B. R., Cheuvront, S. N., Kenefick, R. W. & Sawka, M. N. Limitations of salivary osmolality as a marker of hydration status. *Med. Sci. Sports Exerc.* **43**, 1080–1084 (2011).

31. Fortes, M. B. *et al.* Tear fluid osmolarity as a potential marker of hydration status. *Med. Sci. Sports Exerc.* **43**, 1590–1597 (2011).
32. Ungaro, C. T. *et al.* Non-invasive estimation of hydration status changes through tear fluid osmolarity during exercise and post-exercise rehydration. *Eur. J. Appl. Physiol.* **115**, 1165–1175 (2015).
33. Arroyo, D. *et al.* Intraperitoneal Fluid Overestimates Hydration Status Assessment by Bioimpedance Spectroscopy. *Perit. Dial. Int.* **35**, 85–89 (2014).
34. Dasgupta, I. *et al.* Validating the use of bioimpedance spectroscopy for assessment of fluid status in children. *Pediatr. Nephrol.* **33**, 1601–1607 (2018).
35. Zaloszc, A. *et al.* Hydration measurement by bioimpedance spectroscopy and blood pressure management in children on hemodialysis. *Pediatr. Nephrol.* **28**, 2169–2177 (2013).
36. Meyers, S. M. *et al.* Does hydration status affect MRI measures of brain volume or water content? *J. Magn. Reson. Imaging* n/a-n/a (2016). doi:10.1002/jmri.25168
37. Sawant, A. *et al.* Association between muscle hydration measures acquired using bioelectrical impedance spectroscopy and magnetic resonance imaging in healthy and hemodialysis population. *Physiol. Rep.* **3**, 1–10 (2015).
38. Mirrashed, F. & Sharp, J. C. In vivo quantitative analysis of the effect of hydration (immersion and vaseline treatment) in skin layers using high-resolution MRI and magnetisation transfer contrast. *Ski. Res. Technol.* **10**, 14–22 (2004).
39. Nakamura, K., Brown, R. A., Araujo, D., Narayanan, S. & Arnold, D. L. Correlation between brain volume change and T2 relaxation time induced by dehydration and rehydration: Implications for monitoring atrophy in clinical studies. *NeuroImage Clin.* **6**, 166–170 (2014).
40. Li, M., Vassiliou, C. C., Colucci, L. a & Cima, M. J. ¹H nuclear magnetic resonance (NMR) as a tool to measure dehydration in mice. *NMR Biomed.* **28**, 1031–1039 (2015).
41. Sarvazyan, A., Tatarinov, A. & Sarvazyan, N. Ultrasonic assessment of tissue hydration status. *Ultrasonics* **43**, 661–671 (2005).
42. Sarvazyan, A. P. Ultrasonic water content monitor and methods for monitoring tissue hydration. (2006).
43. Sarvazyan, A. P. INFANT HYDRATION MONITOR. (2007).
44. mx3-Siliva Monitor. Available at: <https://www.mx3diagnostics.com/hydration-science>.
45. Lu, Y. *et al.* A Portable System to Monitor Saliva Conductivity for Dehydration Diagnosis and Kidney Healthcare. *Sci. Rep.* 1–9 (2019). doi:10.1038/s41598-019-51463-8
46. Colucci, L. A. *et al.* Fluid assessment in dialysis patients by point-of-care magnetic relaxometry. *Sci. Transl. Med.* **11**, 1–14 (2019).
47. Sixty-Hydration Monitor. Available at: <https://sixty.ie/>.
48. LVL-Hydration Monitor. Available at: <https://www.kickstarter.com/projects/lactate-threshold/lvl-the-first-wearable-hydration-monitor/description>.
49. Joshi, A., Bennett, D. B. & Stafsudd, O. M. Monitoring Corneal Hydration With a Mid-infrared (IR) Laser. *Ocul. Surf.* **13**, 43–46 (2015).
50. Qassem, M. & Kyriacou, P. Review of Modern Techniques for the Assessment of Skin Hydration. *Cosmetics* **6**, 1–28 (2019).
51. Garrett, D. C., Fear, E. C. & Member, S. Feasibility Study of Hydration Monitoring Using Microwaves – Part 1 : A Model of Microwave Property Changes With Dehydration. *IEEE J. Electromagn. RF Microwaves Med. Biol.* **3**, 292–299 (2019).
52. Garrett, D. C. *et al.* Feasibility Study of Hydration Monitoring Using Microwaves – Part 2 : Measurements of Athletes. *IEEE J. Electromagn. RF Microwaves Med. Biol.* **3**, 300–307 (2019).
53. Shahzad, A., Khan, S., Jones, M., Dwyer, R. M. & O'Halloran, M. Investigation of the effect of dehydration on tissue dielectric properties in ex vivo measurements. *Biomed. Phys. Eng. Express* **3**, 1–9 (2017).
54. Wang, J., Zilic, Z. & Shu, Y. Evaluation of an RF wearable device for non-invasive real-time hydration monitoring. *2017 IEEE 14th Int. Conf. Wearable Implant. Body Sens. Networks* 91–94 (2017). doi:10.1109/BSN.2017.7936015
55. Pollacco, D. A. *et al.* Characterization of the dielectric properties of biological tissues using mixture equations and correlations to different states of hydration. *Biomed. Phys. Eng. Express* **5**, 1–15 (2019).
56. Gu, S., Lin, T. & Lasri, T. Broadband dielectric characterization of aqueous saline solutions by an interferometer-based microwave microscope. *Appl. Phys. Lett.* **108**, 1–4 (2016).
57. Jaspard, F., Nadi, M. & Rouane, A. Dielectric properties of blood : an investigation of haematocrit dependence. *Physiol. Meas.* **24**, 137–147 (2003).

58. Wolf, M., Gulich, R., Lunkenheimer, P. & Loidl, A. Broadband dielectric spectroscopy on human blood. *Biochim. Biophys. Acta - Gen. Subj.* **1810**, 727–740 (2011).
59. Grant, E. H. & Sheppard, R. J. Relationship between the electrical permittivity of whole blood and the haemoglobin content. *Phys. Med. Biol.* **19**, 153–160 (1974).
60. Basey-Fisher, T. H. *et al.* Microwaving blood as a non-destructive technique for haemoglobin measurements on microlitre samples. *Adv. Healthc. Mater.* **3**, 536–542 (2014).
61. Basey-fisher, T. H. *Biosensing with Microwave Debye Relaxation Analysis.* (Imperial College London, 2013).
62. Rose, D. P. *et al.* Adhesive RFID sensor patch for monitoring of sweat electrolytes. *IEEE Trans. Biomed. Eng.* **62**, 1457–1465 (2015).
63. Brueck, A., Iftekhhar, T., Stannard, A. B., Yelamarthi, K. & Kaya, T. A Real-Time Wireless Sweat Rate Measurement System for Physical Activity Monitoring. *Sensors (Basel)*. **18**, 1–12 (2018).
64. Salvo, P., Pingitore, A., Barbini, A. & Francesco, F. Di. A wearable sweat rate sensor to monitor the athletes' performance during training Mise au point d'un capteur de mesure de la sudation durant. *Sci. & Sport.* **33**, 51–58 (2018).
65. Scott, J. *et al.* The effect of the moisture content of a local heat source on the blood flow response of the skin. *Arch. Dermatol. Res.* **301**, 581–585 (2009).
66. Mendelson, Y. Pulse Oximetry : Theory and Applications for Noninvasive Monitoring. *Clin. Chem.* **38**, 1601–1607 (1992).
67. Chen, Y. *et al.* Skin-like biosensor system via electrochemical channels for noninvasive blood glucose monitoring. *Sci. Adv.* **3**, 1–7 (2017).
68. Choi, H. *et al.* Design and In Vitro Interference Test of Microwave Noninvasive Blood Glucose Monitoring Sensor. *IEEE Trans. Microw. Theory Tech.* **63**, 3016–3025 (2015).
69. Hale, G. M. & Query, M. R. Optical Constants of Water in the 200-nm to 200-um Wavelength Region. *Appl. Opt.* **12**, 555–563 (1989).
70. Tsenkova, R. Aquaphotomics Tenth Anniversary. *NIR news* **27**, 45–47 (2016).
71. Berneis, K. & Keller, U. Bioelectrical impedance analysis during acute changes of extracellular osmolality in man. *Clin. Nutr.* **19**, 361–366 (2000).
72. AURA Band. Available at: <https://www.kickstarter.com/projects/1559547824/aura-band-ultimate-fitness-tracker/comments>.
73. Watts, C. *Electromagnetic sensing of cell suspensions in microfluidic systems.* (IMPERIAL COLLEGE LONDON, 2017).
74. Agilent Technologies. *Agilent Basics of Measuring the Dielectric Properties of Materials Application note.* **2005**, (2005).
75. Vinh, N. Q. *et al.* High-precision gigahertz-to-terahertz spectroscopy of aqueous salt solutions as a probe of the femtosecond-to-picosecond dynamics of liquid water. *J. Chem. Phys.* **142**, 1–7 (2015).
76. Gortner, R. A. THE STATE OF WATER IN COLLOIDAL AND LIVING SYSTEMS. *Trans. Faraday Soc.* **36**, 678–686 (1930).
77. Buchner, R., Barthel, J. & Stauber, J. The dielectric relaxation of water between 0°C and 35°C. *Chem. Phys. Lett.* **306**, 57–63 (1999).
78. Li, L., Li, C., Zhang, Z. & Alexov, E. On the Dielectric “ Constant ” of Proteins: Smooth Dielectric Function for Macromolecular Modeling and Its Implementation in DelPhi. *J. Chem. Comput.* **9**, 2126–2136 (2013).
79. Ling, G. What Determines the Normal Water Content of a Living Cell? *Physiol. Chem. Phys. Med. NMR* **36**, 1–19 (2004).
80. Daseler, W., Steinhoff, H. J. & Redhardt, A. A new method for the determination of the permittivity of small samples in the microwave range and its application to hemoglobin single crystals. *J. Biochem. Biophys. Methods* **22**, 69–82 (1991).
81. Foster, K. R. & Schwan, H. P. Dielectric properties of tissues and biological materials: a critical review. *Crit Rev Biomed Eng.* **17**, 25–104 (1989).
82. R.A. Freedman, H. D. Y. *Sears and Zemansky's University Physics With Modern Physics.* (Addison-Wesley, 1999).
83. Petosa, A. & Ittipiboon, A. Dielectric Resonator Antennas : A Historical Review and the Current State of the Art. *EEE Antennas Propag. Mag.* **52**, 91–116 (2010).
84. Keysight. *Keysight 85070E Dielectric Probe Kit 200 MHz to 50 GHz Technical Overview.* (2017).
85. Gregory, A. & Clarke, R. N. Dielectric Metrology with Coaxial Sensors. *Meas. Sci. Technol.* **18**, 1–18 (2007).
86. Zhang, C. & Carloni, P. Salt effects on water / hydrophobic liquid interfaces : a molecular

- dynamics study. *J. Phys. Condens. Matter* **24**, 1–6 (2012).
87. Santorelli, A. *et al.* Investigation of Anemia and the Dielectric Properties of Human Blood at Microwave Frequencies. *IEEE Access* **6**, 1–8 (2018).
 88. Hamouti, N., Del Coso, J. & Mora-Rodriguez, R. Comparison between blood and urinary fluid balance indices during dehydrating exercise and the subsequent hypohydration when fluid is not restored. *Eur. J. Appl. Physiol.* **113**, 611–620 (2013).
 89. Dill, D. B. & Costill, D. L. Calculation of percentage changes in volumes of blood, plasma, and red cells in dehydration. *J. Appl. Physiol.* **37**, 247–248 (1974).
 90. Sawka, M. N., Young, A. J., Francesconi, R. P., Muza, S. R. & Pandolf, K. B. Thermoregulatory and blood responses during exercise at graded hypohydration levels. *J. Appl. Physiol.* **59**, 1394–1401 (1985).
 91. Montain, S. J. & Coyle, E. F. Influence of graded dehydration on hyperthermia and cardiovascular drift during exercise. *J. Appl. Physiol.* **73**, 1340–1350 (1992).
 92. Hamilton, M. T., Gonzalez-Alonso, J., Montain, S. J. & Coyle, E. F. Fluid replacement and glucose infusion during exercise prevent cardiovascular drift. *J. Appl. Physiol.* **71**, 871–877 (1991).
 93. Logan-Sprenger, H. M., Heigenhauser, G. J. F., Jones, G. L. & Spriet, L. L. The effect of dehydration on muscle metabolism and time trial performance during prolonged cycling in males. *Physiol. Rep.* **3**, 1–13 (2015).
 94. Armstrong, L. E. *et al.* Thermal and circulatory responses during exercise: effects of hypohydration, dehydration, and water intake. *J Appl Physiol* **82**, 2028–2035 (1997).
 95. González-Alonso, J., Mora-Rodríguez, R., Below, P. R. & Coyle, E. F. Dehydration markedly impairs cardiovascular function in hyperthermic endurance athletes during exercise. *J. Appl. Physiol.* **82**, 1229–1236 (1997).
 96. González-Alonso, J., Calbet, J. A. & Nielsen, B. Muscle blood flow is reduced with dehydration during prolonged exercise in humans. *J. Physiol.* **513**, 895–905 (1998).
 97. Chevront, S. N., Kenefick, R. W., Heavens, K. R. & Spitz, M. G. A comparison of whole blood and plasma osmolality and osmolarity. *J. Clin. Lab. Anal.* **28**, 368–373 (2014).
 98. Rocks, B. F., Sherwood, R. A. & Cook, J. G. H. Whole blood osmolality. *Ann. Clin. Biochem.* **23**, 106–108 (1986).
 99. Sollanek, K. J., Kenefick, R. W. & Chevront, S. N. Importance of sample volume to the measurement and interpretation of plasma osmolality. *J. Clin. Lab. Anal.* **33**, 1–6 (2018).
 100. Gabriel, C., Gabriel, S. & Corthout, E. The dielectric properties of biological tissues: I. Literature survey. *Phys. Med. Biol.* **41**, 2231–2249 (1996).
 101. Alison, J. M. & Sheppard, R. J. Dielectric properties of human blood at microwave frequencies. *Phys. Med. Biol.* **38**, 971–978 (1993).
 102. Ikegawa, S., Kamijo, Y., Okazaki, K., Masuki, S. & Okada, Y. Effects of hypohydration on thermoregulation during exercise before and after 5-day aerobic training in a warm environment in young men. *J Appl Physiol* **110**, 972–980 (2011).
 103. Armstrong, L. E. Hydration assessment techniques. *Nutr. Rev.* **63**, S40–S54 (2005).
 104. Zhou, J. *et al.* Reference Values for Continuous Glucose Monitoring in Chinese Subjects. *Diabetes Care* **32**, 1188–1193 (2009).
 105. T. Karacolak, E. C. Moreland, E. T. Cole–cole model for glucose-dependent dielectric properties of blood plasma for continuous glucose monitoring. *Microw. Opt. Technol. Lett.* **55**, 1160–1164 (2013).
 106. Yilmaz, T., Foster, R. & Hao, Y. Radio-Frequency and Microwave Techniques for Non-Invasive Measurement of Blood Glucose Levels. *Diagnostics (Basel)* **9**, 1–34 (2019).
 107. Mackowiak, P. A., Wasserman, S. S. & Levine, M. M. A Critical Appraisal of 98.6°F, the Upper Limit of the Normal Body Temperature, and Other Legacies of Carl Reinhold August Wunderlich. *JAMA* **268**, 1578–1580 (1992).
 108. Akerlof, G. Dielectric constant of some organic solvent-water mixtures at various temperatures. *J. Am. Chem. Soc* **54**, 4125–4139 (1932).
 109. Stadie, W. C. & Sunderman, F. W. The osmotic coefficient of sodium in sodium hemoglobinate and of sodium chloride in hemoglobin solution. *J. Biol. Chem.* **91**, 227–241 (1931).
 110. Smith, G. B. Dielectric constants for mixed media Dielectric constants for mixed media. *J. Phys. D Appl. Phys* **10**, 39–42 (1977).
 111. Zhadobov, M. *et al.* Complex Permittivity of Representative Biological Solutions in the 2–67 GHz Range. *Bioelectromagnetics* **33**, 346–355 (2012).
 112. Basey-Fisher, T. H. *et al.* Microwave Debye relaxation analysis of dissolved proteins: Towards free-solution biosensing. *Appl. Phys. Lett.* **99**, 1–3 (2011).
 113. Buchner, R., Hefter, G. T. & May, P. M. Dielectric Relaxation of Aqueous NaCl Solutions.

- J. Phys. Chem. A* **103**, 1–9 (1999).
114. Peyman, A., Gabriel, C. & Grant, E. H. Complex Permittivity of Sodium Chloride Solutions at Microwave Frequencies. *Bioelectromagnetics* **28**, 264–274 (2007).
 115. C, R. M. & Hollis-Hallett, A. C. The static dielectric constant of NaCl, KCl and KBr at temperatures between 4.2°K and 300°K. *Can. J. Phys.* **44**, 2211–2230 (1966).
 116. Debye, P. J. W. *Polar molecules*. Chemical Catalog Company Incorporated (1929).
 117. Barba, A. A. & D'Amore, M. Relevance of Dielectric Properties in Microwave Assisted Processes. in *Microwave Materials Characterization* (ed. Costanzo, S.) 91–118 (2012). doi:10.5772/2687
 118. Template:Globular proteins. *Wikipedia* Available at: https://en.wikipedia.org/wiki/Template:Globular_proteins.
 119. Keysight. *Keysight N1501A Dielectric Probe Kit 10 MHz to 50 GHz Technical Overview*. (2018).
 120. Basey-Fisher, T. H. *et al.* Microwaving blood as a non-destructive technique for haemoglobin measurements on microlitre samples. *Adv. Healthc. Mater.* **3**, 536–542 (2014).
 121. Berkson, J., Magath, T. B. & Hurn, M. Laboratory Standards in Relation to Chance Fluctuations of the Erythrocyte Count as Estimated with the Hemocytometer. *J. Am. Stat. Assoc.* **30**, 414–426 (1935).
 122. Brown, A. & Goodall, A. L. Normal variations in blood haemoglobin concentration. *J. Physiol.* **104**, 404–407 (1946).
 123. Ponder, E. & Barreto, D. THE VARIATION IN THE CORPUSCULAR HEMOGLOBIN CONCENTRATION IN THE HUMAN RED CELL, AS MEASURED BY DENSITOMETRY. *J. Gen. Physiol.* **39**, 23–29 (1955).
 124. Malka, R., Delgado, Francisco Feijó Manalis, S. R. & Higgins, J. M. In Vivo Volume and Hemoglobin Dynamics of Human. *PLoS Comput. Biol.* **10**, 1–12 (2014).
 125. Dunne, E. *et al.* Heparin as an Anticoagulant for the Dielectric Measurement of Blood. *IEEE Trans. Dielectr. Electr. Insul.* **26**, 229–234 (2019).
 126. Salahuddin, S. *et al.* Effects of Standard Coagulant Agents on the Dielectric Properties of Fresh Human Blood. *IEEE Trans. Dielectr. Electr. Insul.* **24**, 3283–3289 (2017).
 127. Dupuy, A. M. *et al.* Stability of routine biochemical analytes in whole blood and plasma / serum: focus on potassium stability from lithium heparin. *Clin. Chem. Lab. Med.* **56**, 413–421 (2018).
 128. Jinks, D., Brooks-white, R. & Bush, V. Evaluation of Refrigerated Stability of 15 Analytes in Lithium Heparin Gel Primary Tubes. *Lab. Med.* **44**, 45–51 (2013).
 129. Jaspard, F. & Nadi, M. Dielectric properties of blood: an investigation of temperature dependence. *Physiol. Meas.* **23**, 547 (2002).
 130. Levinthal, C., Wodak, S. J., Kahn, P. & Dadvanian, A. K. Hemoglobin Interaction in Sick Cell Fibers I : Theoretical Approaches to the Molecular Contacts. *Proc. Natl. Acad. Sci. U. S. A.* **72**, 1330–1334 (1976).
 131. Henry, E. R. *et al.* Allosteric control of hemoglobin S fiber formation by oxygen and its relation to the pathophysiology of sickle cell disease. *Proc. Natl. Acad. Sci. U. S. A.* (2020). doi:10.1073/pnas.1922004117
 132. Statius van Eps, L. W. Sick Cell Disease. in *Atlas of diseases of the kidney* (1999).
 133. Jones, S. B. & Friedman, S. P. Particle shape effects on the effective permittivity of anisotropic or isotropic media consisting of aligned or randomly oriented ellipsoidal particles. *Water Resour. Res.* **36**, 2821–2833 (2000).
 134. Sihvola, A. Dielectric Polarization and Particle Shape Effects Dielectric Polarization and Particle Shape Effects. *J. Nanomater.* 19 (2007). doi:10.1155/2007/45090
 135. Figueiredo, N. M. & Cavaleiro. Dielectric Properties of Shape-Distributed Ellipsoidal Particle Systems. **15**, 379–397 (2019).
 136. Biasio, A. Di & Cametti, C. Effect of shape on the dielectric properties of biological cell suspensions. *Bioelectrochemistry* **71**, 149–156 (2007).
 137. Abay, A. *et al.* Glutaraldehyde – A Subtle Tool in the Investigation of Healthy and Pathologic Red Blood Cells. *Front. Physiol.* **10**, 1–14 (2019).
 138. West African Genetic Medicine Centre. SICKLE CELL DISEASE. Available at: <https://wagmc.org/research/sickle-cell-disease/>.
 139. About NanoVNA. Available at: <https://nanovna.com/>.

Appendix

Appendix 1 - St Mary's ethics approval acceptance letter.



13 October 2017

Unique Ref: SMEC_2017-18_016

Colin Towey & Wesleigh Dawsmith (SHAS): Monitoring Hydration Status in Athletes Using Microwave Technology

Dear Colin and Wesleigh

University Ethics Sub-Committee – provisional approval

Thank you for submitting changes to the previously approved ethics application reference SMEC_2016-17_032, due to a change of proposer.

I confirm that ethical approval is granted by Chair's Action.

Yours sincerely

A handwritten signature in black ink, appearing to read 'Conor Gissane'.

Prof Conor Gissane
Chair of the Ethics Sub-Committee

Cc Dr Mark Glaister

*Appendix 2 - MTA for the movement of human blood between St Mary's university
and Queen Mary University of London.*

St Mary's
University
Twickenham
London



Material Transfer Agreement

This Agreement is made by and between:

a) **St Mary's University, Waldegrave Rd, Strawberry Hill, Twickenham. TW1 4SX**

and

b) **Queen Mary University of London, of Mile End Road, London E1 4NS**

This Agreement records the terms under which St Mary's University will make available whole human blood samples (the "Material"). The term "Material" includes all unmodified progeny generated from the material supplied and that part of all derivatives and the derivative's progeny which contains any of the material supplied or its progeny. The Recipient Institution will hold the Material on the terms of this Agreement and solely for the purpose of analysing the osmolality, dielectric and optical properties of the whole human blood samples ("the Research Project") within the research group of Dr. Tina Chowdhury ("the Recipient Scientist").

1. The Material may only be used by those under the Recipient Scientist's direct supervision in the Recipient Institution's laboratories under suitable containment conditions, and in compliance with all applicable statutes and regulations. **THE MATERIAL MAY NOT BE USED IN HUMAN SUBJECTS OR FOR CLINICAL OR DIAGNOSTIC PURPOSES.**
2. The Recipient Institution will not transfer the Material to any other body, or permit its use within the Recipient Institution other than by the Recipient Scientist's research group, without (in each case) prior written consent from St Mary's University. The Material may not be used by the Recipient Scientist in research which is subject to the provision of any rights to a commercial third party without prior written consent.
3. The Recipient Institution understands that the Material is experimental in nature, and may have hazardous properties. St Mary's University makes no representations and gives no warranties either express or implied in relation to it: for example, no warranties are given about quality or fitness for a particular purpose; or that the use of the Material will not infringe any intellectual property or other rights of third parties. St Mary's University will not be liable for any use made of the Material.
4. Except to the extent prohibited by law, the Recipient Institution assumes all liability for damages which may arise from its receipt, use, storage or disposal of the Material. St Mary's University will not be liable to the Recipient Institution for any loss, claim or demand made by the Recipient Institution, or made against the Recipient Institution by any other party, due to or arising from the use of the Material by the Recipient Institution, except to the extent the law otherwise requires.
5. The liability of either party for any breach of this Agreement, or arising in any other way out of the subject matter of this Agreement, will not extend to loss of business or profit, or to any indirect or consequential damages or losses.
6. The Recipient Scientist will acknowledge the source of the Material in any publication reporting on its use. If the Recipient Scientist wishes to include in a publication any information which has been provided by St Mary's University with the Material and which was clearly marked as "confidential" and "proprietary" at the point of disclosure ("Confidential Information"), the



Recipient Scientist will request permission from St Mary's University, providing a copy of the text before publication takes place.

7. **Nothing in this Agreement grants the Recipient Institution any rights over the Material (other than as specifically granted by this Agreement) or under any patents, nor any right to use, or permit the use of, any products or processes containing, using, or directly derived from the Material for profit-making or commercial purposes ("Commercial Use").** If the Recipient Institution wishes to make Commercial Use of the Material or a product directly derived from the Material it agrees to negotiate in good faith with St Mary's University or its representative for the grant of an appropriate licence or the conclusion of a revenue sharing agreement, if justified. St Mary's University will have no obligation to grant a licence.
8. Nothing included in this Agreement shall prevent St Mary's University from being able to distribute the Material to other commercial or non-commercial entities, including any intellectual property protection being undertaken by the Recipient Institution on any new use made with the Material.
9. This Agreement shall commence on the date of last signature below and will (subject to earlier termination pursuant to clause 10) continue for the duration of the Research Project.
10. St Mary's University may terminate this Agreement if the Recipient Institution is in material breach of any of the terms of this Agreement and, where the breach is capable of remedy, the Recipient Institution has failed to remedy the same within one month of service of a written notice from St Mary's University specifying the breach and requiring it to be remedied.
11. Upon completion of the Research Project or earlier termination under clause 10 the Recipient Institution will discontinue all use of the Material, and upon St Mary's University's direction, return or destroy the Material, unless permission to retain the Material is specifically provided in writing by St Mary's University to the Recipient Institution.
12. This Agreement shall be governed by English Law, and the English Courts shall have exclusive jurisdiction to deal with any dispute which may arise out of or in connection with this Letter Agreement.

Accepted and Agreed by an authorised signatory on behalf of

Queen Mary University of London

Name: *Jan Clarke*
 Position: Operations Manager
(Post Award)
 Signature: *[Signature]*
 Date: 17th Nov 2017

Accepted and Agreed by an authorised signatory on behalf of

St Mary's University

Name: Colin Towey
 Position: Lab Technician & Physiologist
 Signature: *[Signature]*
 Date: 26th Oct 2017



APPENDIX 1: Study description and details of Materials

TO BE COMPLETED BY THE RECIPIENT INSTITUTION'S SCIENTIST:

1. STUDY DESCRIPTION:

The use of blood osmolality, dielectric and optical properties as a measure of hydration status – whole blood osmolality, dielectric and optical of samples is being analysed in to determine a level of correlation between the three measures.

2. DETAILS OF MATERIALS REQUESTED (type of material, quantity, numbers of material):

The whole human blood samples are being transported for analysis at Queen Mary of University for analysis of osmolality, dielectric and optical properties.

3. DETAILS OF COURIER TO BE USED AND COURIER ACCOUNT CODE:

4. LOCATION OF LABORATORY WHERE MATERIALS ARE TO BE HELD/USED:

Queen Mary University of London
School of Engineering and Material Science, Mile End Road, London E1 4NS

5. HTA LICENCE / ETHICS APPROVAL:

Complete one of the following:

This Study has been given a favourable opinion by an ethics committee, which, within the UK, is recognised under the Human Tissue Act 2004. Please provide the reference of the opinion and name of the committee: St. Mary's University Ethics sub-committee (project reference: SMEC_2015-16_115).

Or:

The Materials are to be stored in premises licensed by the Human Tissue Authority, until favourable ethical approval has been obtained for the proposed Study at which point the Recipient Scientist shall notify St Mary's University. Please provide the licence number:

Or:

Where the Materials are supplied by St Mary's University from a research tissue bank which may be a diagnostic archive and which has been granted REC approval for specific research projects, this REC approval may cover the research Study with the materials at the Recipient Institution. If this is the case, the Designated Individual (or their duly authorised

St Mary's
University
Twickenham
London



delegate) of St Mary's University confirms that its REC approval for the tissue bank will cover the proposed Study by signing here:

.....

APPENDIX 2: Delivery and Storage of Materials

TO BE COMPLETED BY ST MARY'S UNIVERSITY:

1. QUANTITY OF MATERIALS TO BE DELIVERED:

80 x 9mL whole blood samples

2. COST OF SAMPLE PREPARATION:

N/A

3. CONDITIONS OF STORAGE

Samples will arrive chilled (2-4°C) and will be stored in a fridge upon arrival.

4. RETURN/DESTRUCTION OF SURPLUS MATERIALS ON COMPLETION OF STUDY

If there are any Materials left over from the Study, the Recipient Institution needs to provide confirmation to St Mary's University that any remaining Material will be returned to St Mary's University or destroyed in the appropriate manner.